

Studies on T-even Bacteriophage DNA

Thesis by
Jungsuh Park Kim

In Partial Fulfillment of the Requirements
For the Degree of
Doctor of Philosophy

California Institute of Technology
Pasadena, California

1972

(Submitted May 26, 1972)

To My Family

Acknowledgments

Although words may not adequately describe my indebtedness to the many people who helped make this work possible, I feel pleasantly obliged to mention some of them here:

My foremost gratitude goes to Professor Norman Davidson who so kindly and continuously supplied valuable suggestions, guidance and encouragement throughout the course of this study.

I deeply appreciate the help of Professor William Wood, Drs. Steven Beckendorf and John Wilson in preparing Part I of this Thesis. Thanks are due also to Drs. Ray Bowman, Tom Broker, Davis Hershey, and Sheldon York for their patience in correcting parts of this Thesis.

Encouragement from all my family and friends has always been with me.

Abstracts

Part I. The regions of sequence homology and non-homology between the DNA molecules of T2, T4, and T6 have been mapped by the electron microscopic heteroduplex method. The heteroduplex maps have been oriented with respect to the T4 genetic map. They show characteristic, reproducible patterns of substitution and deletion loops. All heteroduplex molecules show more than 85% homology. Some of the loop patterns in T2/T4 heteroduplexes are similar to those in T4/T6.

We find that the *rII*, the lysozyme and *ac* genes, the D region, and gene 52 are homologous in T2, T4, and T6. Genes 43 and 47 are probably homologous between T2 and T4. The region of greatest homology is that bearing the late genes. The host range region, which comprises a part of gene 37 and all of gene 38, is heterologous in T2, T4, and T6. The remainder of gene 37 is partially homologous in the T2/T4 heteroduplex (Beckendorf, Kim and Lielausis, 1972) but it is heterologous in T4/T6 and in T2/T6. Some of the tRNA genes are homologous and some are not. The internal protein genes in general seem to be non-homologous.

The molecular lengths of the T-even DNAs are the same within the limit of experimental error; their calculated molecular weights are correspondingly different due to unequal glucosylation. The size of the T2 genome is smaller than that of T4 or T6, but the

terminally repetitious region in T2 is larger. There is a length distribution of the terminal repetition for any one phage DNA, indicating a variability in length of the DNA molecules packaged within the phage.

Part II. E. coli cells infected with phage strains carrying extensive deletions encompassing the gene for the phage ser-tRNA are missing the phage tRNAs normally present in wild type infected cells. By DNA-RNA hybridization we have demonstrated that the DNA complementary to the missing tRNAs is also absent in such deletion mutants. Thus the genes for these tRNAs must be clustered in the same region of the genome as the ser-tRNA gene. Physical mapping of several deletions of the ser-tRNA and lysozyme genes, by examination of heteroduplex DNA in the electron microscope, has enabled us to locate the cluster, to define its maximum size, and to order a few of the tRNA genes within it. That such deletions can be isolated indicates that the phage-specific tRNAs from this cluster are dispensable.

Part III. Genes 37 and 38 between closely related phages T2 and T4 have been compared by genetic, biochemical, and heteroduplex studies. Homologous, partially homologous and non-homologous regions of the gene 37 have been mapped. The host range determinant which interacts with the gene 38 product is identified.

Part IV. A population of double-stranded ϕ X-RF DNA molecules carrying a deletion of about 9% of the wild-type DNA has been discovered in a sample cultivated under conditions where the phage lysozyme gene is nonessential. The structures of deleted monomers, dimers, and trimers have been studied by the electron microscope heteroduplex method. The dimers and trimers are shown to be head-to-tail repeats of the deleted monomers. Some interesting examples of the dynamical phenomenon of branch migration in vitro have been observed in heteroduplexes of deleted dimer and trimer strands with undeleted wild-type monomer viral strands.

Table of Contents

	<u>Page</u>
Acknowledgments	ii
Abstracts	iii
Part I. Sequence Homology Studies between T2, T4 and T6 DNAs by Electron Microscopy	1
(a) The T2/T4 Heteroduplex	11
(b) The T4/T6 Heteroduplex	42
(c) The T2/T6 Heteroduplex	46
(d) Molecular Weight Determination of T-even DNAs by Electron Microscopy	67
Part II. Bacteriophage T4 Transfer RNA—Clustering of the Genes for the T4 Transfer RNA	81
Part III. Structure of Bacteriophage T4 Genes 37 and 38 .	115
Part IV. Electron Microscopic Studies of Heteroduplex DNA from a Deletion Mutant of Bacteriophage ϕ X-174	171
Propositions	198

Part I

Sequence Homology Studies between
T2, T4, and T6 DNAs by Electron Microscopy

The regions of sequence homology and non-homology between the DNA molecules of T2, T4, and T6 have been mapped by the electron microscopic heteroduplex method. The heteroduplex maps have been oriented with respect to the T4 genetic map. They show characteristic, reproducible patterns of substitution and deletion loops. All heteroduplex molecules show more than 85% homology. Some of the loop patterns in T2/T4 heteroduplexes are similar to those in T4/T6.

We find that the rII, the lysozyme and ac genes, the D region, and gene 52 are homologous in T2, T4, and T6. Genes 43 and 47 are probably homologous between T2 and T4. The region of greatest homology is that bearing the late genes. The host range region, which comprises a part of gene 37 and all of gene 38, is heterologous in T2, T4, and T6. The remainder of gene 37 is partially homologous in the T2/T4 heteroduplex (Beckendorf, Kim and Lielausis, 1972) but it is heterologous in T4/T6 and in T2/T6. Some of the tRNA genes are homologous and some are not. The internal protein genes in general seem to be non-homologous.

The molecular lengths of the T-even DNAs are the same within the limit of experimental error; their calculated molecular weights are correspondingly different due to unequal glucosylation. The size of the T2 genome is smaller than that of T4 or T6, but the terminally repetitious region in T2 is larger. There is a length

distribution of the terminal repetition for any one phage DNA, indicating a variability in length of the DNA molecules packaged within the phage.

Introduction

The bacteriophages T2, T4, and T6 are known to be closely related by the criteria of serological cross-reaction, genetic complementation, genetic recombination and morphology. Genetic relatedness can also be investigated by DNA-DNA homology. In the case of T-even phages, such studies have been made by classical hybridization experiments (Schildkraut, Wierzchowski, Marmur, Green and Doty, 1962; Cowie, Avery and Champe, 1971). A more penetrating study of the DNA-DNA homology between related phages can be made by the electron microscope heteroduplex method (Davis and Davidson, 1968; Westmoreland, Szybalski and Ris, 1969; Davis, Simon and Davidson, 1971; Davis and Hyman, 1971).

The closely related lambdoid phages undergo genetic recombination and can complement each other genetically. The regions of homology in several lambdoid phages have been mapped by electron microscopy (Simon, Davis and Davidson, 1971). Perfect DNA sequence homology was found in most of the essential genes and non-homology in some silent regions. The regions of homology and non-homology are large, at least gene size.

Genetic recombination between the closely related bacteriophages T3 and T7 is rare and they exclude each other in mixed infection. Partial homology throughout most of the genome is observed for T3 and T7 (Davis and Hyman, 1971).

T2, T4, and T6 are expected to be perfectly homologous in most essential genes and non-homologous in the regions which genetic studies have already shown to be non-homologous such as the host range region and exclusion genes (Russell, 1967). Less essential genes could be either homologous or non-homologous.

The particle morphologies of the three phages are very similar except that both T4 and T6 have a thin collar in the neck region which is absent in T2. Their genetic maps are largely congruent. In T2, 46 of the 53 identified genes are homologous to T4 genes. In T6, 34 of the 42 identified genes are homologous to T4 genes and 3 genes are homologous to T2 genes not yet identified in T4 (Russell, 1967). There are, however, a few differences among these bacteriophage, which indicate that they have diverged far enough to have new functions. For example, T4 induces an enzyme involved in the repair of UV-damaged DNA which is absent in T2 (Yasuda and Sekiguchi, 1970). T2 induces a DNA methylase not found in T6 infected cells (Hausman and Gold, 1966). The most striking genetic difference is in the host range region (Russell, 1967; Beckendorf *et al.*, 1972). This difference is expected because the receptors for T4 reside in the lipopolysaccharide layer of the cell wall, while those for T2 and T6 are in the lipoprotein layer. Furthermore, several bacterial strains exist which are resistant to one phage but not to the others. The products of genes 37 and 38 are compatible between T2 and T6, but incompatible between T2 and T4, and between T4 and T6.

T-even DNAs contain glucosylated hydroxymethylcytosine (HMC), but the pattern of glucosylation is species-specific (Sinsheimer, 1954; Lehman and Pratt, 1960). All three phages induce an HMC- α -glucosyl transferase. T4 induces an additional HMC- β -glucosyl transferase, while T6 (and probably T2) induces a "di-glucosylating" enzyme (Kornberg, Zimmerman and Kornberg, 1961; Zimmerman, Kornberg and Kornberg, 1962). T4 excludes T2 and T6 very strongly, while T6 excludes T2 weakly (Russell, 1967). All these observations suggest that there is closer genetic relationship between T2 and T6 than between the other pairs. A similar conclusion was drawn by Cowie et al. (1971) from their DNA-DNA hybridization studies.

In this paper we present our results on base sequence homology between T-even DNAs as studied by the electron microscope heteroduplex method. We compare the physical map with that derived from genetic studies. Physical measurements of the molecular weight, the genome size, and the size of the terminal repetition for each T-even phage are also presented.

Materials and Methods

(a) Phages

Wild type T4D, T4B, T2L, and T6 as well as T4BrII deletion mutants (rH23, rH88 and r638) and T4rEDdf41 were obtained from Dr. William Wood. The lysozyme deletion mutant, T4BeG19 was provided by Dr. George Streisinger. T4tRNA deletion mutants

$psu_b^- \Delta 8$, $psu_b^- \Delta 27$, $psu_b^- \Delta 33$, and $psu_b^- \Delta 119$ were obtained from Dr. John Wilson.

Several hybrid phages between T2 and T4 were used. Hybrids in the host range region, $T2h^{4+}$ and $T4r22[Bx28T2Lh^{2+}]$ ($T4h^{2+}$) were obtained from Dr. Frank Stahl through Dr. William Wood. T2L was crossed to T4BrH23, rH88, and r638 by Dr. John Wilson. $T2am^+$ progeny were selected on a restrictive host at low temperature by Dr. Steven Beckendorf from crosses of T2 bearing am mutations in genes 43 and 47 and a temperature-sensitive mutation in gene 34 with UV-irradiated wild type T4D.

(b) Bacteria

E. coli BB, S/4, S/6 and CR63r⁻ were obtained from Dr. William Wood.

(c) Media

Hershey broth, used for phage and bacterial growth, and enriched Hershey top and bottom agar, used for plating assays, contained the following (Russell, 1967): a) Hershey broth; 8 g Difco nutrient broth (dehydrated), 5 g Difco bacto peptone, 5 g NaCl, 1 g glucose, and 1 ℓ H₂O, all adjusted to pH 7.4; b) enriched Hershey bottom agar; 10 g Difco bacto agar, 13 g Difco bacto-peptone, 8 g NaCl, 2 g sodium citrate dihydrate, 1.3 g glucose and 1 ℓ H₂O; c) enriched Hershey top agar, same as bottom agar except with 6.5 g agar.

Citrate top and bottom agar used for preparation of plate stocks of the lysozyme deletion mutant contained the following:

a) citrate bottom agar; 10 g tryptone, 11 g Noble agar, 5 g NaCl and 1 l H₂O, all autoclaved and cooled to 55°, with 50 ml 1 M Tris, pH 8.0 and 10 ml 25% sodium citrate dihydrate being added just before pouring; b) citrate top agar; same as bottom agar except with 7 g agar.

(d) Growth of bacteriophage

E. coli BB were grown to about 2×10^8 cells/ml in Hershey broth and then infected with 2 to 5 bacteria. In growing the T4B strain, 20 µg/ml L-tryptophan was added 2-3 min before infection. 30 minutes after infection, 1 M Tris, pH 8.5 was added to raise the pH of the culture medium to between 7.5 and 8.0 to minimize introducing single-strand breaks in DNA (Drs. Hyman and Davis have suggested that after phage infection, when bacterial lysis occurs, phage are usually exposed to a slightly acidic medium. Under this condition DNA is depurinated, so that a break in the phosphodiester chain is introduced upon treatment with alkali). A few drops of chloroform were added to lyse the remaining unlysed cells.

The phage were purified by several cycles of differential centrifugation and stored in 0.1 M NaCl, 0.01 M MgSO₄ and 0.01 M Tris, pH 8.5.

The lysozyme deletion mutant phage were prepared on citrate-lysozyme plates by the confluent lysis technique (Epstein, Bolle, Steinberg, Kellenberger, Boy, Chevally, Susman, Denhardt and

Lielausis, 1963).

(e) Hybridization

When a mixture of two closely related phage DNAs, AA' and BB' is denatured and renatured, the renatured sample will contain homoduplexes, AA' and BB' and heteroduplexes, AB' and A'B. To prepare such heteroduplexes, a solution containing equal numbers of two different phages (total phage concentration about 4×10^{10} phages/ml) was made 0.1 N in NaOH, 0.01 M in EDTA to lyse the phage and to denature the DNA. The solution was left at room temperature for 10 min after which it was neutralized by adding 100 μ l 1.8 M Tris-HCl, 0.2 M Tris base and 1 ml of formamide per ml of phage solution. The phage DNAs were renatured by dialysis against 0.9 M NaCl, 0.1 M Tris, pH 8.5, 0.01 M EDTA and 60% formamide at room temperature for 1 hr. Finally, the renatured DNA was dialyzed against 0.1 M NaCl, 0.01 M Tris, pH 8.5 and 0.001 M EDTA to remove formamide.

(f) Electron microscopy

Our electron microscopic techniques have been described in detail (Davis, Simon and Davidson, 1971). The procedure is basically as follows: 50 μ l spreading solution containing phage DNA, cytochrome c (50 γ /ml), 0.1 M Tris, pH 8.5, 0.01 M EDTA and 40% formamide were spread on a hypophase containing 0.01 M Tris, pH 8.5, 0.001 M EDTA and 10% formamide. Both single- and double-stranded ϕ X-174 DNAs were added to the spreading solution as

internal length standards (5200 bases long, Davidson and Szybalski, 1971). Grids picked up from the protein film were stained with uranyl acetate and shadowed with Pt-Pd. Photographs were taken using a Philips EM300. Negative images of the DNA molecules were traced with the aid of a Nikon Shadowgraph.

One per cent formamide lowers the melting temperature of native DNA by 0.7°C (McConaughy, Laird and McCarthy, 1969). The cation concentration of the spreading solution described above is 0.06 M . The melting temperature of sheared T4DNA at 0.06 M $[\text{Na}^+]$ is 75.5° (Wetmur and Davidson, 1968). Our mounting condition of DNA at 25°C is therefore equivalent to $T_m - 23^{\circ}$. The denaturing power of the hypophase described above is about the same as that of the spreading solution.

(g) The schematic representations of the heteroduplex loop patterns correspond, from left to right, to the clockwise direction of the T4 genetic map.

Results

(a) The T2/T4 Heteroduplex

The T2/T4 heteroduplex map shows a characteristic and reproducible pattern of substitution and deletion loops. The electron micrograph shown on Plate 1 is an entire circular heteroduplex molecule carrying the T4BrH23 deletion (a deletion of length 4200 base pairs in both the rIIA and B cistrons). The rH23 deletion loop is indicated by an arrow. Both T2 and T4 DNAs are circularly permuted and terminally repetitious (MacHattie, Ritchie and Thomas, 1967), so that unbroken heteroduplex molecules form circles having two single-strand branches. The heteroduplex map, constructed from the loop patterns in a number of whole molecules and by matching overlapping patterns from many broken molecules, is shown in Fig. 1. About 87% of the T4DNA molecule is homologous to T2DNA. The positions of the loops are reproducible except for one or two regions which will be described later.

To orient this physical heteroduplex map with respect to the genetic map (Edgar and Wood, 1966), three T4rII deletions and the deletion eG19 in the lysozyme gene of T4 were used. The deletion rH23 spans all of the rII region and extends past the right-hand boundary of the rIIB cistron into the D region. (The D region is apparently dispensable for the multiplication of T4 phage in all known hosts (Bautz and Bautz, 1967).) Deletion rH88 is inside the rIIA

Plate 1. T2/T4BrH23 heteroduplex circular molecule. The letters ("A" and "H") identify the loops in Fig. 2. Double- and single-stranded circular ϕ X-174 DNA molecules are in the background. Two single-stranded branches corresponding to terminal repetition region are indicated by thinner arrows, and rH23 deletion loop by a thick arrow.

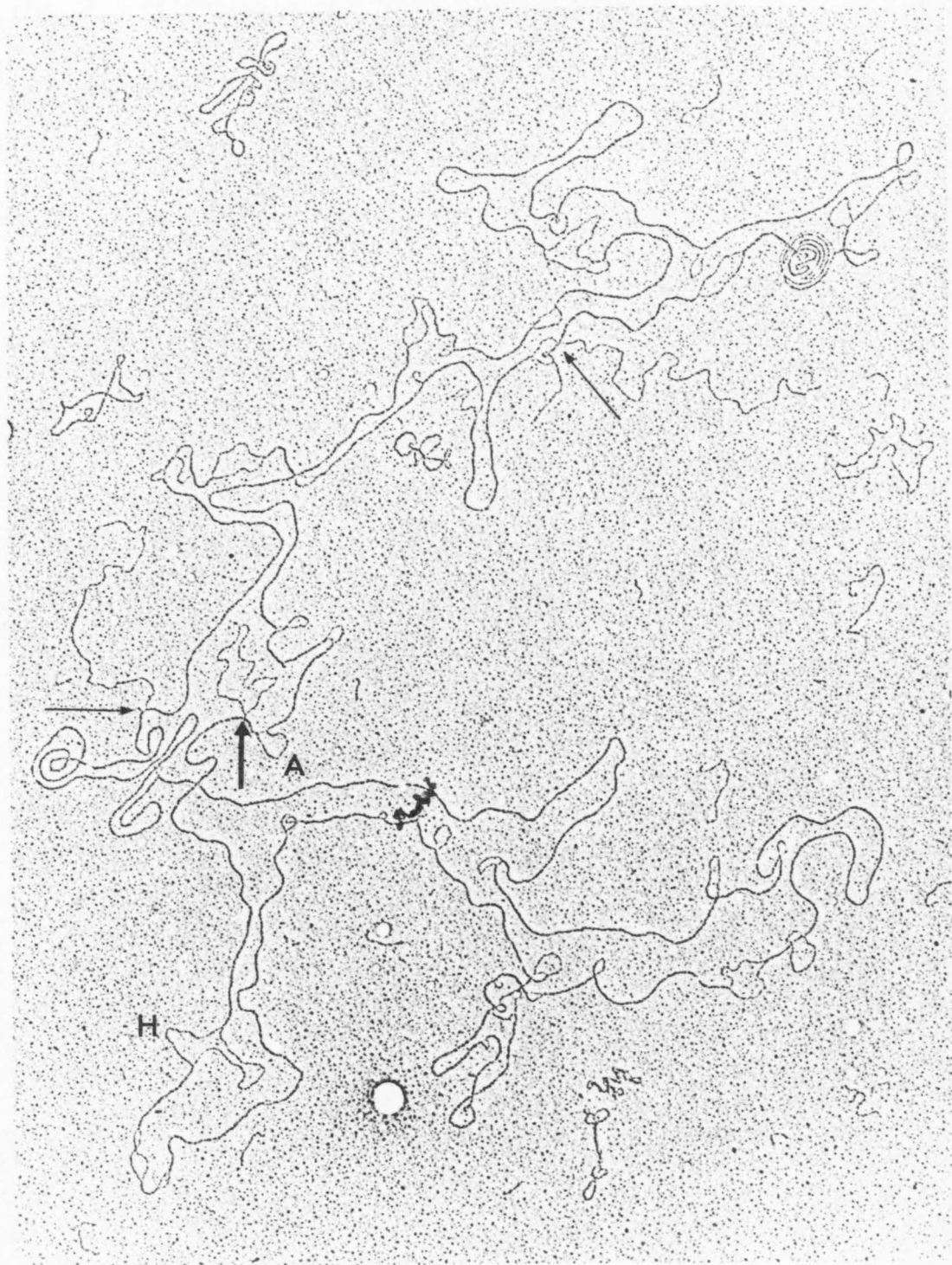
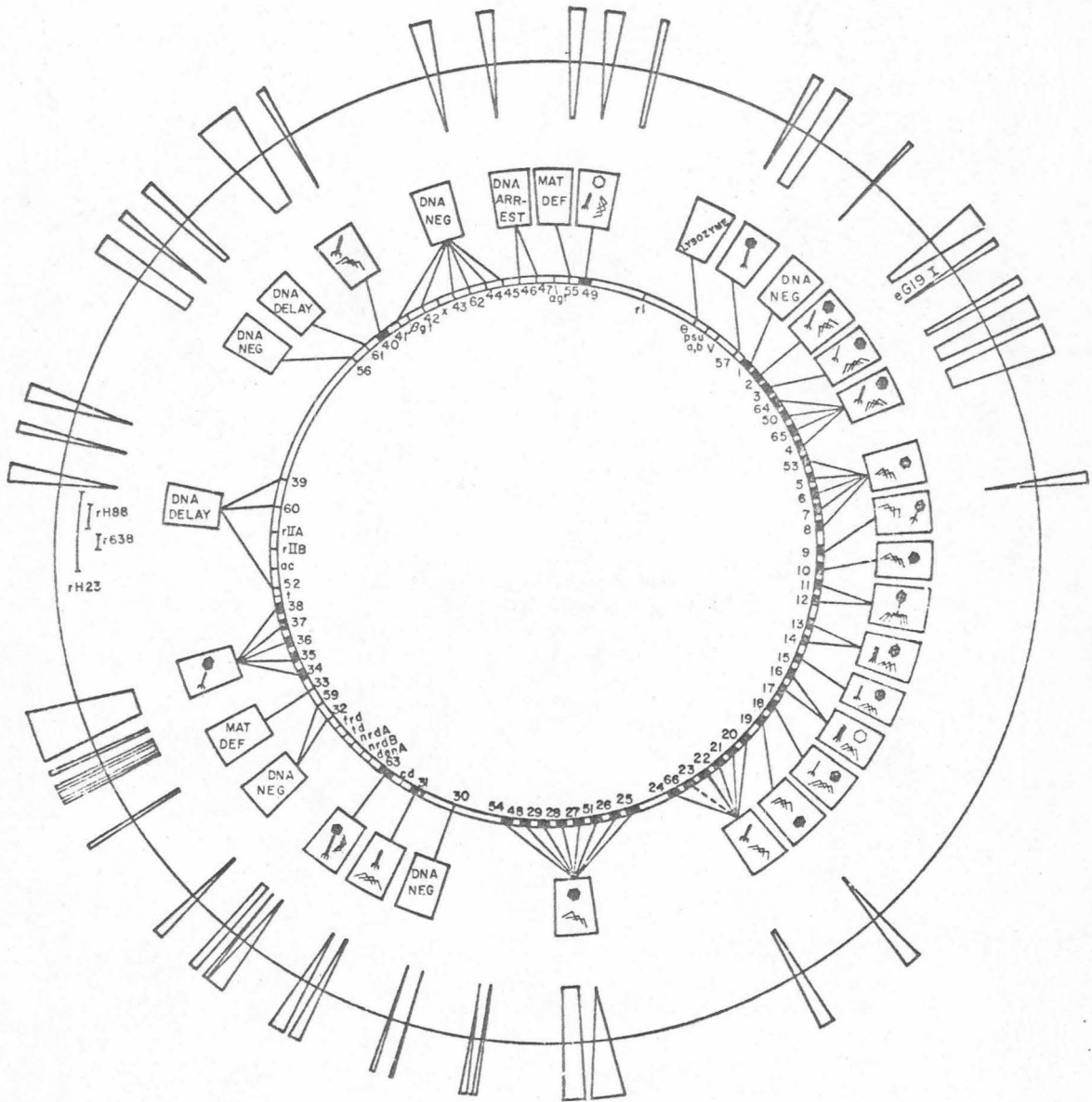


Fig. 1. T2/T4 heteroduplex map oriented relative to the T4 genetic map (Edgar and Wood, 1966; Wood and Edgar, 1967). In the heteroduplex map, outer and inner arcs represent a longer strand and a shorter strand, respectively. The surrounding duplex segments are separated by the average of the two arms of a substitution loop or one-half the length of a deletion type loop.



Outer Circle: T2/T4 Map
Inner Circle: Genetic Map of T4

cistron. Deletion r638 deletes all of the rIIB cistron and extends into region D.

Electron micrographs of the T2/T4B, T2/T4BrH23, T2/T4BrH88 and T2/T4Br638 heteroduplexes around the rII region are shown in Plate 2. Figure 2 is a schematic representation of the loop patterns of these heteroduplexes. Since the rH23 deletion loop lies between deletion loop A and substitution loop H of the regular T2/T4 heteroduplex map, these two features can be used as position markers. The deletion rH88 loop is closer to loop A than is the deletion r638 loop. Therefore the direction loop A \rightarrow loop H corresponds to the rIIA \rightarrow rIIB cistron. This orients our physical map relative to the genetic map (see Fig. 1).

If the right end of the deletion rH23 coincides with that of the rIIA cistron, we estimate the size of rIIA cistron to be 2400 base pairs. If the deletion rH23 extends beyond the right end of rIIA cistron, it will be smaller. The deletion r638 starts at the beginning of rIIB cistron (Benzer, 1961) and extends into half way of the D region. Thus the rIIB cistron should be smaller than r638 deletion (960 base pairs). The region D adjacent to the rIIB cistron has been identified as a DNA sequence which is transcribed early during infection. The region D is subdivided into three regions; D₁ (a delayed-early gene), D_{2a} and D_{2b} (immediate-early gene) (Sederoff, Bolle and Epstein, 1971). It seems that the left end of the rH23 deletion is located at the boundary between D₁ and D_{2a} regions (Sederoff et al., 1971). From the relative position of the deletions

Plate 2. Electron micrographs of T2/T4B(a), T2/T4-BrH23(b), T2/T4BrH88(c) and T2/T4Br638(d) heteroduplex DNA molecules around rII region. Each rII deletion loop, the deletion-type loop A and the substitution loop H are indicated. The loops A and H are separated by 11,500 base pairs in (a). The distances from the loop A and to the deletion loop, rH23, rH88 and r638 correspond to 400, 1,100 and 2,800 base pairs. Double-stranded ϕ X-174 molecules in the background.

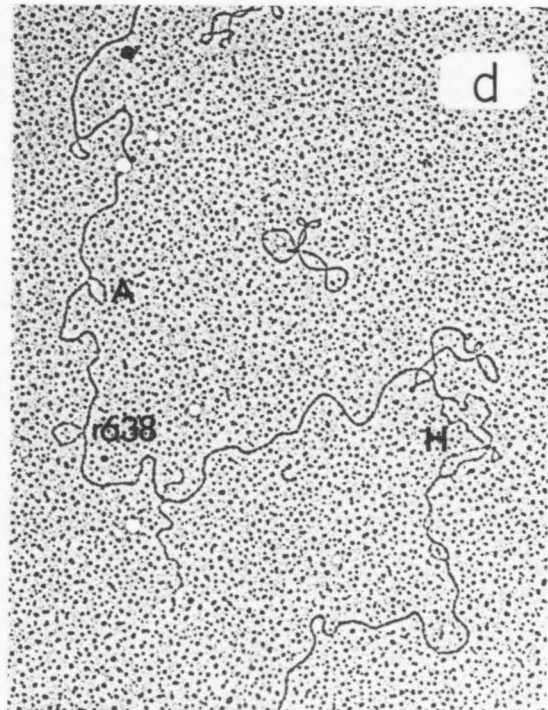
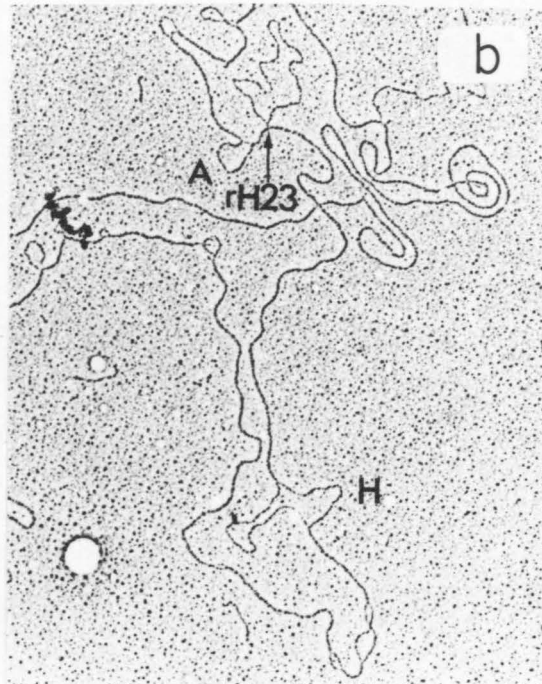
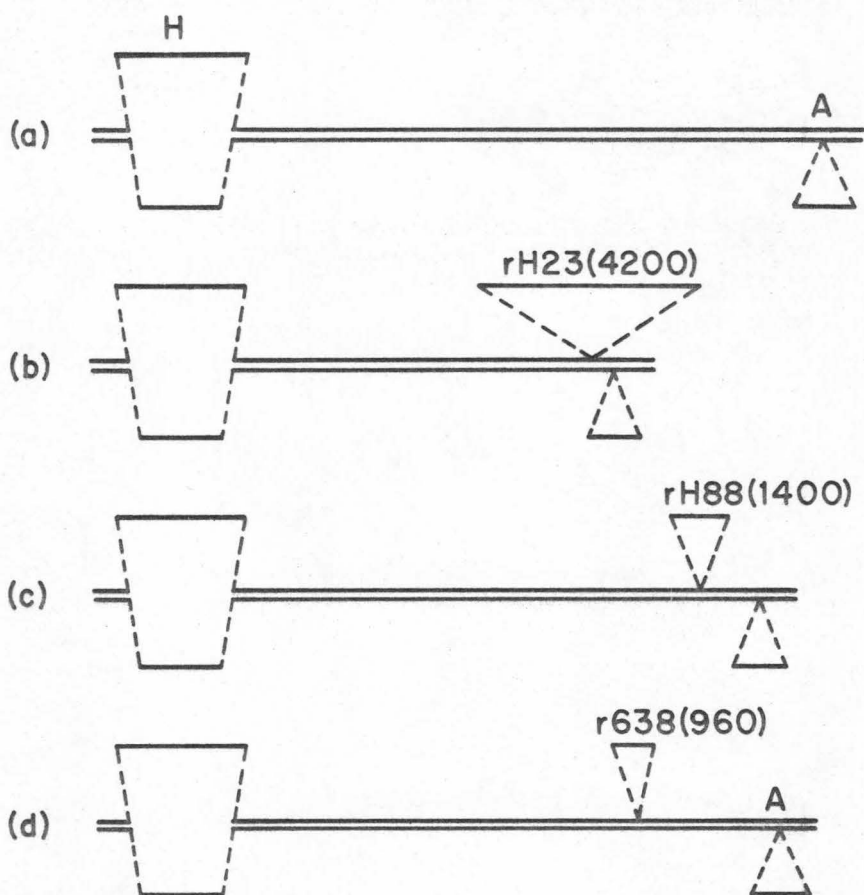
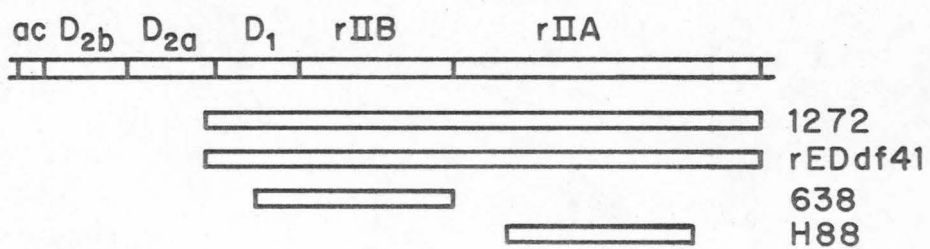


Fig. 2. Genetic map of rII deletion mutants of T4, and schematic representation of the loop patterns of T2/T4B(a), T2/T4BrH23(b), T2/T4BrH88(c) and T2/T4Br638(d) heteroduplex DNA around rII region. The size of region D is estimated from the recombination distance between r73 and ac (Edgar and Epstein, 1961). In T2/T4BrH23 heteroduplex, the rH23 and "A" deletion loops have opened up together to give an asymmetric substitution loop. Therefore the "A" loop corresponds to T4 DNA. The size of each rII deletion is given in base-pairs. All the figures (a) - (d) are in scale.



rIIB ← rIIA

rH23 and r638, we conclude that the size of the region D_1 is at least 1000 base pairs.

There are two strains of T4, T4D (Doerman) and T4B (Benzer). Most of the rII mutants of T4 have been isolated from the Benzer strain, while most of the amber and temperature-sensitive mutants have been isolated from the Doerman strain. They were derived from a common ancestor, but T4D has lost its requirement for L-tryptophan. To investigate the sequence relationship between T4D and T4BrH23, the T4D/T4BrH23 heteroduplexes were examined in the electron microscope. These heteroduplex molecules seem to be entirely double-stranded throughout the molecule except for the rH23 deletion loop. We thus conclude by heteroduplex criteria that they are homologous. Should there be any regions of non-homology smaller than 100 base pairs, they may not be resolved with our present technique, especially when we do not know where to expect to find non-homology. Another well-known rII deletion mutant, T4rEDdf41 (derived from T4D by Edgar, Feynman, Klein, Lielausis and Steinberg (1962)) seems to be identical to T4BrH23 by heteroduplex mapping.

Our measurements made on the T4BrH23/T4BeG19 heteroduplex show that eG19 is located 140° from the rH23 deletion. Plate 3 shows electron micrographs of the T2/T4BeG19 heteroduplex DNA around the e gene. Figure 3 schematically represents loop patterns of the heteroduplex T2/T4BeG19. The eG19 deletion loop

Plate 3. Electron micrographs of T2/T4B(a) and T2/T4-BeG19(b and c) heteroduplex DNAs around the e gene. Size of the double-stranded region between loops B and C correspond to 1050 base pairs in (a). In (b) there is a eG19 deletion loop (700 bases) between loops B and C. The double-stranded region between loops B and eG19 is variable in length. The largest length observed was 180 base-pairs. Frequently the loops B and eG19 opened up together to give a symmetric substitution loop (indicated by an arrow) shown in (c). Letters relate the loop pattern in the micrograph to the schematic representation in Fig. 3.

Originally these electron micrographs were taken at such low magnifications that they were undergone two-step enlargements. The contrast is relatively poor and there is no good distinction between single- and double-stranded regions.

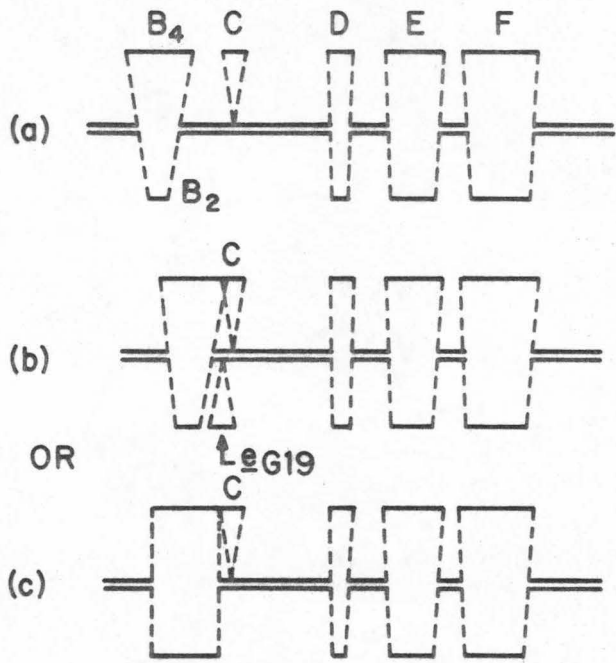


Fig. 3. Schematic representations of the three heteroduplex molecules for which electron micrographs are shown in Plate 3.

(a) T2/T4B.

(b) and (c) T2/T4BeG19.

→ Clockwise



(700 bases) was found between the loops B and C. This position is about 135° from the rII region around the circular map by the shorter spanning. This result confirms the map order that was obtained with the rII deletion mutants. The eG19 deletion loop and substitution loop B (with single-strand sizes of 1250 and 480 bases, respectively) often open up together to give a substitution loop in which both strands are about equal in length (Fig. 3c). From this observation it is possible to deduce that the longer strand (B_4) of the loop corresponds to the T4 molecule and the shorter one (B_2) to T2.

(i) Homology in the tail fiber and neighboring genes

Tail fiber assembly in T4 requires at least 6 phage genes; 34, 35, 36, 37, 38, and 57. Genes 34 and 37 code for the two major structural proteins. The products of T4 gene 37 and 38 (P37 and P38) interact during tail fiber assembly, and they are incompatible with P37 and P38 of T2 (Russell, 1967). Russell's genetic studies indicated that the host range determinants for T4 were closer to gene 38 than to gene 37 among the tail fiber genes. We therefore suspected that gene 37 and gene 38 should map in the large substitution loop H of Figs. 1 and 2.

To test this, we examined heteroduplexes $T2h^{4+}/T2rH23$ and $T4h^{2+}/T4rH23$. The history of T2rH23 mutant will be described later. $T2h^{4+}$ and $T4h^{2+}$ were made to be isogenic to T2 and T4, respectively, except for the host range region (Sechaud, Streisinger, Emrich, Newton, Lanford, Reinhold, and Stahl, 1965). As expected, the loop H did indeed appear in these heteroduplexes; however,

it is also possible that the loop H contained genes other than the host range determinant. By heteroduplex methods, quite a few T4 and T2 genes were found in T2h⁴⁺ and T4h²⁺, respectively.

These conclusions were confirmed by the more extensive biochemical, genetic and heteroduplex studies of Beckendorf et al. (1972). They showed that the host range determinant as well as gene 38 maps in the loop H. The longer strand (H₂, 2600 bases) comes from T2 and the shorter strand (H₄, 1560 bases) from T4 (Beckendorf et al., 1972). This observation is consistent with the fact that the molecular weight of P37 from T2 is 13,000 daltons (approximately 400 bases) larger than that from T4. The difference in length between the H₂ and H₄ arms of the substitution loop H therefore suggests that gene 38 of T2 is also bigger than gene 38 of T4. The results of Beckendorf et al. (1972) indicate that the rest of gene 37 consists of homologous, partially homologous and heterologous segments which map counterclockwise from loop H (Fig. 4).

There has been conflicting evidence as to the relative sizes of T2 and T4 genes 34 and 35. Genetic recombination studies suggest that their lengths were greater in T4 than in T2 (Russell, 1967). Mosig's physical mapping (1968) however indicated genes 34 and 35 of T4 are smaller than indicated by the genetic studies. It was then found (Beckendorf and Wilson, 1972), that the molecular weight of P34 in T2 and T4 are same (130,000 daltons) and that T4 gene 34 has a sharp gradient of increasing recombination near one end of its ends. Russell (1967) observed intragenic recombination in gene 34

between T2 and T4, suggesting that the genetic sequences are homologous.

The following physical argument suggests that the gene 34 and 35 of T2 and T4 are at least partly homologous and not greatly different in size. The sizes of the relevant peptide gene products (Ward and Dickson, 1971; King and Laemmli, 1971) and corresponding numbers of coding nucleotides for T4 are: P38, 240 amino acids, 720 nucleotides; P37, 1180 amino acids, 3540 nucleotides; P36, 220 amino acids, 660 nucleotides; P35, 360 amino acids, 1080 nucleotides (personal communication with Dr. Dickson); P34, 1360 amino acids, 4080 nucleotides (assuming an average residue molecular weight of 110 per amino acid). Figure 4 shows these spacings on the heteroduplex map, assuming that genes are contiguous. This map suggests that gene 35 is homologous, and about 90% of gene 34 is homologous.

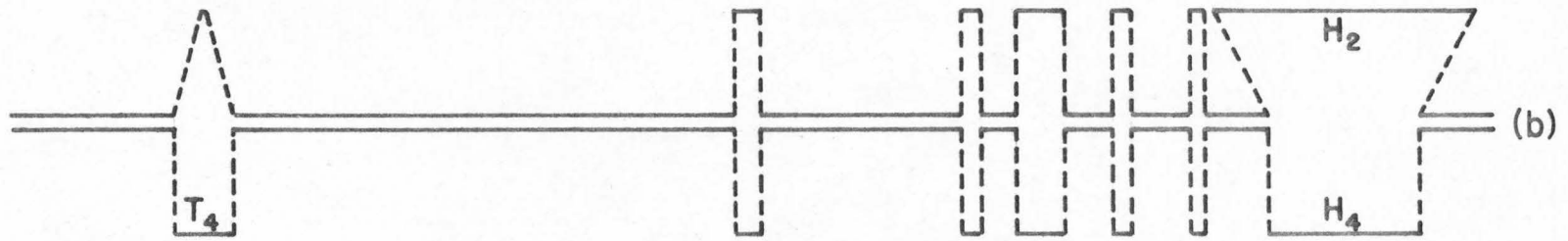
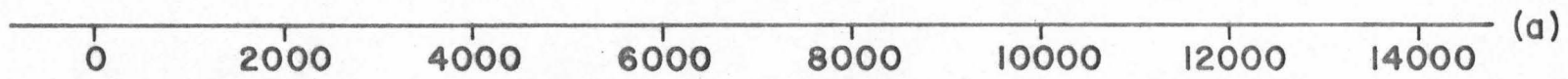
There are three known genes between the rII cistron and gene 38: the D region, the ac gene (acriflavine resistant) and gene 52 (DNA-delayed). In T2/T4 heteroduplexes all three genes map in homologous region about 8000 base-pairs long.

(ii) Homology in genes 43 and 47

A triple mutant of T2 (amber mutations in genes 43 and 47 and a temperature-sensitive mutation in gene 34) was crossed to wild type T4D, which had been subjected to an average of 17-19 lethal hits of UV irradiation per molecule. The input ratio of T2 to T4 was 10:1. Progeny from this cross were plated on CR63r⁻ (CR63r⁺ is

Fig. 4. T2/T4 heteroduplex map and translational map (based on the size of peptide gene product) around the tail fiber genes.

- (a) Scale in base-pairs.
- (b) T2/T4 heteroduplex map. The deletion type loop in the left end corresponds to T4 DNA. This will be shown in section (c). For the loop H, the spacing between the surrounding duplex segments is equal to the length of the T4 single-strand, i. e., H_4 .
- (c) Translational map of T4. Map position of gene 37 is drawn from Beckendorf et al. (1972).
- (d) Partially homologous region of gene 37 in the T2/T4 heteroduplex.



30



restrictive to T2) at 30°C. Each plaque was replated on a mixture of S/4 and S/6 at 30°C to select T2 phage (clear plaque) containing T4 genes 43 and 47 (T4 phage give turbid plaques), but still retaining their temperature sensitive mutation (this was tested by replating at 43°C).

Heteroduplexes formed from three independently isolated hybrid phages and T4 were examined. Loop patterns observed here were identical to those from 9 to 1 o'clock--that is, in the region spanning genes 43 and 47 on the wild type T2/T4 heteroduplex map (see Fig. 1). This result indicates that genes 43 and 47 in T2 are homologous to T4 within the limits of our present technique.

(iii) Homology in tRNA genes

Upon infection of E. coli with T-even phages, phage-coded tRNAs are induced (Daniel, Sarid and Littauer, 1970). Polyacrylamide gel electrophoresis of low molecular weight RNA from cells infected with wild type T4D gives 6 distinct bands (Wilson, Kim and Abelson, 1972a). Wilson and Kells (1972b) have isolated phage-coded nonsense suppressors in T4 and deletion mutants in the serine suppressor tRNA gene (Wilson and Abelson, 1972c). Most of the tRNA genes are clustered around the e gene and are non-essential. A few tRNA genes in T4 have been mapped by electron microscopy and by polyacrylamide gel electrophoresis of RNA isolated from cells infected with deletion mutants (Wilson et al., 1972a).

We used several T4 tRNA deletion mutants ($\text{psu}_b^- \Delta 8$, $\text{psu}_b^- \Delta 27$, $\text{psu}_b^- \Delta 119$ and $\text{psu}_b^- \Delta 33$) to study which T4 tRNA genes are homologous to T2 tRNA genes. The physical map of the \underline{e} and psu_b deletions has been constructed and relative positions of tRNA genes have been determined (Wilson *et al.*, 1972a). Electron micrographs of the heteroduplex molecules between T4 tRNA deletion mutants and T2 are in Plate 4. Their schematic representation of the loop patterns is shown in Fig. 5. Figure 5(a) shows loop patterns around the tRNA gene in T2/T4. The two arrows indicate the extreme limits of the tRNA gene clusters. Figures 5(b)-(e) represent the position of each deletion (colored area) in the T2/T4 tRNA deletion mutants heteroduplex. All information shown in Figs. 5(a)-(e) is presented together in Fig. 5(f). The loop E is an asymmetric substitution loop (the difference in the size of the two strands is about 210 bases). From the size of the loop E appearing in T2/T4 $\text{psu}_b^- \Delta 8$, it is possible to conclude that the longer strand is from T2DNA. We have compared the sizes of deletions $\text{psu}_b^- \Delta 119$ and $\text{psu}_b^- \Delta 33$ in T4 with the sizes of the loops occurring due to deletion of the tRNA genes in T2/ $\text{psu}_b^- \Delta 119$ and T2/ $\text{psu}_b^- \Delta 33$ heteroduplexes, respectively. We suggest that the longer strand of the loop F also corresponds to T2 DNA. Band 1- and ser-tRNA genes are homologous and band 2- and gly-tRNA genes map at a non-homologous region. The leu-tRNA gene could be homologous in T2 and T4. The band 1- and band 2-tRNA genes have not yet been characterized. McClain and Barrel (personal communication with Dr. Wilson) have shown that a ser-tRNA is separated by

Plate 4. Electron micrographs of the heteroduplexes between T2 and T4 tRNA deletion mutants around tRNA gene. The loops are labelled as B → F to correspond to Fig. 5.

- (a) T2/T4 heteroduplex around the tRNA genes. The double-stranded region between loops E and F (indicated by an arrow) as well as E₄ strand was decreased slightly.
- (b) T2/T4 $\text{psu}_b^- \Delta 8$ heteroduplex.
- (c) T2/T4 $\text{psu}_b^- \Delta 27$ heteroduplex.
- (d) T2/T4 $\text{psu}_b^- \Delta 119$ heteroduplex.
- (e) T2/T4 $\text{psu}_b^- \Delta 33$ heteroduplex.

The arrows in (b), (c), (d) and (e) represent loops occurring due to deletion of tRNA genes in T4. The loop patterns in (d) and (e) support that the loop F₄ (see p. 37) is indeed T4 DNA.

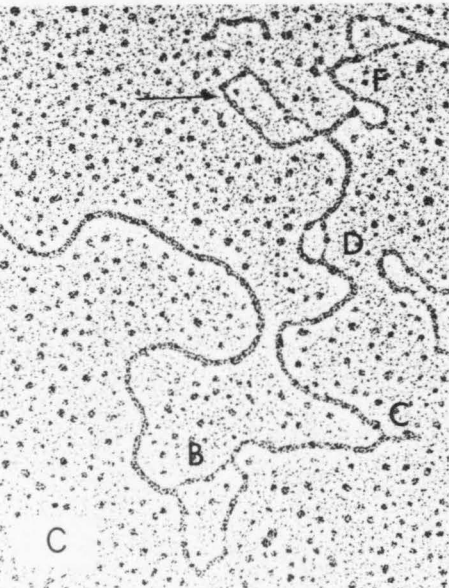
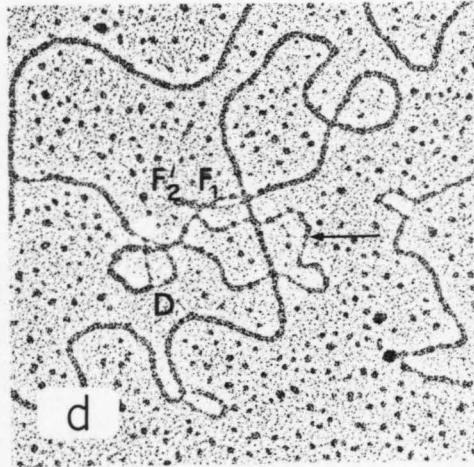
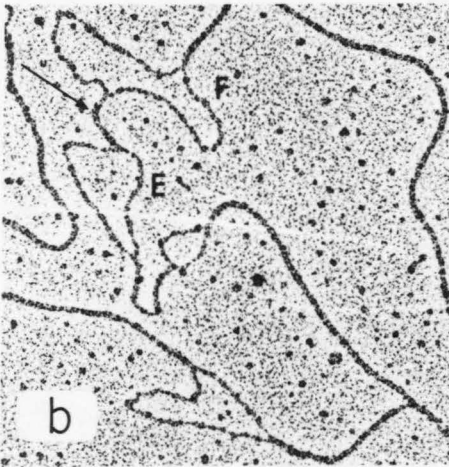
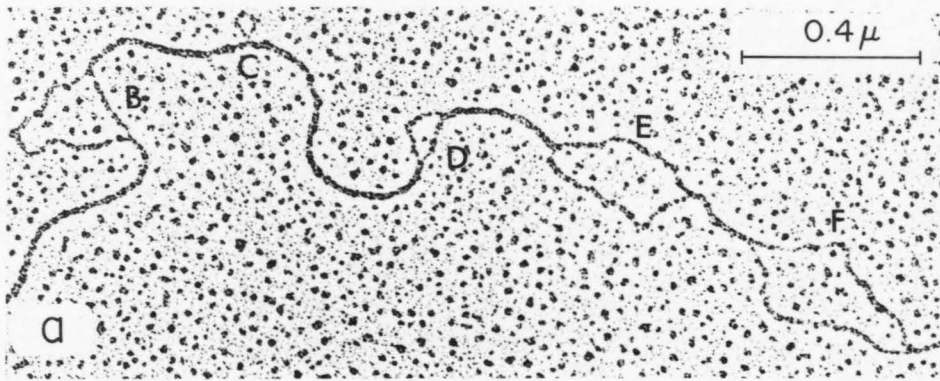
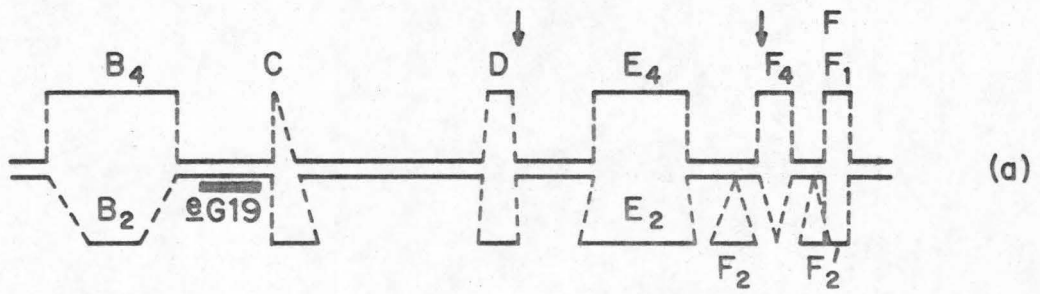


Fig. 5. Schematic representation of the loop patterns between T2 and T4 tRNA deletion mutants. The colored areas represent size and map position of the deletions.

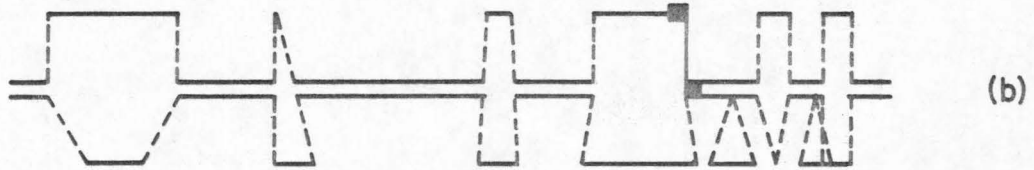
- (a) T2/T4 heteroduplex around tRNA genes. The two arrows indicate the extreme limits of the tRNA gene clusters.
- (b) T2/T4 $\text{psu}_b^- \Delta 8$ heteroduplex. Glycine- and ser-tRNA genes are deleted in T4 $\text{psu}_b^- \Delta 8$ (Wilson *et al.*, 1972a).
- (c) T2/T4 $\text{psu}_b^- \Delta 27$ heteroduplex. Band 2-, gly- and ser-tRNA genes are deleted in T4 $\text{psu}_b^- \Delta 27$.
- (d) T2/T4 $\text{psu}_b^- \Delta 119$ heteroduplex. Glycine- and ser- and leu-tRNA gene are deleted in T4 $\text{psu}_b^- \Delta 119$.
- (e) T2/T4 $\text{psu}_b^- \Delta 33$ heteroduplex. All the tRNA genes are deleted in T4 $\text{psu}_b^- \Delta 33$.
- (f) The results in (a) → (e) are presented all together in (f).

For the loops B, E and F the spacing between the surrounding duplex segments is equal to the length of the T4 single-strand, *i. e.*, B_4 , E_4 and F_4 . For loops, such as C and D, where the identity of the strand(s) is not known, the surrounding duplex segments are separated by the average of the two arms of a substitution loop or one-half of the length of a deletion type loop.

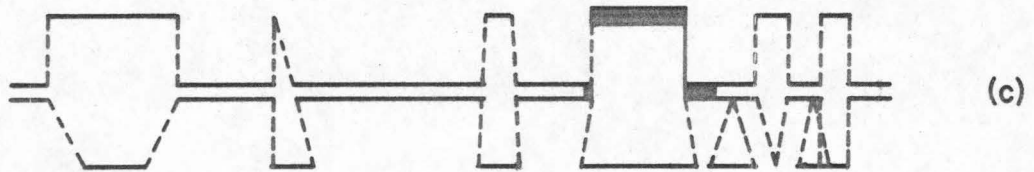
→ Clockwise



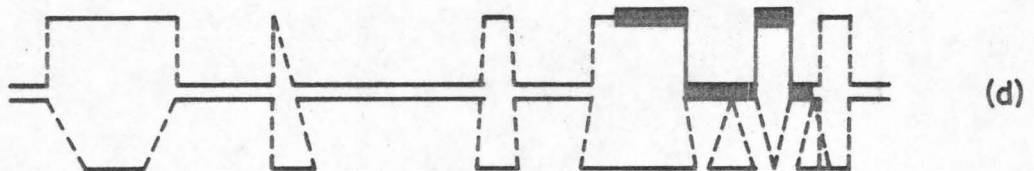
(a)



(b)



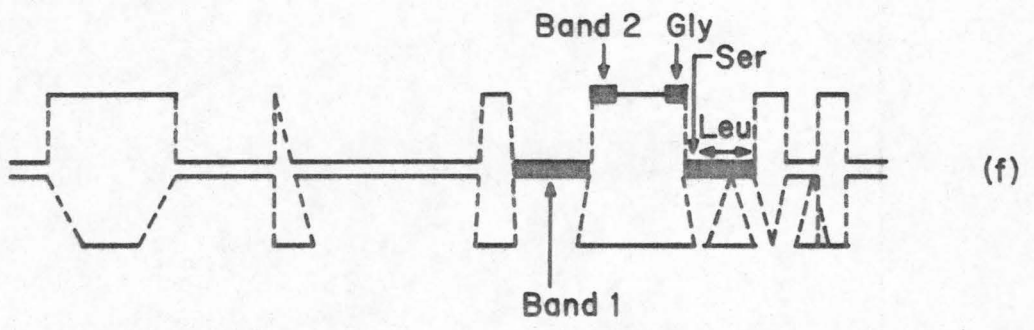
(c)



(d)



(e)

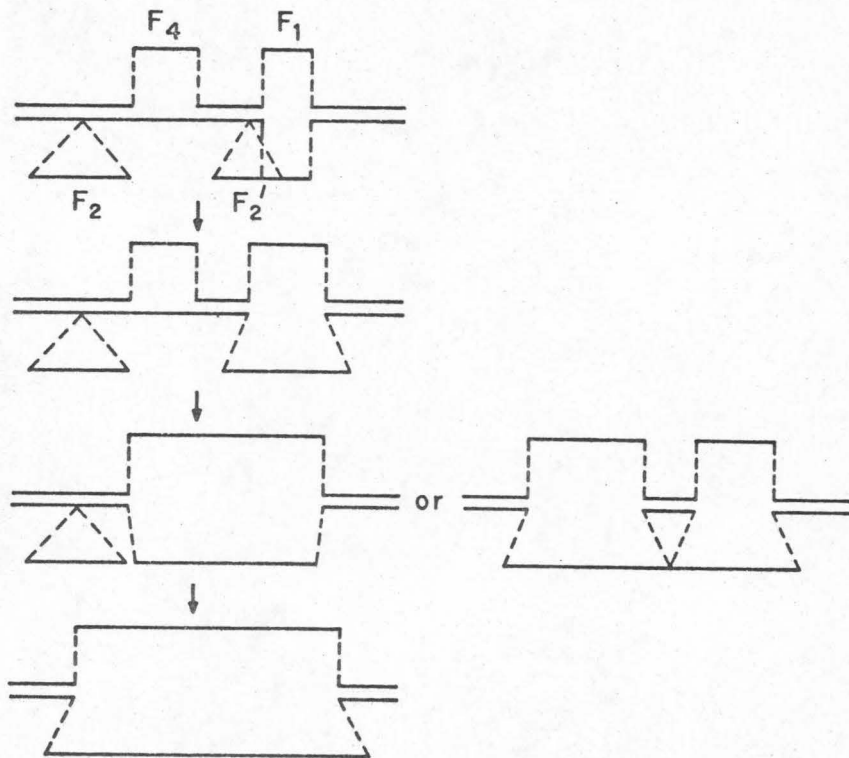


(f)

fewer than 10 nucleotides from a proline-tRNA. Ser-tRNA and some of the tRNAs in band 5 were not present in cells infected with T4 $\text{psu}_b^- \Delta 53$ (Wilson *et al.*, 1972a). These two observations imply that the pro-tRNA gene might be on the right side of the ser-tRNA gene, which is a homologous region in T2/T4.

The overall picture then is that some of the tRNA genes of T4 are homologous to genetic sequences in T2 and some are not.

The loop F has a variable structure, consisting of up to 4 small loops, as shown below. The single-stranded regions can



expand by opening up of the short double-stranded region between the loops until there is finally one large loop. The patterns of loop opening show that F_2' and F_4 , and F_2 and F_4 could not belong to the same DNA. The longer strand of the completely opened loop F seems to be T2 DNA. We therefore suggest that F_2 and F_2' correspond to T2 DNA, and F_4 to T4 DNA. It is fair to assume that the double-stranded regions between the loops F_2 and F_4 , and between the loops F_2' and F_4 are homologous (instead of only partially homologous), because in T4 DNA, a region of known perfect homology about 250 base-pairs long between rH88 and r638 deletion loops was observed to open up completely about 50% of the time (unpublished result) under the same denaturing conditions.

(iv) Homology in internal proteins

Three low molecular weight internal proteins (IP I, IP II and IP III) are present in relatively large amounts within the phage head. These basic proteins can bind to DNA at low salt concentrations, but are completely dissociated from DNA at high salt concentration. Black (1971) isolated mutants in the structural genes of each of the internal proteins. Mutants in IP II and IP III gene were amber. The single and double mutants grow normally on su^- bacteria. The three genes are arranged in the following order: -r48 II III e I v 57-. IP III undergoes assembly-dependent cleavage (Laemmli, 1971). T2 DNA does not direct the synthesis of any T4 internal proteins (Black and Gold, 1971). Black (personal communication through Dr. Wood) purified the internal proteins from several T4 lysozyme

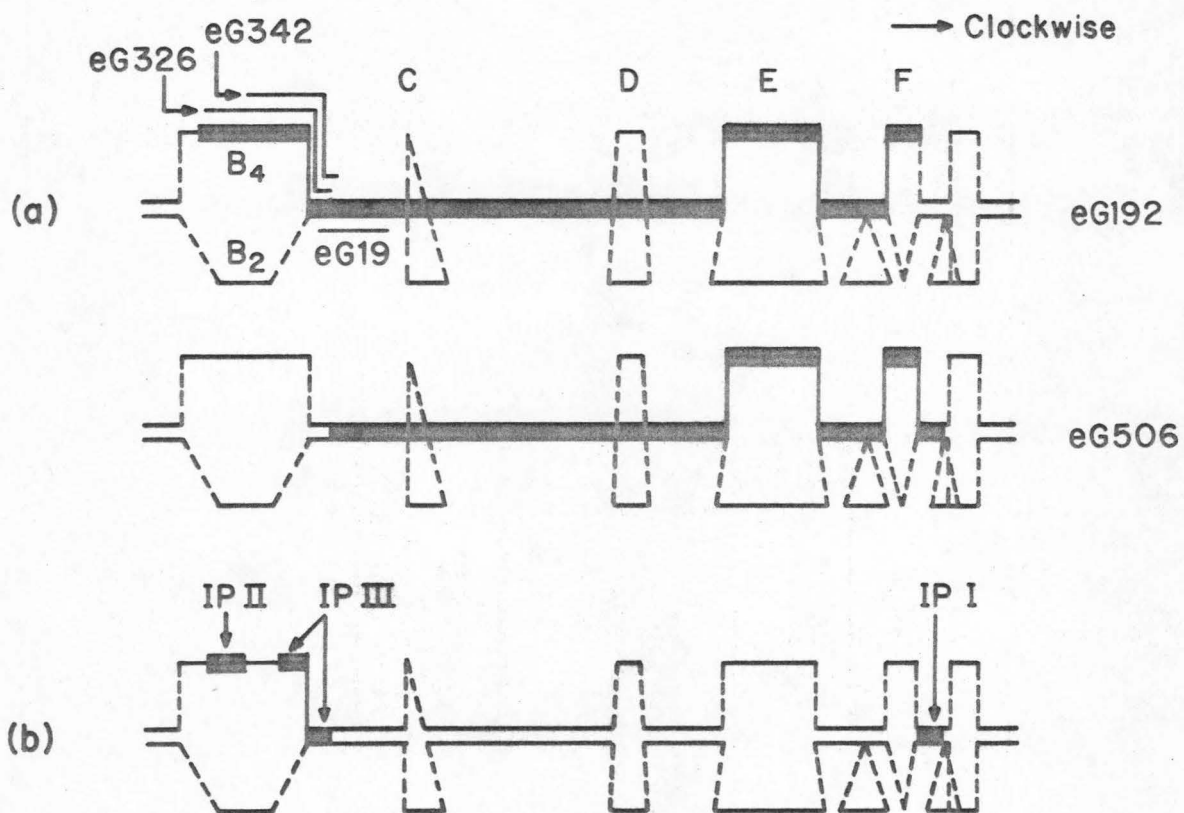
deletion mutant phages (eG192, eG506, eG326, eG342 and eG19) and looked for missing proteins. A physical map of these deletions has been constructed (Wilson et al., 1972a). Figure 6 presents the loop patterns of T2/T4 e deletion mutants which show how much T4 DNA is deleted and whether there are internal proteins missing.

The results show that the IP III gene is very close to the e gene, and the IP I gene is far from the IP II and IP III genes. IP I contains about 90 amino acids (Black and Ahmad-Zadeh, 1971), which correspond to 270 bases on the DNA template, in reasonable agreement with the size of the IP I gene on the map. IP III consists of about 160 amino acids (480 base-pairs) and its gene is adjacent to the e gene. Thus one can map the IP III gene accurately. A spacer of about 300 bases is between the IP II gene (220 base-pairs) and the IP III gene. The results show that the gene for IP II is completely non-homologous between T2 and T4; gene for IP III contain homologous and non-homologous segments. The IP I gene seems to be homologous. In T2, the sum of the B₂ loop (480 bases) and the overlapping region (180 base-pairs) between eG342 and eG19 is barely large enough to correspond to the template for the synthesis of IP II and IP III. It is also possible that the IP II and IP III genes are smaller in T2, since polyacrylamide gel patterns of the T2L internal proteins showed that they have mobilities different from those of T4 internal proteins (Black and Ahmad-Zadeh, 1971). The internal proteins in T4 are dispensable because T4 deletion mutants in one or two of these genes give viable particles.

Fig. 6. (a) Schematic representations of the loop patterns of T2/T4BeG19, T2/T4BeG326, T2/T4BeG342, T2/T4BeG192 and T2/T4BeG506 heteroduplexes. Dark areas and lines indicate the sizes and ends of the deletions.

(b) Map positions of IP I, IP II, and IP III in the T2/T4 heteroduplex.

(c) The table shows an internal protein(s) missing in each lysozyme deletion mutant. These results obtained by Dr. Black, were provided to us by Dr. Wood ("+", present; "-", absent).



(c)

	IP I	IP II	IP III
eG192	+	-	-
eG506	-	+	+
eG326	+	-	-
eG19	+	+	-
eG342	+	+	-

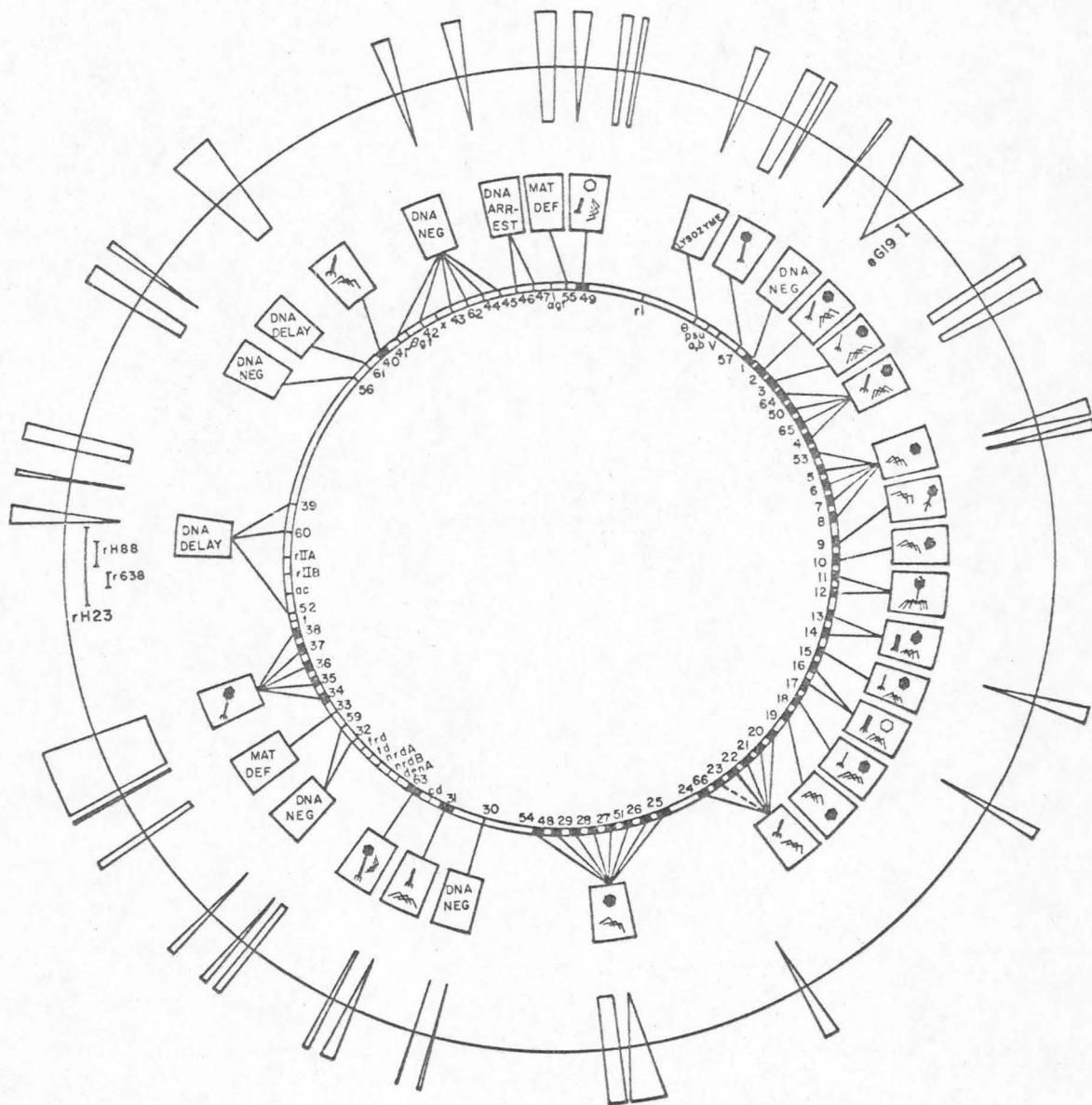
(b) The T4/T6 Heteroduplex

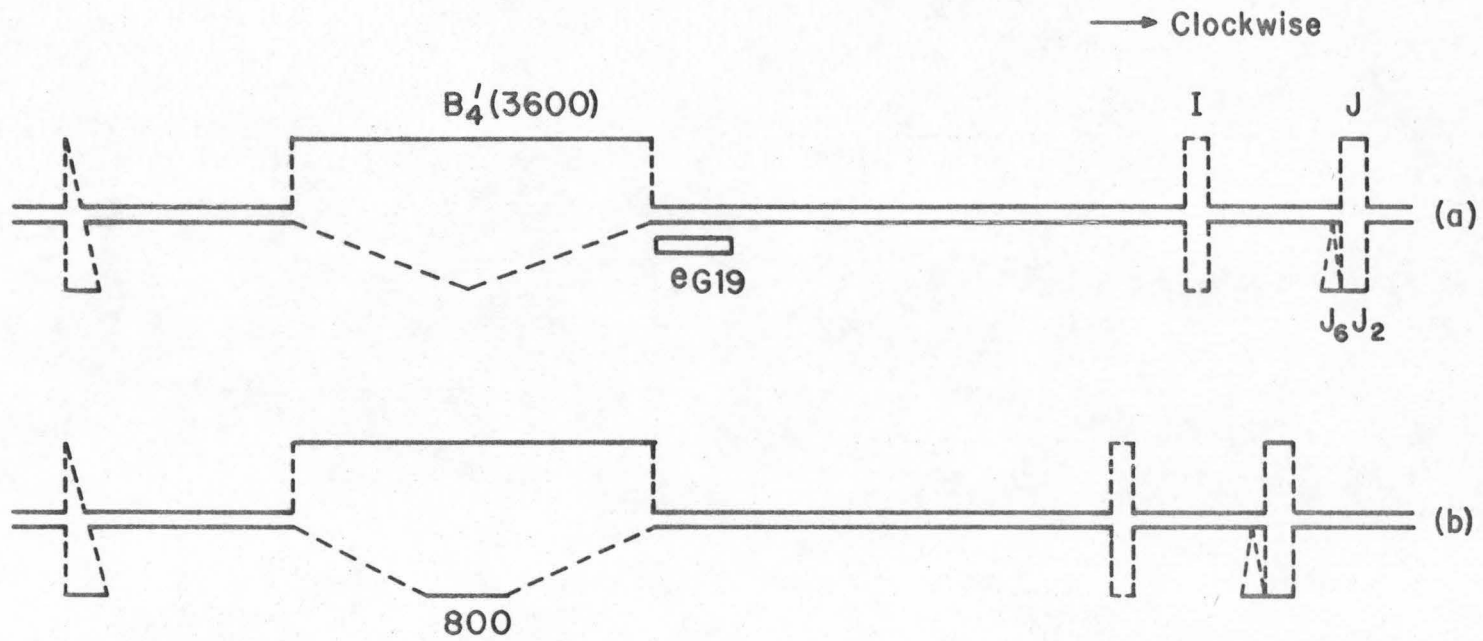
The heteroduplex T4/T6 map has been constructed and oriented in a manner similar to the one described previously for T2/T4 (Fig. 7). Eighty-eight per cent of T4 DNA is homologous to T6 DNA. The rII and lysozyme genes are homologous. Some of the loop patterns are similar to those observed in the heteroduplex T2/T4.

A schematic representation of the loop patterns around the e gene is shown in Fig. 8. In the heteroduplex T4BeG19/T6, we have observed a substitution (3600 bases, 800 bases) which is absent in wild type T4/T6. The size of the eG19 deletion is 700 bases and the double-stranded region between loops I and B₄' (3600 bases) was decreased by the size of this deletion in T4BeG19/T6. Thus the right end of the eG19 deletion must start within the double-stranded region near the loop B₄'. Also we know loop B₄' consists of T4 DNA because its size was unaffected by the presence of the eG19 deletion.

The host range region (part of gene 37 and all of gene 38) is heterologous, as is the rest of gene 37. In contrast, the latter region is partially homologous in the T2/T4 system. This observation is consistent with genetic result that the products of genes 37 and 38 from T4 and T6 are incompatible (Russell, 1967). The two strands of the host range loop are about equal in length, indicating that there is no large difference in the size of the respective genes 37 and 38.

Fig. 7. The T4/T6 heteroduplex map oriented with respect to the T4 genetic map. This heteroduplex map was oriented by using three rII deletion mutants of T4 and confirmed by using the eG19 deletion mutant of T4.





45

Fig. 8. Schematic representation of the loop patterns of T4/T6 (a) and T4BeG19/T6 (b) heteroduplexes around the e gene. Size of the loops is given in base-pairs.

A map of the tRNA gene cluster was obtained by forming the heteroduplexes T4psu_b⁻Δ27/T6 and T4psu_b⁻Δ33/T6. The loop patterns observed in these heteroduplexes are shown in Fig. 9. The band 1-, band 2-, leu-, and probably pro-tRNA genes are homologous. Since loop I is present in only 50% of the T4/T6 heteroduplexes and is somewhat variable in size, we don't know whether loop I is an AT-rich or a partially homologous region. If the latter possibility is correct, the gly- and ser-tRNA genes may be non-homologous.

The IP I gene was mapped in a homologous region (Fig. 9-(d)) by comparing loops J₁ and J₆ in T4/T6 with loops F₁ and F₂' in T2/T4. It seems that loop J₆ is equivalent to F₂' and loop J₁ to F₁. If this is true, loop J₆ comes from T6 DNA. The map position for the IP II and the IP III genes in T4 is the loop B₄' in the T4/T6 heteroduplex, suggesting that in T6 either there are no genes corresponding to the T4 IP II and IP III genes or they map elsewhere.

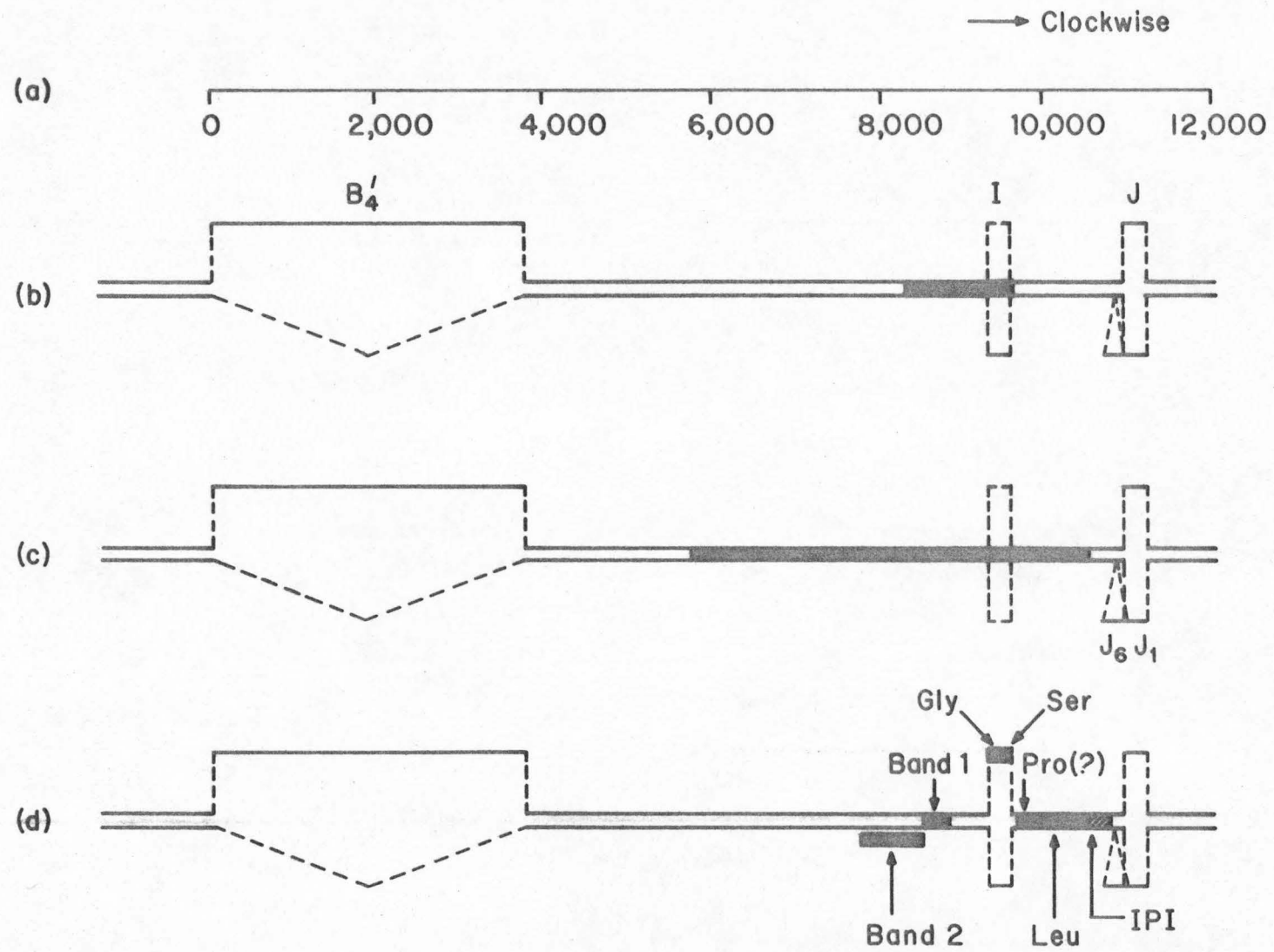
(c) The T2/T6 Heteroduplex

The T2/T6 heteroduplex map is shown in Fig. 10. Eighty-nine per cent of the heteroduplex appears double-stranded. It seemed probable that the largest substitution loop in this map would be the host range region. Unfortunately, there was no immediate way available to orient the T2/T6 map with respect to the two other heteroduplex maps, T2/T4 and T4/T6.

To make an orientation possible, we introduced rII deletions (rH23, rH88 and r638) into T2 by crossing T2 to T4rII deletion

Fig. 9. Schematic representation of the loop patterns around tRNA genes in the following heteroduplex molecules:

- (a) Scale in base-pairs.
- (b) T4 $\text{psu}_b^- \Delta 27$ /T6. Band-2, gly- and ser-tRNA genes are deleted in $\text{psu}_b^- \Delta 27$.
- (c) T4 $\text{psu}_b^- \Delta 33$ /T6. All the tRNA genes are deleted in $\text{psu}_b^- \Delta 33$.
- (d) Map position of each tRNA gene on T4/T6 heteroduplex. IP I gene is also mapped. Some results obtained in the T2/T4 system were used to locate tRNA genes on T4/T6 heteroduplex.



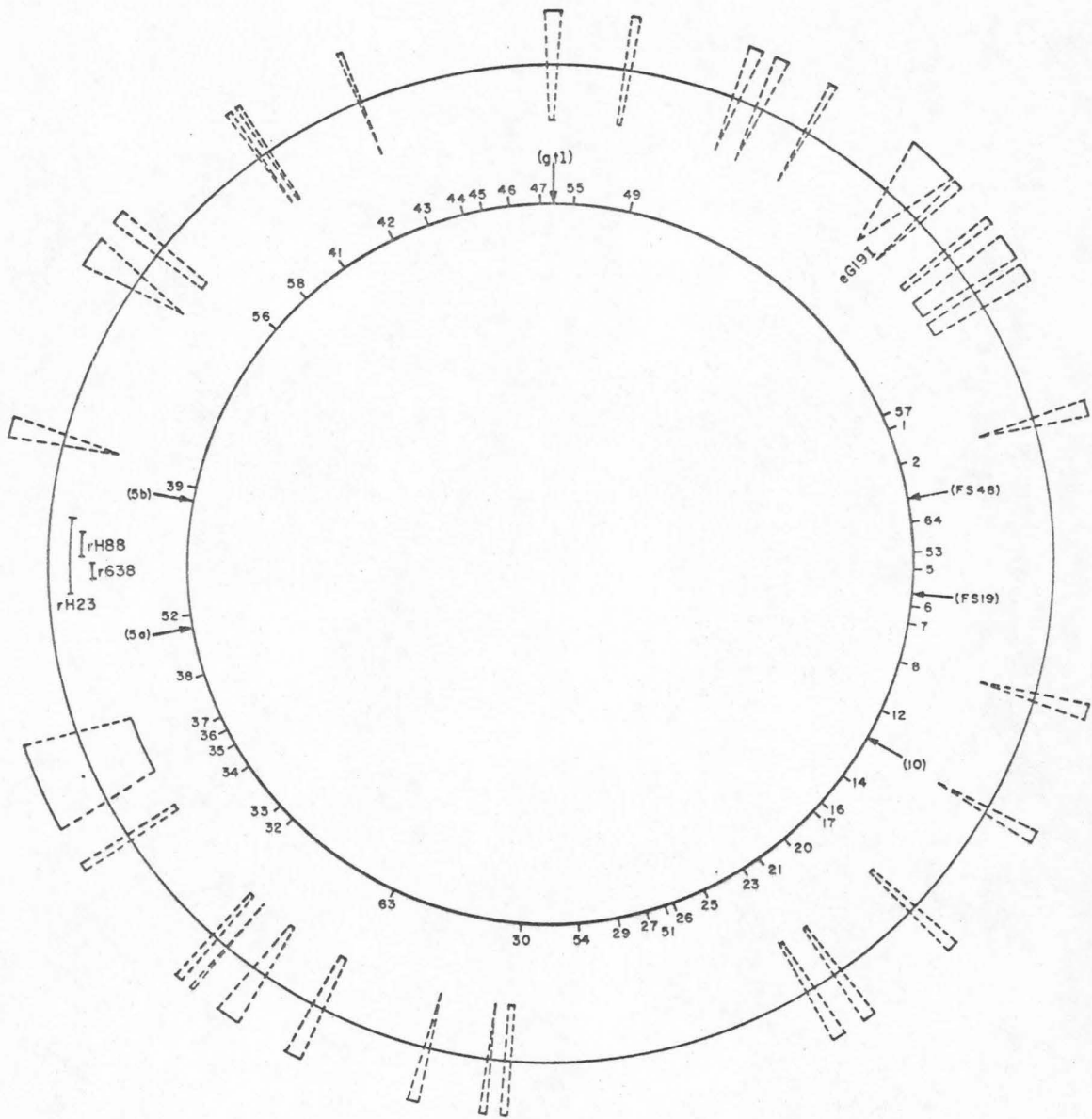


Fig. 10. The T2/T6 heteroduplex map with T2 genetic map (Russell, 1967).

mutants. The characteristics of the original T4rII deletions are summarized in Table 1. To prevent the markers of T2 from being partially excluded (which they normally would be in a mixed infection with T4 (Russell, 1967)) the T4rII deletion mutants were exposed to UV radiation sufficient to give 20 lethal hits per phage. The input ratio of T2 to any T4rII deletion was 10:1 except in the case of T4BrH23, where the ratio was 1:1. The progeny from these crosses were plated on S/4 from which several r-type plaques were picked and tested for the characteristics of the original deletions by complementation (T2rH88-1, T2r638 and T2rH23). T2rH88-1 was back-crossed to T2 to make it as isogenic as possible with T2 (T2rH88-2).

Table 1

Characteristics of the original T4rII deletions

	rIIB point mutant			rIIA point mutant		
	HB232	EM84	NT332	HB118	HB122	EM640
rH88	c	c	c	+	-	-
r638	-	-	-	c	c	c
rH23	-	-	-	-	-	-

c: complementation

+: recombination

-: neither complementation nor recombination
(indicating that the deletion overlaps
the point mutant).

DNA from these phages was examined to see how many T4 genes were picked up. Figure 11 is a schematic representation of the loop patterns of the heteroduplex T2rH88-1/T2, T2rH88-2/T2 and T2r638/T2. In general, these DNA heteroduplex molecules looked like T2 except in 3 or 4 regions and the rII deletions appeared where they were expected. At about 10 o'clock (loop M) T2rH88-2 lost a piece of T4DNA which appeared in T2rH88-1. A loop at 12 o'clock (loop N) on each circle was mapped by its disappearance in the heteroduplexes T2rH88-1/T4rH88, T2rH88-2/T4rH88 and T2r638/T4r638. An increase in the double-stranded region between the closest loops on either side of the loop indicates that loop N corresponds to T4 DNA. Loop O in the T2/T2rH88 heteroduplexes is not identical to loop P in T2/T2r638. From heteroduplexes with T4, one finds that both loops O and P come from T4 DNA. Also, by forming heteroduplexes with T6, we have shown that loop O in T2/T2rH88 appears in T4/T6 but not in T2/T6. Thus T4 has a region of 600 base-pairs long which T2 and T6 lack. On the other hand, loop P in T2/T2r638 appears in T2/T6 but not in T4/T6, showing that T4 and T6 contain a region of 1000 base-pairs long which T2 lacks. We don't understand why these 3 or 4 pieces of T4 DNA are consistently introduced to T2.

The recombinant phage T2rH23 contains very many T4 genes, including the rH23 deletion. It is homologous to T2 throughout the tail fiber gene. It was not used further in our experiment.

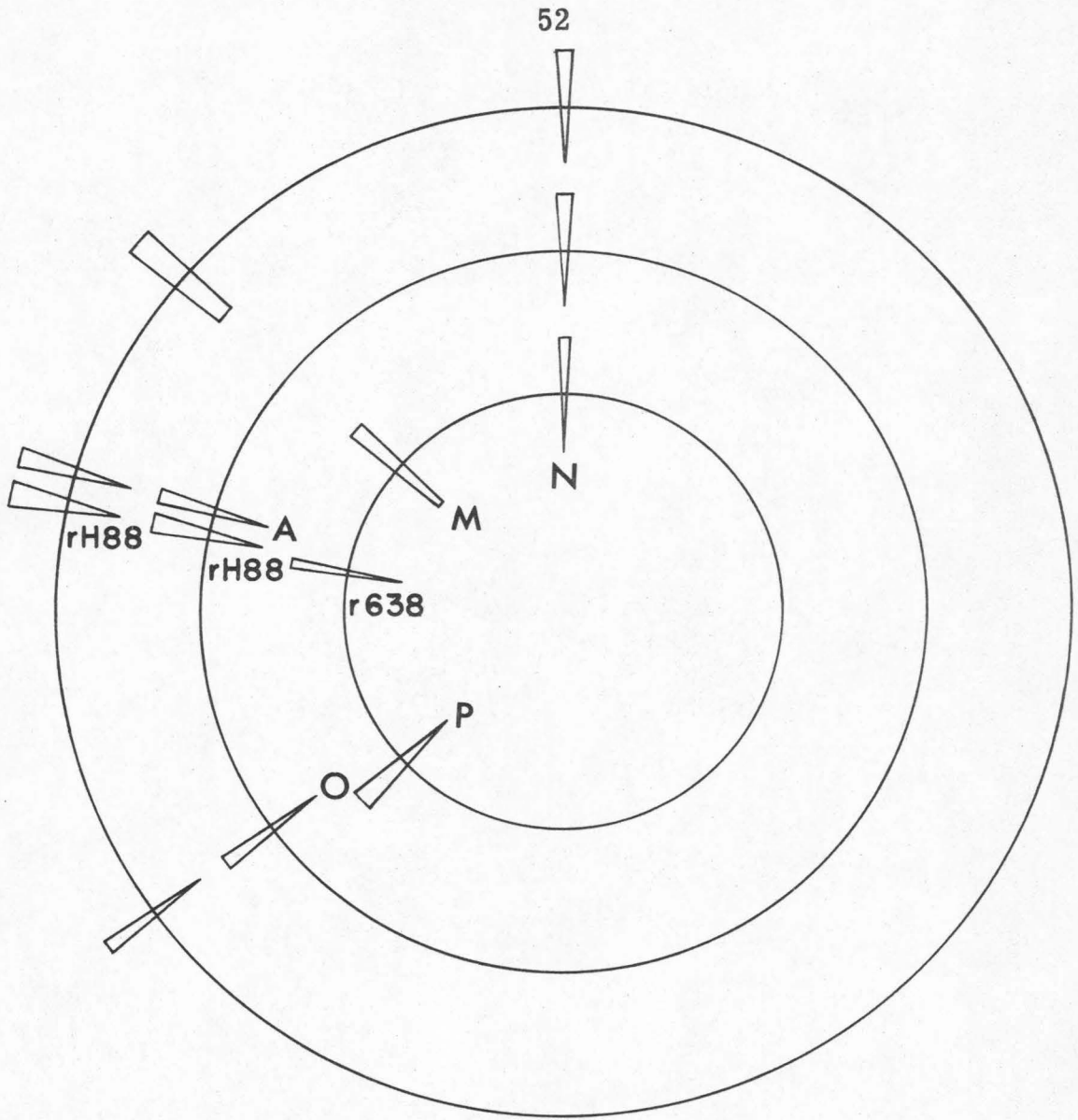


Fig. 11. Heteroduplex maps of T2/T2rH88-1,
 T2/T2rH88-2 and T2/T2r638.

All three rII deletions are not needed to orient the T2/T6 heteroduplex map, because each rII deletion mutant contains several other markers as well. The pattern of the loops around the rII region in the T2rH88-1/T6 heteroduplex is shown in Fig. 12. The regions of loops A and M appearing in both T2/T4 and T4/T6 map at homologous region in T2/T6. The direction loop A \rightarrow loop rH88 corresponds to the rIIA \rightarrow rIIB direction (see also Fig. 2). This information allows orientation of the T2/T6 heteroduplex map, as shown in Fig. 10. The rII gene is homologous. The largest non-homologous region is that bearing genes 37 and 38. The combined size of genes 37 and 38 in T2 is greater by 900 base-pairs than that in T4. In T2/T6, one strand of the host range loop is larger by 1000 bases than the other. If the longer strand corresponds to T2 DNA, then one would expect to observe a symmetric loop in T4/T6, which is indeed the case. We therefore conclude that the size of genes 37 and 38 in T2 is larger by about 1000 base-pairs than that in T4 and in T6. The electron microscopic observation that there is less DNA homology in gene 37 between T2 and T6 and between T4 and T6 than between T2 and T4 seems to be inconsistent with the genetic results that P37 and P38 are more compatible between T2 and T6 than between T2 and T4 (Russell, 1967). Perhaps non-homology in DNA sequences does not necessarily imply incompatibility of the gene product.

The position of the e gene can be deduced on the T2/T6 map by comparison with the T2/T4 and the T4/T6 heteroduplex maps. Figure 13 shows loop patterns around the e and the tRNA genes in

Fig. 12. Schematic representation of the loop patterns of T2/T6 (a) and T2rH88-1/T6 (b) heteroduplexes around the rII region. The direction loop A \rightarrow loop rH88 corresponds to the rIIA \rightarrow rIIB cistron. The shorter strand of the host range loop is labelled as H6, because that seems to be T6 DNA. The other strand is labelled as H₂' to avoid confusion with H₂ loop in Fig. 4. The size of the loops is given in base-pairs.

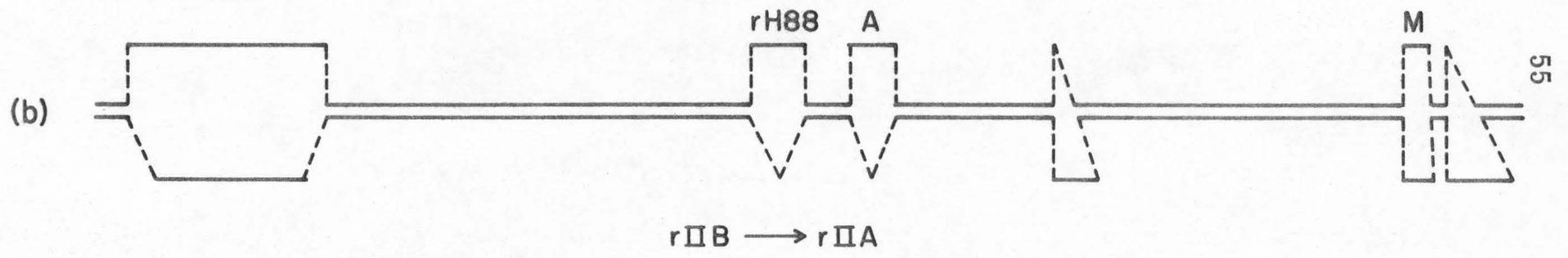
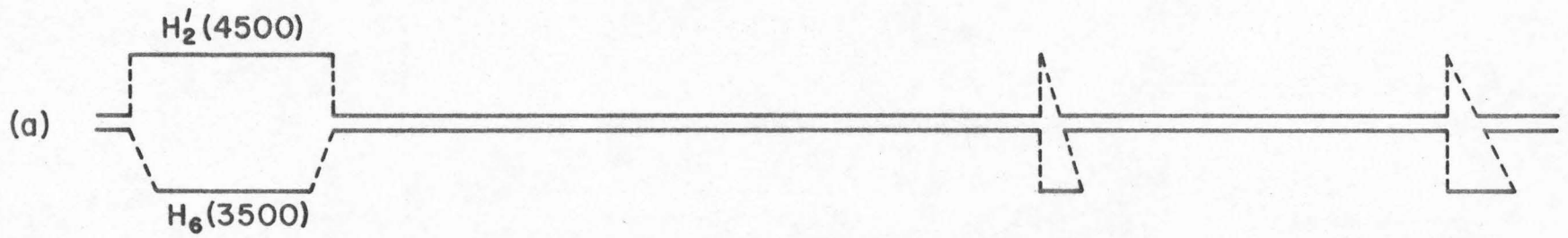
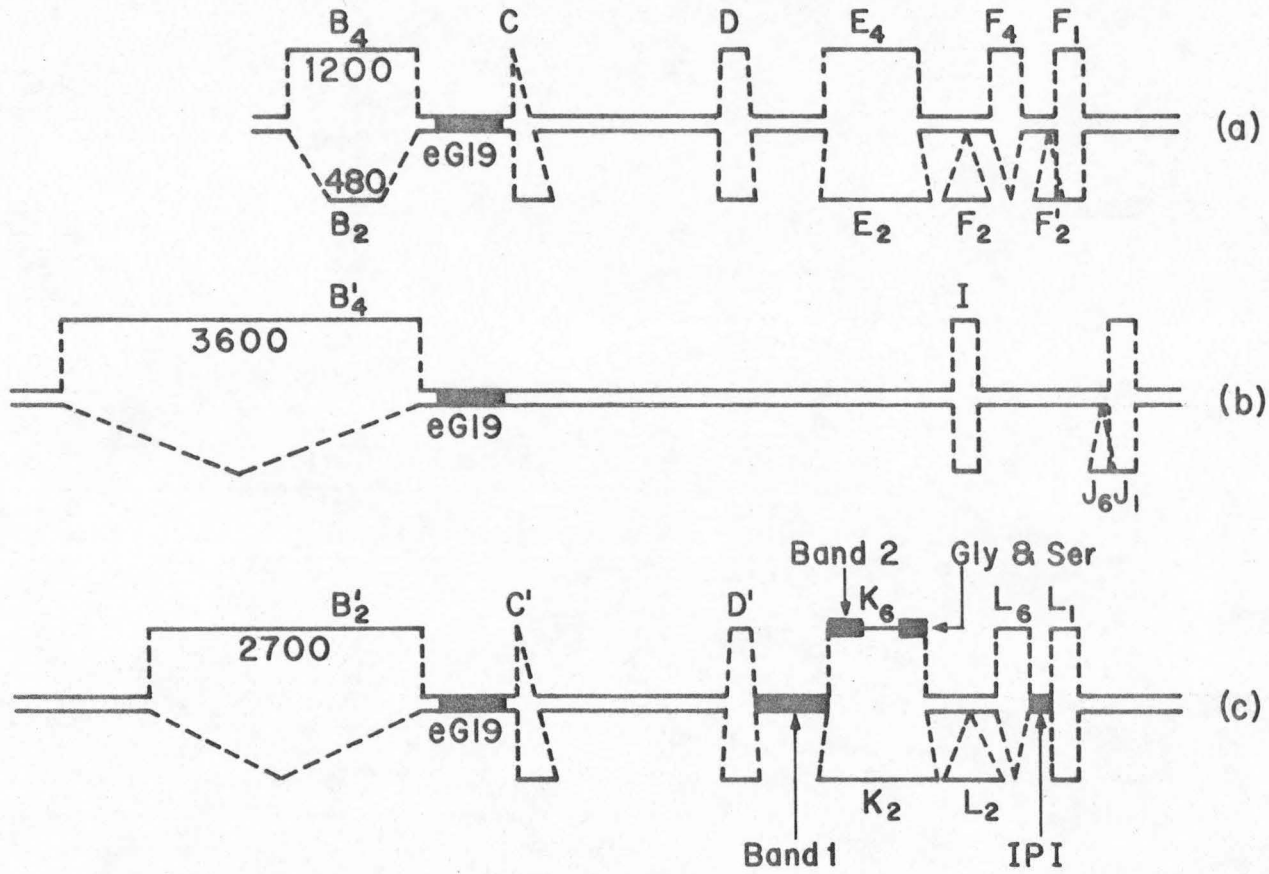


Fig. 13. Schematic representation of the loop patterns of T2/T4 (a), T4/T6 (b), and T2/T6 (c) heteroduplex around the e, the tRNA and the internal protein genes. The shorter strand of the loop K is likely to be T6 DNA, because shorter strand of the loop E is known to be T4 DNA and the sequence for the loop E is homologous in T4/T6. Similarly the L₂ and L₆ loops seem to be T2 and T6 DNAs, respectively. The loops L₁, L₂ and L₆ open up together in a similar fashion to that of loop F.

→ Clockwise

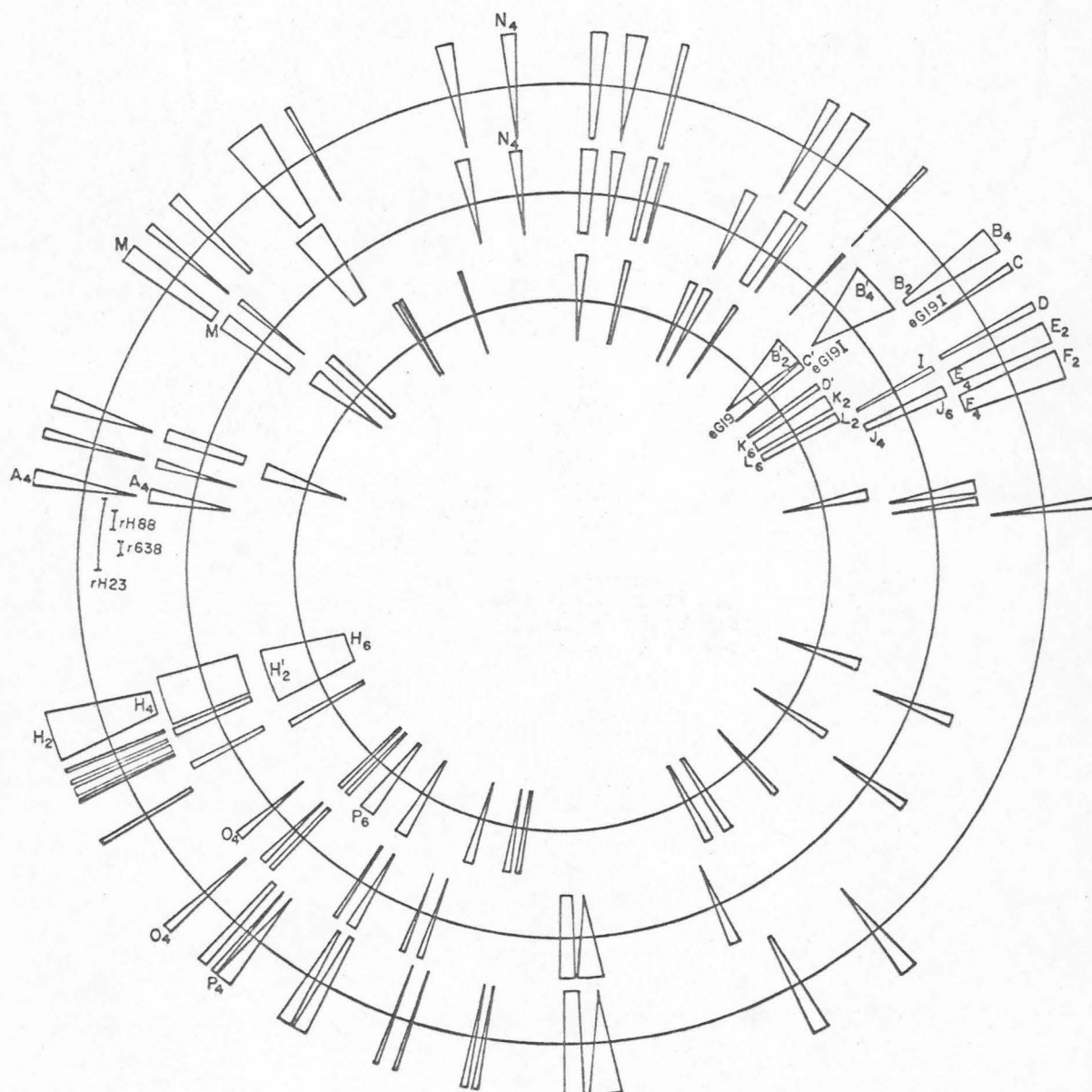


each heteroduplex. The T2/T4 map contains a substitution loop B with T4 and T2 arms of length 1200 and 480 bases, respectively, just counterclockwise of the eG19 region. In T4/T6, there is a large loop of 3600 bases at this site. In T2/T6, there is a loop (B_2') of 2700 bases. The simplest interpretation is that the B region is entirely missing in T6; the eG19 region therefore maps as indicated in Fig. 13.

One can approximately map the tRNA genes in T2/T6 in a manner similar to the one described for the e gene mapping. The lengths of the double-stranded regions between loops B and C, C and D, and D and E in T2/T4 are equal to those between loops B_2' and C' , C' and D' and D' and K respectively in T2/T6. Therefore the band 1-tRNA gene is homologous, and the band 2- and gly-tRNA genes are non-homologous. The ser-tRNA gene could be heterologous because the size of the loop K is slightly larger than that of the loop E. The situation for the leu-tRNA is uncertain.

The three heteroduplex maps (T2/T4, T4/T6 and T2/T6) were oriented by matching the rII region relative to one another (Fig. 14). All the loops we have discussed were labelled "loops A P". Where the identity of the strand is known, subscripts 2, 4, and 6 were used to represent T2, T4 and T6 DNAs, respectively.

Fig. 14. The T2/T4, T4/T6, and T2/T6 heteroduplex maps oriented by matching the rII region relative to one another. All the loops we have discussed were labelled. Subscripts 2, 4, and 6 represent T2, T4 and T6 DNAs, respectively.



Outer Circle: T2/T4 Map
 Middle Circle: T4/T6 Map
 Inner Circle: T2/T6 Map

Discussion

We have examined the T2/T4, the T4/T6 and the T2/T6 heteroduplex molecules in the electron microscope. Heteroduplex loop patterns of substitution and deletion loops were oriented with respect to the T4 genetic map by using rII and e deletion mutants. T-even DNAs are such large molecules that it is not easy to get complete heteroduplex molecules in which all the loops are measurable, because there is non-specific interaction between single-strand loops. Therefore the heteroduplex maps were constructed from complete molecules or from broken molecules by superimposing one on another.

Genes rII, D, ac, 52 and e are in homologous regions in all heteroduplexes. T2 and T4 seem to be homologous in early genes 43 and 47. Generally, the morphogenesis genes (from gene 57 to gene 24) have a high degree of homology. Gene 38 and the host range determinant are non-homologous in T2, T4 and T6. Genes 35 and 34 seem to be highly homologous in all cases. The overall homology is greater than 85% for all heteroduplexes. We infer from the similarity of loop patterns in T4/T6 with those in T2/T4 that T2 and T6 are the most closely related species. This observation agrees with the biochemical and genetic results obtained by other workers.

Cowie et al. (1971) performed DNA-DNA hybridization studies using labelled DNA fragments from one type of T-even phage and

excess unlabelled DNA fragments from another type of T-even phage. (The DNA fragments were 300-400 nucleotides long.) From hydroxyapatite column chromatography of heteroduplex DNAs, they have estimated the degree of homology and the lowering of melting temperature (Table 2). The average homology in T2/T4, T4/T6 and T2/T6 were calculated to be 87%, 84% and 91%, respectively. Our estimates based on electron microscopic observation are 87%, 88% and 89% for T2/T4, T4/T6, and T2/T6, respectively. Table 2 shows that the T2/T6 heteroduplex is the most stable to thermal melting. They therefore suggested that T2 and T6 are the most closely related and that T4 and T6 are the most distantly related species.

Table 2
DNA-DNA hybridization of T-even DNAs

Labelled DNA fragment	Unlabelled DNA fragment	Per cent homology	ΔT_m
T2	T6	95	1.3
T6	T2	87	1.5
T2	T4	91	2.3
T4	T2	82	2.5
T4	T6	83	4.5
T6	T4	85	4.5

Data are drawn from Cowie, Avery and Champe (1971).

Both tRNA and internal protein genes map around the e gene. The tRNA genes are non-essential for the growth of the phage on the laboratory strain of E. coli. We mapped a few tRNA genes in T2/T4, T4/T6, and T2/T6. The results are summarized in Table 3. The tRNA genes of T4 and T6 are the most homologous. It might be possible that some of the tRNA genes in T2 have been inverted with respect to those in T4 and T6. The IP II gene maps in a non-homologous region in T2 and T4 (to the left side of the e gene), but IP III gene of T2 and T4 maps in a homologous and non-homologous region. The gene for IP I in T2, T4, and T6 seems to be homologous. The IP II and IP III genes if they exist in T6 must map in some other part of the chromosome.

Table 3

Homology in tRNA genes between T-even phage

	T2/T4	T4/T6	T2/T6
Band 1	+	+	+
Band 2	-	+	-
Gly	-	-	-
Ser	+	-(?)	-(?)
Leu	+(?)	+	+(?)

+: homologous

-: non-homologous

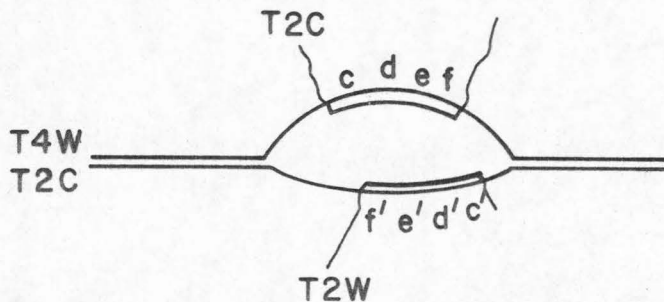
?: uncertain

All the heteroduplex molecules were mounted at $T_m - 23^\circ$. When a duplex segment between two substitution loops is only partially homologous, its length is frequently more variable than for an exactly homologous segment. For most of the segments in the heteroduplexes studied here, the standard deviations in length were in the range expected for exactly complementary sequences. A known region of perfect homology about 250 base-pairs long between T4BrH88 and T4Br638 was observed to open up completely about 50% of the time. There are several possible explanations: (1) the region is AT-rich; (2) the denaturation conditions in hyperphase and hypophase were not exactly the same; thus the heteroduplexes were not spread under the equilibrium conditions; (3) a shear force is applied perpendicular to the short double-stranded region during spreading; or some combination of these three effects.

There is some electron microscopic evidence for partial homology in part of gene 37 between T2 and T4 (Beckendorf *et al.*, 1972). The present studies do not add to this evidence. Furthermore, our observations do not give any definite information as to partially homologous sequences in other regions of the genome. The best way to study partial homology is to examine heteroduplexes spread at varying formamide concentrations, but this was not done as part of our studies.

In the heteroduplex formed between lambdoid phages or between T7 and T3, very few deletion type loops were found. Deletion loops of 1000 bases long (about an average gene size) appear

with very high frequency in T-even heteroduplexes, suggesting that some genes present in one phage are absent in the other, or a gene is substantially larger in one phage than in the other. Furthermore, the two strands of a substitution loop are frequently different in length (see Fig. 14). We therefore suggest that during evolution the DNA molecules of the T-even phages may have undergone deletions and substitutions as well as single, random base changes. It is also possible that substitution loops arise because sequences of T4 DNA, for example, are inverted relative to T2 DNA. This could be tested in the following way. T2/T4 heteroduplexes formed from unsheared DNA are hybridized with sheared T2 or with T4 DNA (1500 base-pairs long). If a particular non-homologous sequence is inverted, we would observe that both strands of the substitution loop are hybridized with small pieces of DNA and appear double-stranded. If it is not inverted, only one strand of the loop is hybridized with sheared DNA, so that we can assign which strand of the loop comes from T2 or T4 DNA.



A more accurate heteroduplex map could be constructed utilizing amber mutants in various genes of T2 or T4. For example, a triple mutant of T4, containing amber mutations in genes 55 and 49 and a temperature sensitive mutation in gene 47 could be crossed to wild type T2 and selection made for a predominant T4 progeny phage containing the genes 55 and 49 of the T2 parent and 47 of T4. Such progeny could be selected easily from a cross where the T2 parent had been subjected to a large dose (20-25 lethal hits) of UV irradiation. This progeny phage DNA would then be hybridized to T2 DNA and the loop patterns in the resulting heteroduplex molecules analyzed. If genes 55 and 49 are in a region homologous in T2 and T4, then the same loop patterns should be observed in this heteroduplex molecule as is observed when wild type T4 and T2 DNA are observed. If, on the other hand, the genes are in a region of non-homology, a heteroduplex molecule of the selected progeny with T2 would lack a loop(s) normally found at that region in T2/T4 heteroduplexes. This kind of analysis can be extended to other regions where loops occur in the heteroduplex map.

Large deletions have been isolated from T4 strains carrying a tandem duplication of the rII region. Those deletion mutants give minute plaques (Homyk and Weil, 1971), and fall into 4 recombinational classes. One is a silent region between genes 39 and 56, a second is between genes 31 and 32 whose functions are known, but non-essential genes (Ray, Sinha, Warner and Snustad, 1972). The other 2 classes are unknown. Homyk and Weil are mapping the

deletions by electron microscopy to locate silent regions and non-essential genes on the T4 chromosome (personal communication). These results will be helpful to interpret our heteroduplex maps.

(d) Molecular Weight Determination of T-even DNAs by
Electron Microscopy

Cowie, Avery and Champe (1971) have predicted that the molecular weights of T4 and T6 DNAs are respectively 10 and 8% larger than that of T2 DNA. This prediction was based on unequal results obtained in DNA-DNA hybridization between labelled fragments from one type of T-even phage and excess unlabelled DNA fragments from another type of phage. For example, in the reaction of labelled T2 DNA with excess unlabelled T6 DNA, 95% of the T2 DNA was hybridized with T6 DNA. On the other hand, only 87% of labelled T6 DNA was hybridized with T2 DNA. To investigate these observations, we have measured the molecular lengths and genome sizes of T-even DNAs by electron microscopy.

Wild type hydrogen-bonded λ circular DNA was used as an internal length standard. Since the DNA was mounted in the presence of 40% formamide ($T_m - 23^\circ$), the cohesive ends of λ DNA were near their melting point and were always pulled apart during the mounting procedures. However, their ends were so close to each other that intact λ molecules were readily recognized. We take the molecular weight of λ to be 30.8×10^6 daltons. From the relative length, the following molecular weights for non-glucosylated DNA may be

computed: T2, 112×10^6 ; T4B, 112×10^6 ; T6, 113×10^6 (Table 4). These DNAs contain hydroxymethyl cytosine which is glucosylated to different extents (Lehman and Pratt, 1960). If we take the average sodium nucleotide weight of non-glucosylated DNA as 331amu, the correction factors for glucosylation of T2, T4 and T6 DNAs are 1.088, 1.103 and 1.147, respectively. After correction for glucosylation, the molecular weights of T2, T4 and T6 DNAs are 122×10^6 , 124×10^6 and 130×10^6 daltons. Therefore there is no difference in the molecular length of T-even DNAs, but their molecular weights are different due to unequal glucosylation.

Differences in the genome size among T-even phages, if any, can be determined in the following way. The T-even DNAs are circularly permuted and terminally repetitious (Thomas and Rubenstein, 1964; Streisinger, Emrich and Stahl, 1967). Upon denaturation and renaturation circular molecules with two single-stranded branches are formed (Thomas and MacHattie, 1964; Lee, Davis and Davidson, 1970). A schematic representation for the formation of such circular molecules is shown in Fig. 15. From the circular duplex region we can measure the genome size, and from the length of single-stranded branches, we can measure the size of the terminal repetition. In our experiments the relative amounts of circular and linear duplex species in the renatured population were about 20 and 80%, respectively.

Table 4

Molecular weight, genome size and size of terminal repetition
of T-even bacteriophage DNAs

	Molecular weight			Size of terminal repetition** ($\times 10^6$ daltons)	Size of genome† (nonglucosylated)	% Terminal repetition
	From length measurements†	Glucosylated	Lang*			
T2L	112 \pm 2	122 \pm 2	116	5.6 \pm 1.0	106 \pm 1	5.3 \pm 1.0
T4B	112 \pm 2	124 \pm 2	119	2.0 \pm 0.8	110 \pm 1	1.8 \pm 0.7
T4BrH23	—	—	—	4.4 \pm 3.4	107 \pm 1	4.2 \pm 3.2
T6	113 \pm 2	130 \pm 2	—	2.2 \pm 1.1	109 \pm 1	2.0 \pm 1.0

† Relative to $\lambda c_{26} = 30.8 \times 10^6$ daltons.

* Relative to T7 = 25.1×10^6 daltons (Lang, 1970).

** Relative to $\phi X174$ single-stranded = 1.7×10^6 daltons.

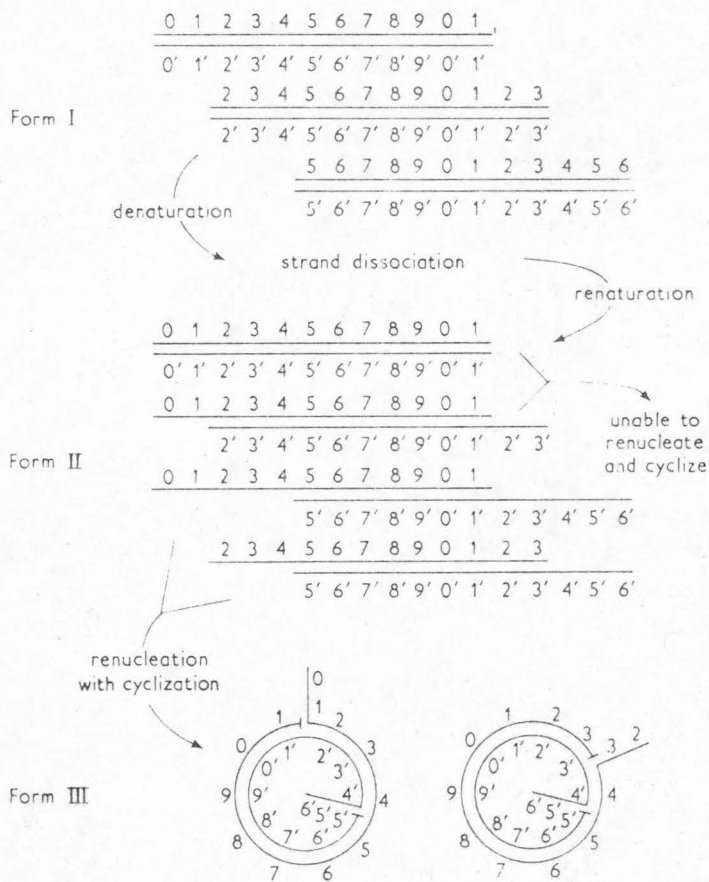


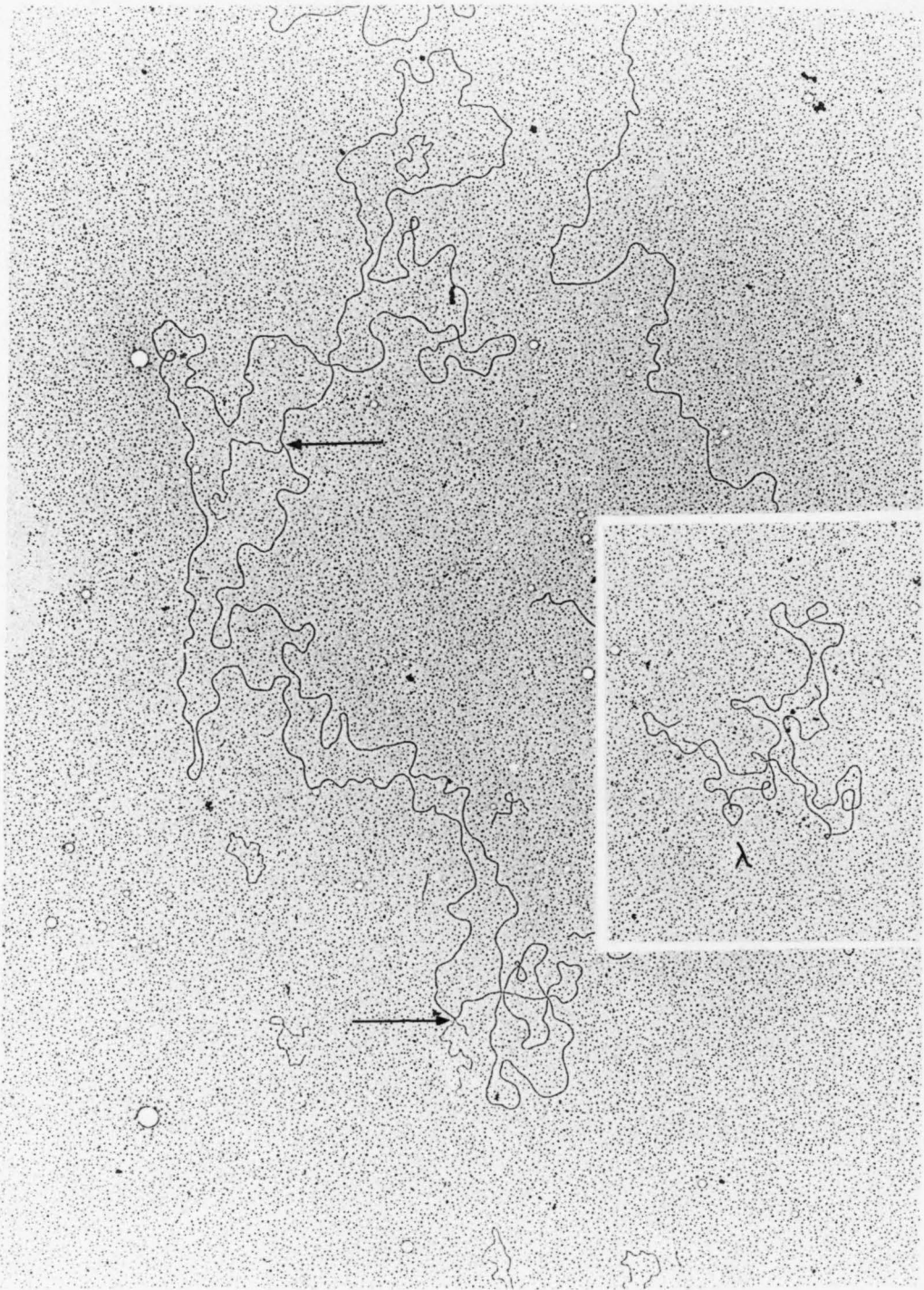
Fig. 15. Schematic representation for studying circularly permuted and terminally repetitious DNA. This figure is redrawn from Lee, Davis and Davidson (1970).

Plate 5 is an electron micrograph of a circular T2 homoduplex molecule. Two single-stranded branches representing terminal repetitions are indicated by arrows. One of the branches is forked as a result of single-strand branch migration as is generally observed for the terminal repetition branches of E. coli 15 phage homoduplexes (Lee, Davis and Davidson, 1970). In our work the observed ratio of unforked to forked branches in T4BrH23 homoduplexes was 3:7. The expected statistical ratio is $1:6600 \pm 5100$. This confirms the conclusion of Lee et al. (1970) that there is an intrinsic difference in free energy between an unforked and a forked branch contributing a factor of about $(3/7) (6600) \approx 2800$ to the equilibrium ratio between them.

The genome sizes of T2, T4 and T6 DNAs are measured as $106(\pm 1)$, $110(\pm 1)$ and $109(\pm 1) \times 10^6$ daltons, respectively, calculated for non-glucosylated molecules (Table 4). The genome sizes of T4 and T6 are greater than that of T2; in contrast, the terminal repetitions of T4 and T6 are smaller than that of T2. The discrepancy between Cowie et al. (1971) and our results can now be clarified. Cowie et al. assumed that the terminal repetitions of T-even DNAs are about the same, which is shown by our work not to be the case. Therefore they measured the genome sizes, instead of the molecular weights of T-even DNAs.

We estimate the size of the terminal repetitions as 5.3 ± 1.0 , 1.8 ± 0.7 , 4.1 ± 3.2 and $2.0 \pm 1.0\%$ of the non-repetitious region in T2, T4, T4BrH23 and T6, respectively. The standard deviations

Plate 5. Electron micrograph of T2 homoduplex molecule. Two single-stranded branches are indicated by the arrows. The small circular molecules in the background is single-stranded ϕ X-174 DNA. The insert is a λ molecule used as a length standard for double-stranded region.



for the size of terminal repetitions given above are larger than expected for homogeneous samples. The variation in size may arise, from breakage during preparation, or from a small natural variability in the amount of DNA packaged in the head. Let p be the fraction of each unbroken strand present in a sample of denatured DNA.

Renaturation takes place with equal probability for any two complementary strands. Then p^2 is the number fraction of renatured molecules between two unbroken strands. Experimentally 23% of the duplex molecules in a T4BrH23 homoduplex sample were circles. So $p^2 = 0.23$ and $p = 0.48$. Therefore 48% of the strands were unbroken. Let a be the average number of breaks per initial strand. The probability that a break will occur in a terminal repetition would be $2af$, where f is the fractional length of the terminal repetition. Since we know a is smaller than 1, and $f = 0.04$, $2af$ is smaller than 0.08. Thus we conclude that it is unlikely that the large variations are due to breakage in the terminal repetition. We therefore believe that the observed variability in the size of repetition for any one kind of DNA is due to natural variability in the length packaged.

Figure 16 shows size distributions of the terminal repetitions regions of T2, T4 and T4BrH23. None of the distributions displays a sharp peak, indicating that the terminal repetitions in T-even phages are heterogeneous in size. The terminal repetition of T4BrH23 (having a deletion of 4200 base-pairs long) is larger than that of wild type T4. It is believed that mature T4 phage particles,

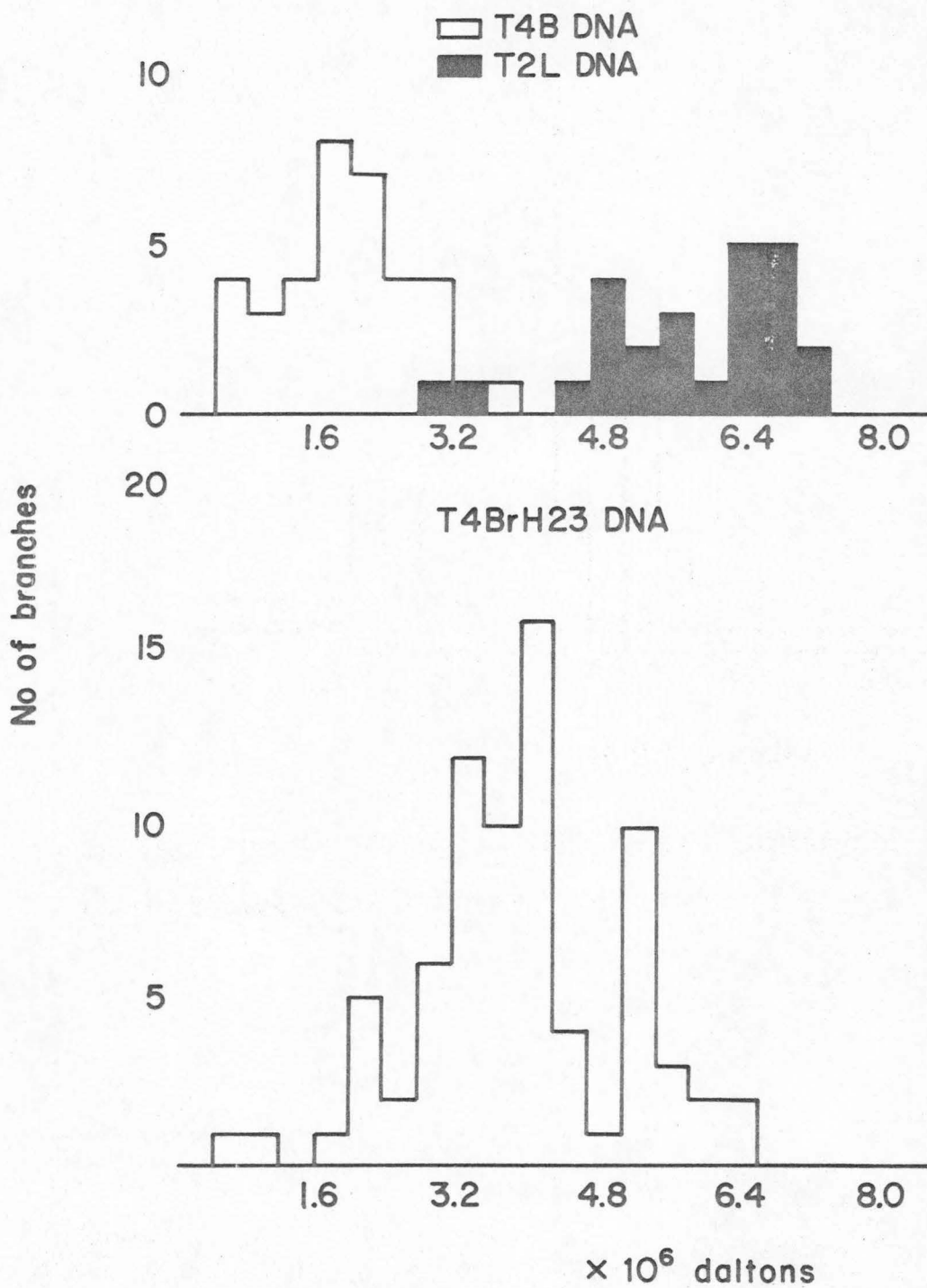


Fig. 16. Size distribution of the terminal repetitions in T2, T4 and T4BrH23 DNAs.

on the average, contain a "headful" of DNA (Streisinger, Emrich and Stahl, 1967). When the genome is shorter due to the presence of deletion, terminal repetition is increased to compensate for the loss of deleted base pairs. The "headful" mechanism is thus consistent with our observation that there are larger terminal repetitions in deletion mutants than in the wild type.

In summary, the molecular length of T-even phage DNAs are the same within the limit of experimental error. The genome sizes of T4 and T6 are greater than that of T2, as a result, the terminal repetition of T2 is larger than that of T4 and T6.

References

- Bautz, F. A. and Bautz, E. K. (1967). *J. Mol. Biol.* 28, 345.
- Beckendorf, S., Kim, J. P. and Lielausis, I. (1972). Part III of this Thesis.
- Beckendorf, S. and Wilson, J. H. (1972). Manuscript in preparation.
- Benzer, S. (1961). *Proc. Natl. Acad. Sci. U.S.* 47, 403.
- Black, L. W. and Gold, L. M. (1971). *J. Mol. Biol.* 60, 365.
- Black, L. W. and Ahmad-Zadeh, C. (1971). *J. Mol. Biol.* 57, 71.
- Black, L. W. (1971). Phage Meeting Abstracts at Cold Spring Harbor, p. 85.
- Cowie, D. S., Avery, R. J. and Champe, S. P. (1971). *Virology* 45, 30.
- Daniel, V., Sarid, S. and Littauer, U. V. (1970). *Science* 167, 1682.
- Davidson, N. and Szybalski, W. (1971). In "The Bacteriophage λ " (A. D. Hershey, Editor), Cold Spring Harbor Laboratory, New York, Chapter 3.
- Davis, R. W. and Davidson, N. (1968). *Proc. Natl. Acad. Sci.* 60, 243.
- Davis, R. W., Simon, M. N. and Davidson, N. (1971). In "Methods in Enzymology", XXID, 413.
- Davis, R. W. and Hyman, R. W. (1971). *J. Mol. Biol.* 62, 287.
- Edgar, R. S. and Epstein, R. H. (1961). *Science* 134, 327.
- Edgar, R. S., Feynman, R. P., Klein, S., Lielausis, I. and Steinberg, C. M. (1962). *Genetics* 47, 179.

- Edgar, R. S. and Wood, W. B. (1966). Proc. Natl. Acad. Sci. U.S. 55, 498.
- Epstein, R. H., Bolle, A., Steinberg, C. M., Kellenberger, E., Boy de la Tour, E., Chevally, R. S., Susman, M., Denhardt, G. H. and Lielausis, I. (1963). Cold Spr. Harb. Symp. Quant. Biol. 28, 375.
- Hausman, R. and Gold, M. (1966). J. Biol. Chem. 241, 1985.
- Homyk, T. and Weil, J. (1971). Phage Meeting Abstracts at Cold Spring Harbor, p. 89.
- King, J. and Laemmli, U. K. (1971). J. Mol. Biol. 62, 465.
- Kornberg, S. R., Zimmerman, S. B., and Kornberg, A. (1961). J. Biol. Chem. 236, 487.
- Lang, D. (1970). J. Mol. Biol. 54, 557.
- Laemmli, U. K. (1971). Nature 227, 680.
- Lee, C. S., Davis, R. W., and Davidson, N. (1970). J. Mol. Biol. 23, 163.
- Lehman, I. R. and Pratt, E. A. (1960). J. Mol. Chem. 235, 3254.
- MacHattie, L. A., Ritchie, D. A. and Thomas, C. A., Jr. (1967). J. Mol. Biol. 23, 355.
- McConaughy, B. L., Laird, C. D. and McCarthy, B. J. (1969). Biochemistry 8, 3289.
- Mosig, G. (1968). Genetics 59, 137.
- Mosig, G. (1970). Advances in Genetics 15, 7.
- Ray, P., Sinha, N. K., Warner, H. R. and Snustad, D. P. (1972). J. Virology 9, 184.

- Russell, R. L. (1967). Ph.D. Thesis, California Institute of Technology.
- Schildkraut, C. L., Wierzchowski, K. L., Marmur, J., Green, D. M. and Doty, P. (1962). *Virology* 18, 43.
- Séchaud, J., Streisinger, G., Emrich, J., Newton, J., Lanford, H., Reinhold, H. and Stahl, M. M. (1965). *Proc. Natl. Acad. Sci. U.S.* 54, 1333.
- Sederoff, R., Bolle, A. and Epstein, R. H. (1971). *Virology* 45, 440.
- Simon, M. N., Davis, R. W. and Davidson, N. (1971). In "The Bacteriophage λ " (A. D. Hershey, Editor), Cold Spring Harbor Laboratory, New York, p. 313.
- Sinsheimer, R. L. (1954). *Science* 120, 551.
- Streisinger, G., Emrich, J. and Stahl, M. M. (1967). *Proc. Natl. Acad. Sci.* 57, 292.
- Thomas, C. A., Jr. and Rubenstein, I. (1964). *Biophys. J.* 4, 93.
- Ward, S., Luftig, R. B., Wilson, J. H., Eddleman, H., Lyle, H. and Wood, W. B. (1970). *J. Mol. Biol.* 54, 15.
- Ward, S. and Dickson, R. C. (1971). *J. Mol. Biol.* 62, 479.
- Westmoreland, B. C., Szybalski, W. and Ris, H. (1969). *Science* 163, 1343.
- Wetmur, J. G. and Davidson, N. (1968). *J. Mol. Biol.* 31, 349.
- Wilson, J. H., Kim, J. P. and Abelson, J. N. (1972a). Part II of this Thesis.

Wilson, J. H. and Abelson, J. N. (1972c). Manuscript in preparation.

Wilson, J. H. and Kells, S. (1972b). Manuscript in preparation.

Wood, W. B. and Edgar, R. S. (1967). *Scientific American* 217, 60.

Yasuda, S. and Sekiguchi, M. (1970). *J. Mol. Biol.* 47, 243.

Zimmerman, S. B., Kornberg, S. R. and Kornberg, A. (1962).

J. Biol. Chem. 237, 512.

Part II

Bacteriophage T4 Transfer RNA

III. Clustering of the Genes for the T4 Transfer RNAs

John H. Wilson*

Division of Biology, California Institute of Technology
Pasadena, California, U.S.A. 91109

Jung Suh Kim

Division of Chemistry and Chemical Engineering
California Institute of Technology
Pasadena, California, U.S.A. 91109

John N. Abelson

Department of Chemistry, University of California (San Diego)
La Jolla, California, U.S.A. 92037

* Present address: Department of Biochemistry, Stanford
University Medical Center, Stanford, California

E. coli cells infected with phage strains carrying extensive deletions encompassing the gene for the phage ser-tRNA are missing the phage tRNAs normally present in wild type infected cells. By DNA-RNA hybridization we have demonstrated that the DNA complementary to the missing tRNAs is also absent in such deletion mutants. Thus the genes for these tRNAs must be clustered in the same region of the genome as the ser-tRNA gene. Physical mapping of several deletions of the ser-tRNA and lysozyme genes, by examination of heteroduplex DNA in the electron microscope, has enabled us to locate the cluster, to define its maximum size, and to order a few of the tRNA genes within it. That such deletions can be isolated indicates that the phage-specific tRNAs from this cluster are dispensable.

Introduction

The bacteriophage T4 upon infection of its host bacterium directs the synthesis of 6 to 10 phage specific tRNAs (Weiss, Hsu, Foft and Scherberg, 1968; Daniel, Sarid and Littauer, 1968; Tillack and Smith, 1968; Wilson and Abelson, 1972). T4 tRNAs specific for arginine, glycine, isoleucine, proline, leucine, and serine have been identified (Daniel, Sarid and Littauer, 1970; Scherberg and Weiss, 1970; Wilson and Kells, 1972; W. H. McClain, personal communication). The T4-coded nonsense suppressors psu_a^+ , psu_b^+ and psu_1^+ all result from mutations within the T4 ser-tRNA gene and map about 8 map units clockwise from gene e on the standard T4 genetic map (McClain, 1970; Wilson and Kells, 1972; Wilson and Abelson, 1972). Since many genes in T4 are clustered into functionally related groups, we anticipated that genes for some of the other phage tRNAs might be located in the region of the genome between genes e and 57.

To test this notion we assayed by polyacrylamide gel fractionation the tRNAs produced by Escherichia coli cells after infection with phage strains carrying deletions of gene e or of the gene for the phage ser-tRNA (Wilson and Abelson, 1972). The altered band patterns of RNA from these cells suggest that the genes for the phage tRNAs are clustered around the site of the ser-tRNA gene. By correlating the physical map position of the deletions as determined

by examination of heteroduplex DNA in the electron microscope (Davis, Simon and Davidson, 1971) with the presence or absence of tRNAs, we have been able to locate this cluster, to define its maximum size, and to order a few of the tRNA genes within it.

Materials and Methods

(a) Phage and bacterial strains

Deletion mutants of gene e , derived from wild type T4B, were obtained from the collection of Dr. G. Streisinger through Dr. W. Salser and Dr. J. Owen. Those obtained from Dr. W. Salser also carry the spackle mutation, S12, which permits growth of the deletion mutants on plates which do not contain egg-white lysozyme (Emrich, 1969). $psu_b^- \Delta$ strains were derived from psu_b^+ strains and characterized as deletions as described by Wilson and Abelson (1972). CR63 was used as the permissive host for $psu_b^- \Delta$ strains, all of which carry the mutation amN133. S/6/5 was used as the host for growth of lysozyme deletion mutants.

(b) Media and buffers

Media and buffers are described by Wilson and Kells (1972) and Wilson and Abelson (1972).

(c) Transfer RNA from phage-infected cells

Methods for preparation of ^{32}P -labelled RNA, electrophoresis in 10% polyacrylamide gel slabs and autoradiography of the gel slabs are described by Wilson and Abelson (1972).

(d) DNA-RNA hybridization

Wild type T4B and the gene e deletion mutant carrying a spackle mutation, eG506:S12, were grown on E. coli B and purified by differential centrifugation and a step CsCl gradient (Thomas and Abelson, 1966). The purified phage were dialyzed at 4°C against 0.1 M NaCl, 0.01 M Tris-HCl pH 7.4.

DNA was extracted as described by Thomas and Abelson (1966) and then sonicated for 2 min using a Branson sonifier. The sonicated DNA was denatured by heating for 5 min in boiling water followed by quick chilling in ice.

The liquid hybridization technique of Nygaard and Hall (1964) was carried out as described by Bolle, Epstein, Salser and Geiduschek (1968). Hybridization was for 6 hr at 65°C.

³²P-Labelled T4 RNA was prepared and fractionated by electrophoresis on a 10% polyacrylamide gel slab as described by Wilson and Abelson (1972). Bands were located by autoradiography and cut out of the gel slab. The RNA was removed from the gel by homogenizing the gel segment in 0.3 M NaCl. The gel slurry was centrifuged in glass centrifuge tubes and the supernatant solution containing most of the ³²P-labelled RNA was removed. The gel was reextracted twice with 0.3 M NaCl. This procedure removed more than 90% of the RNA from the gel. Small particles of gel were removed by filtration of the RNA solution through a Millipore filter. The RNA was concentrated by ethanol precipitation.

Two samples of T4 RNA which had been pulse labelled with ^3H -uridine between 2 and 5 min and 17 and 20 min after phage infection at 37°C were given to us by Dr. G. Notani.

(e) Electron microscopy

Electron microscope techniques for examining heteroduplex DNA are described in Davis et al. (1971), and Westmoreland, Szybalski and Ris (1969). Heteroduplex DNA was prepared as follows. 1.3 μg of each of two phages were mixed with 0.25 ml of 0.1 N NaOH, 0.02 M EDTA at room temperature for 10 min to lyse the phage and denature the DNA. To neutralize the solution and renature the DNA 25 μl of 1.8 M Tris-HCl, 0.2 M Tris-OH and 0.25 ml formamide were added. Samples were dialyzed against 0.9 M NaCl, 0.1 M Tris pH 8.5, 0.01 M EDTA, 60% formamide for 1 hr and then exhaustively against 0.1 M NaCl, 0.01 M Tris pH 8.5, 0.001 M EDTA. 0.5 μg of the heteroduplex DNA was mixed with 50 μl of hyperphase containing 0.1 M Tris pH 8.5, 0.05 mg/ml cytochrome c, 40% formamide and spread onto 0.01 M Tris pH 8.5, 0.001 M EDTA, 10% formamide. Both single- and double-stranded ϕX174 DNA (5200 nucleotides in length; N. Davidson, personal communication) were added as internal standards. Grids were stained with uranyl acetate and shadowed with platinum-palladium. Under these conditions, single-stranded DNA is extended into a measurable form and appears thinner and kinkier than double-stranded DNA.

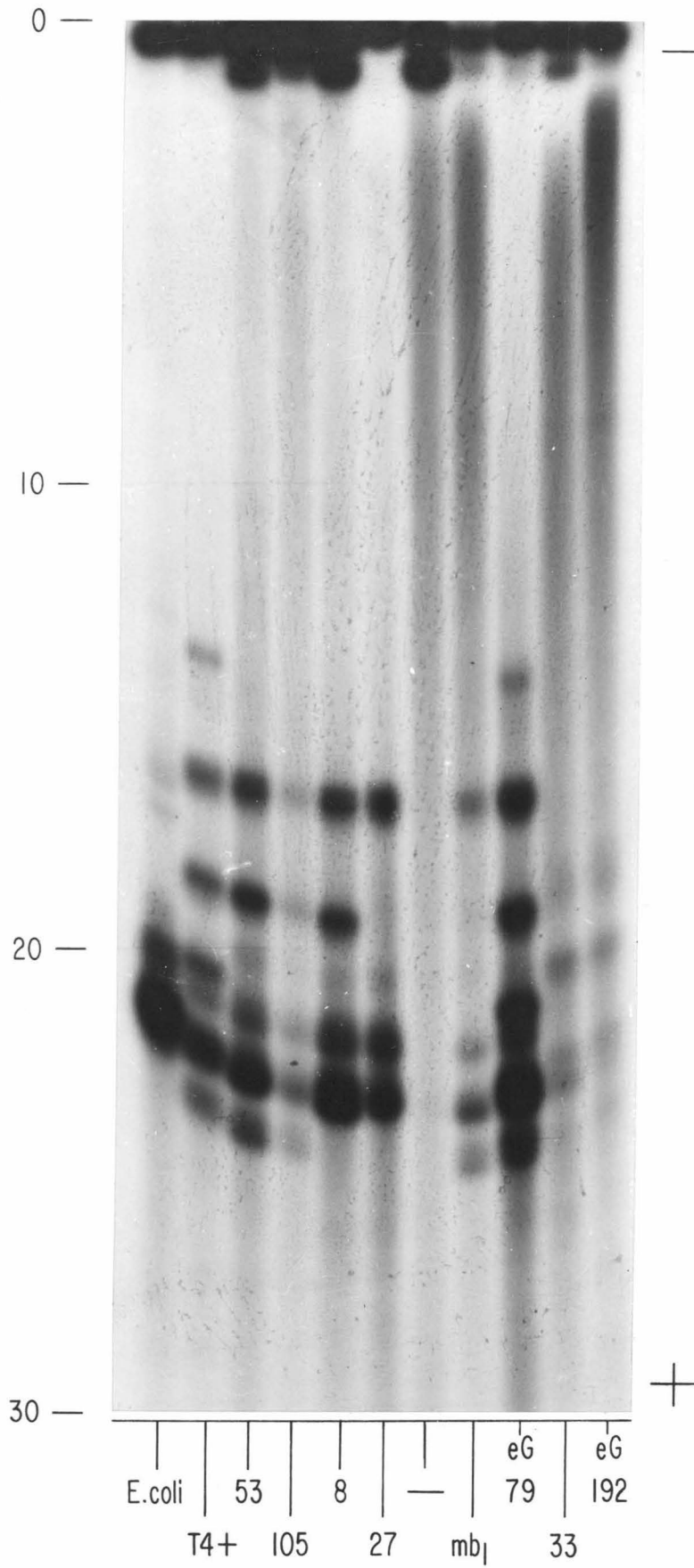
Results

(a) Production of T4 tRNA in deletion-infected cells

The phage-coded nonsense suppressors which result from an alteration in the T4 ser-tRNA (psu_a^+ , psu_b^+ and psu_i^+) are located between genes e and 57 about 8 map units from gene e (McClain, 1970; Wilson and Kells, 1972). To determine whether the genes for any of the other phage tRNAs are located in the same region of the genome, we compared the stable low molecular weight RNAs present in cells infected with wild type T4 and strains carrying deletions of gene e or of the gene for the phage ser-tRNA. Plate 1 shows the fractionation by polyacrylamide gel electrophoresis of low molecular weight RNA from infected and uninfected cells.

The wild type T4 RNA separates into several distinct bands. Five of these bands (1, 2, 3, 4 and 6) contain single species of RNA as judged by their oligonucleotide maps and one, band 5, is a mixture of some 3 to 5 different species (J. Abelson, G. Paddock and T. Pinkerton, unpublished experiments; W. H. McClain and B. G. Barrell, personal communication). Bands 1 and 2 and additional high molecular weight bands may contain tRNA precursors (W. H. McClain and B. G. Barrell, personal communication; G. Paddock and J. Abelson, unpublished experiments). Band 3 contains a serine tRNA (W. H. McClain and B. G. Barrell, personal communication) and band 4 contains a leucine tRNA (Pinkerton, Paddock and Abelson,

Plate 1. Separation of ^{32}P -labelled RNAs from uninfected and T4-infected cells. ^{32}P -Labelled RNA was extracted from cells, electrophoresed on 10% polyacrylamide gel slabs and autoradiographed as described in Material and Methods. eG192 carries S12. All the $\text{psu}_b^- \Delta$ strains, indicated only by their isolation number, carry amN133. mb1 is a point mutant (Wilson and Abelson, 1972). The numbers at left indicate the distance of migration (cm).



1971). Bands 5 and 6 also contain tRNAs (W. H. McClain and B. G. Barrell, personal communication; J. Abelson, G. Paddock and T. Pinkerton, unpublished experiments).

The e deletions which we have examined were known to extend beyond the end of gene e toward gene 57. Two, eG192 and eG506, had been demonstrated by the decreased recombination of outside markers to be quite large and were estimated to extend approximately half the way from gene e to gene 57 (J. Powers, personal communication). As shown in Plate 1, eG79 and wild type are indistinguishable in their band patterns, while both eG192 and eG506 (not shown) are missing most of the RNA bands prominent in wild type infected cells. These results suggest that the genes responsible for the missing bands might be located in that portion of the genome which is deleted in both eG192 and eG506 but not deleted in eG79.

The deletions of the ser-tRNA gene were isolated from among those phage mutants which no longer make functional suppressor tRNA (ser-tRNA) as described by Wilson and Abelson (1972). The RNA band patterns observed with some of these deletion mutants are shown in Plate 1. As predicted from the genetic analysis, all are missing band 3, the ser-tRNA band. $\text{psu}_b^- \Delta 53$ and $\text{psu}_b^- \Delta 105$ are missing only band 3. $\text{psu}_b^- \Delta 8$ is missing bands 3 and 6. $\text{psu}_b^- \Delta 27$ is missing bands 2, 3, and 6. $\text{psu}_b^- \Delta 119$ (gel not shown) is missing bands 3, 4 and 6. The above mutants all show RNA at the position of band 5. However, since we have not yet separated the band 5 RNA species, we do not know if all or only some of the band 5 species are present. $\text{psu}_b^- \Delta 33$

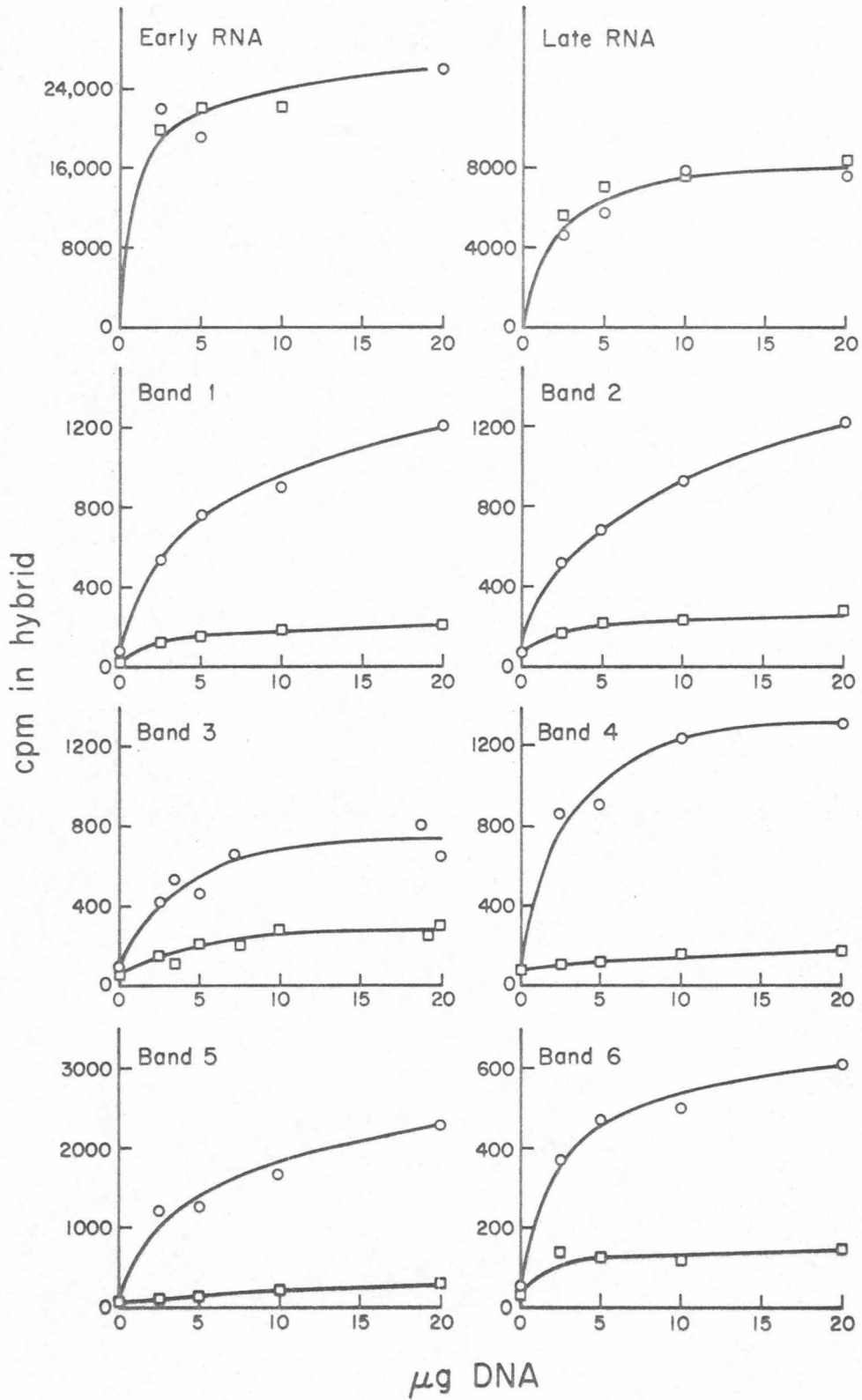
and $\text{psu}_b^- \Delta 64$ (gel for $\text{psu}_b^- \Delta 64$ is not shown) are missing all the prominent phage bands and give gel patterns identical to that of eG192. These observations are consistent with the interpretation that the above deletions encompass some of the genes for the other phage tRNAs. The gel pattern of the point mutant mb1 (Wilson and Abelson, 1972) has been included to emphasize that deletion of the structural genes is not the only possible explanation for the disappearance of RNA bands.

As can be seen in Plate 1, there are faint bands present in the gel patterns of the various deletion mutants. The relative intensities of these bands have varied from experiment to experiment. It is unclear whether they represent phage RNA or residual host RNA synthesis. Most faint bands can be aligned with host bands, lending some support to the second alternative.

(d) Hybridization of T4 tRNAs with wild type and deletion DNA

To determine whether the absence of an RNA band indicates absence of the corresponding structural gene, we extracted the DNAs from eG506 and wild type phage and compared their capacity to hybridize with RNA species from wild type-infected cells as shown in Fig. 1. As a control to measure the relative quality of the two DNA preparations, we compared their capacity to hybridize with bulk RNA extracted from wild type-infected cells which had been pulse labelled with ^3H -uridine early or late after infection (these samples were kindly given to us by Dr. G. Notani). As shown in Fig. 1 wild type

Fig. 1. DNA-RNA hybridization. Hybridization procedures are as described in Materials and Methods. Hybridization plateaus with wild type T4B DNA averaged 10% of the input radioactivity. Early and late RNA were pulse labelled with ^3H -uridine between 2 and 5 min and 17 and 20 min after infection at 37°C. O-O represents wild type T4B DNA. □-□ represents eG506 DNA.



and eG506 DNA hybridize with both these RNA preparations equally well, indicating the DNA preparations are equivalent. The low hybridization values for bands 1, 2, 3, 4 and 6 (each contains one unique RNA species) with eG506 DNA indicate that the DNA complementary to these species is missing in eG506. Wild type band 5 RNA hybridizes only about 10% as much with eG506 DNA as with wild type DNA, suggesting that most, if not all, of the DNA complementary to the 3 to 5 different RNA species present in band 5 is also missing from eG506.

These data indicate that the absence of the RNA bands from eG506-infected cells results from deletion of corresponding genes. Thus the genes for the majority of the stable, low molecular weight T4 RNAs are located in a cluster in a region of the T4 genome which is missing in eG506 but present in eG79.

(c) Physical mapping of deletions of gene e and of the gene for the T4 ser-tRNA

In order to locate and define the size of the cluster of T4 tRNA genes we physically mapped several deletions of gene e and of the gene for the ser-tRNA by examination of heteroduplex DNA in the electron microscope. The general techniques we have used are those of Davis et al. (1971) and Westmoreland et al. (1969).

Heteroduplex DNA from a mixture of T2 and T4 phage (T2/T4 heteroduplex) shows a characteristic pattern of substitution and deletion loops when examined in the electron microscope (Kim and

Davidson, in preparation). This pattern of loops has been oriented relative to the standard T4 genetic map by using deletions of genes e and rII as markers (Kim and Davidson, in preparation). Plate 2 shows an electron micrograph of the gene e region of a T2/T4 heteroduplex DNA molecule. Figure 2 is a schematic representation of the same picture. Except for loop A we do not know which strands of the loops correspond to T4 and which to T2. We have positioned the gene e deletions absolutely by mapping them relative to this loop pattern. The deletions of the ser-tRNA gene were subsequently mapped relative to defined gene e deletions.

The procedure for locating a particular gene e deletion relative to this loop pattern varied depending on the size and location of the deletion. We measured small deletions which extended neither past loop B nor all the way through loop A in a single step by heteroduplexing with T2. Their size and location was determined from the decreases in length of A_4 (the single-stranded portion of loop A which comes from T4) and of the double-stranded region between loops A and B. Deletions eG19, eG223, eG326 and eG342 were mapped in this way.

Those deletions which extended past B, or in the case of eG298 past the next marker loop in the direction of gene rI (not shown in Fig. 2) were mapped generally in three steps. The first step was to position the deletion approximately by heteroduplexing with wild type T2. The second step was to position one end of the deletion precisely by heteroduplexing with a defined gene e deletion, which it

Plate 2. These electron micrographs show the portion of T2/T4 (a) and T2/eG79 (b) heteroduplex DNA molecules in the region of gene e. The letters relate the loop pattern in the micrograph to the corresponding schematic representation in Fig. 2. The arrow in (b) indicates the substitution loop formed by the eG79 deletion.

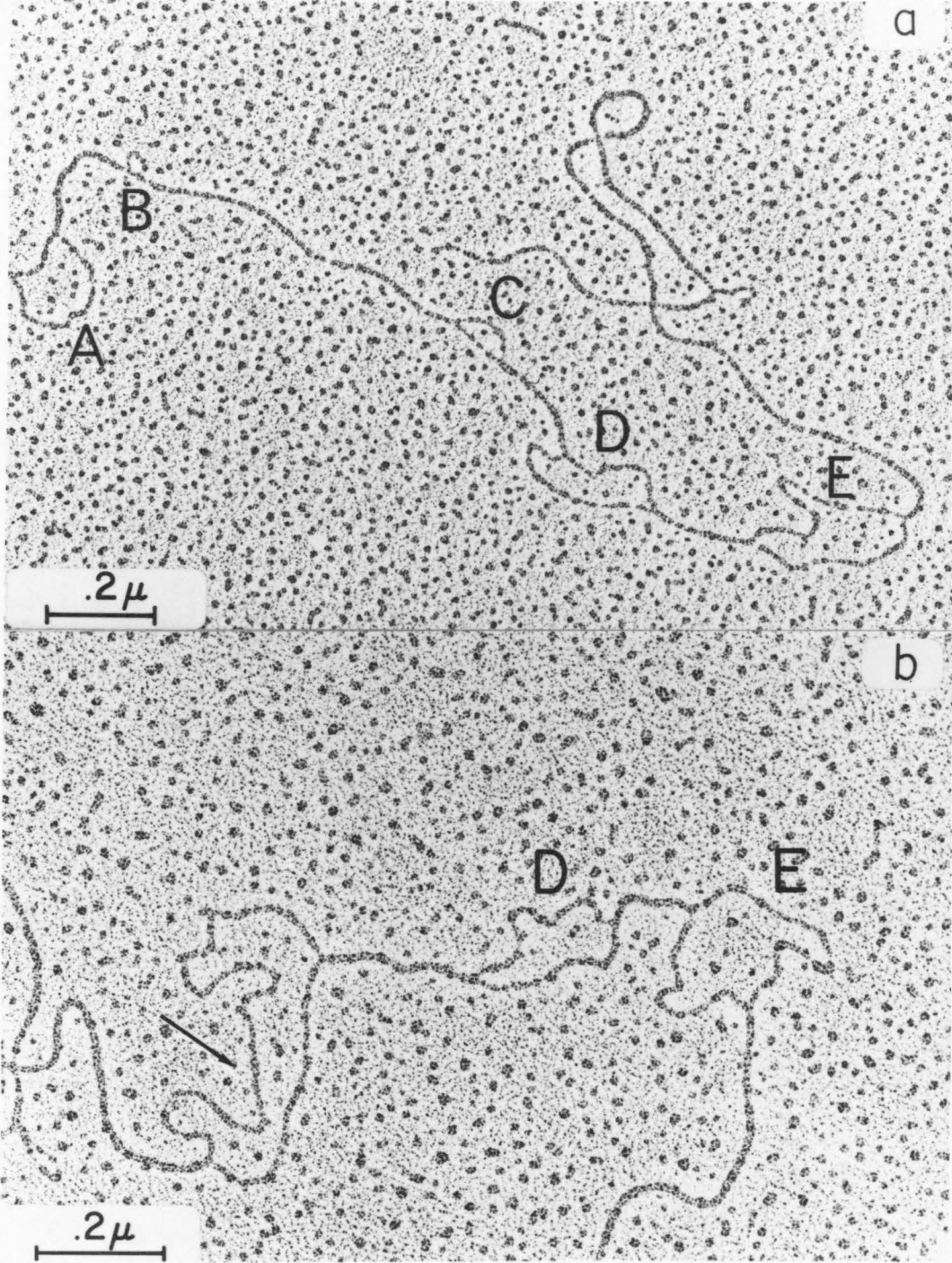
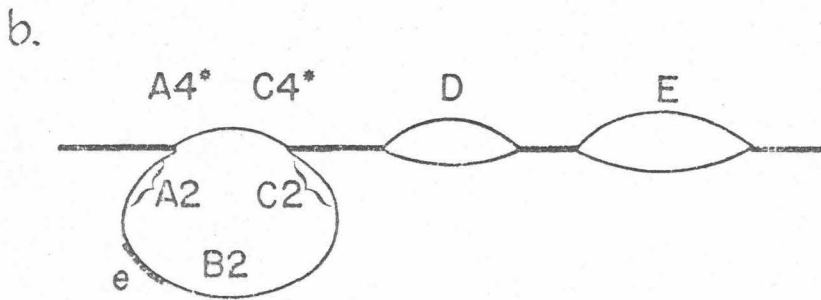
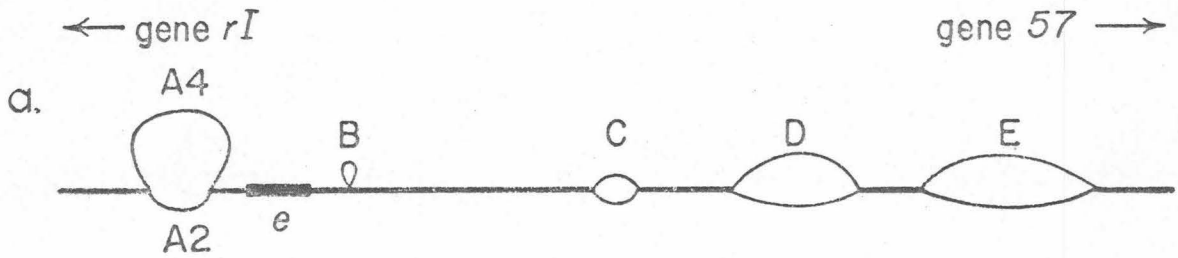


Fig. 2. Schematic representation of T2/T4 (a) and T2/eG79 (b) heteroduplex DNAs. The letters identify the loops in the electron micrograph in Plate 2. A_2 and A_4 indicate those strands of loop A which come from T2 and T4 respectively. The position of gene e is represented by the thickened segments on both strands. A_4^* and C_4^* indicate the portions of A_4 and C which are not deleted by eG79. The positions of A_2 and T2 gene e are indicated on the longer strand of the substitution loop in (b).



partially overlapped. The third step was to define the size of the deletion by heteroduplexing with wild type T4. The orientation, position of one end, and size uniquely locate the deletion. Step one for eG79 is illustrated in Plate 2b. Figure 2b shows the corresponding schematic representation of the eG79/T2 heteroduplex molecule. The loops D and E are intact while loops A, B and C have been replaced by a substitution loop. This pattern indicates that the right end of eG79 begins in loop C and that the left end starts in A₄. The orientation of the deletion is clear but neither end has been positioned precisely. Heteroduplexing these undefined deletions with defined gene e deletions which they partially overlap yields heteroduplex molecules with a single substitution loop. One strand of the substitution loop is equal to the length of the defined deletion minus the length of the overlap, and the other strand is equal to the length of the undefined deletion minus length of the overlap. Knowledge of the size of the undefined deletion from step three allows the size of the overlap to be calculated, thereby locating precisely one end of the undefined deletion relative to the ends of the defined deletion. The size of the deletion was determined by measuring the single strand length of the single deletion loop in the heteroduplex molecule of the gene e deletion and wild type T4. The mapping data for the gene e deletions is summarized graphically in Fig. 3.

Six deletions of the ser-tRNA gene were measured and located by heteroduplexing with defined gene e deletions as shown for $\text{psu}_b^- \Delta 8$, $\text{psu}_b^- \Delta 27$, and $\text{psu}_b^- \Delta 119$ in Plate 3. The single strand length of the

Fig. 3. Physical map of gene e and of the ser-tRNA gene deletions. The heavy black lines represent the lengths and relative positions of the deletions. The distance between adjacent vertical dotted lines is 2000 nucleotides. The vertical rectangle labelled e represents the genetic position of gene e relative to the deletions. The vertical rectangle designated ser-tRNA represents the minimum overlap of the ser-tRNA gene deletions. All gene e deletion mutants except eG19, eG79 and eG298 carried the spackle mutation, S12. The $psu_b^- \Delta$ strains all carried amN133.

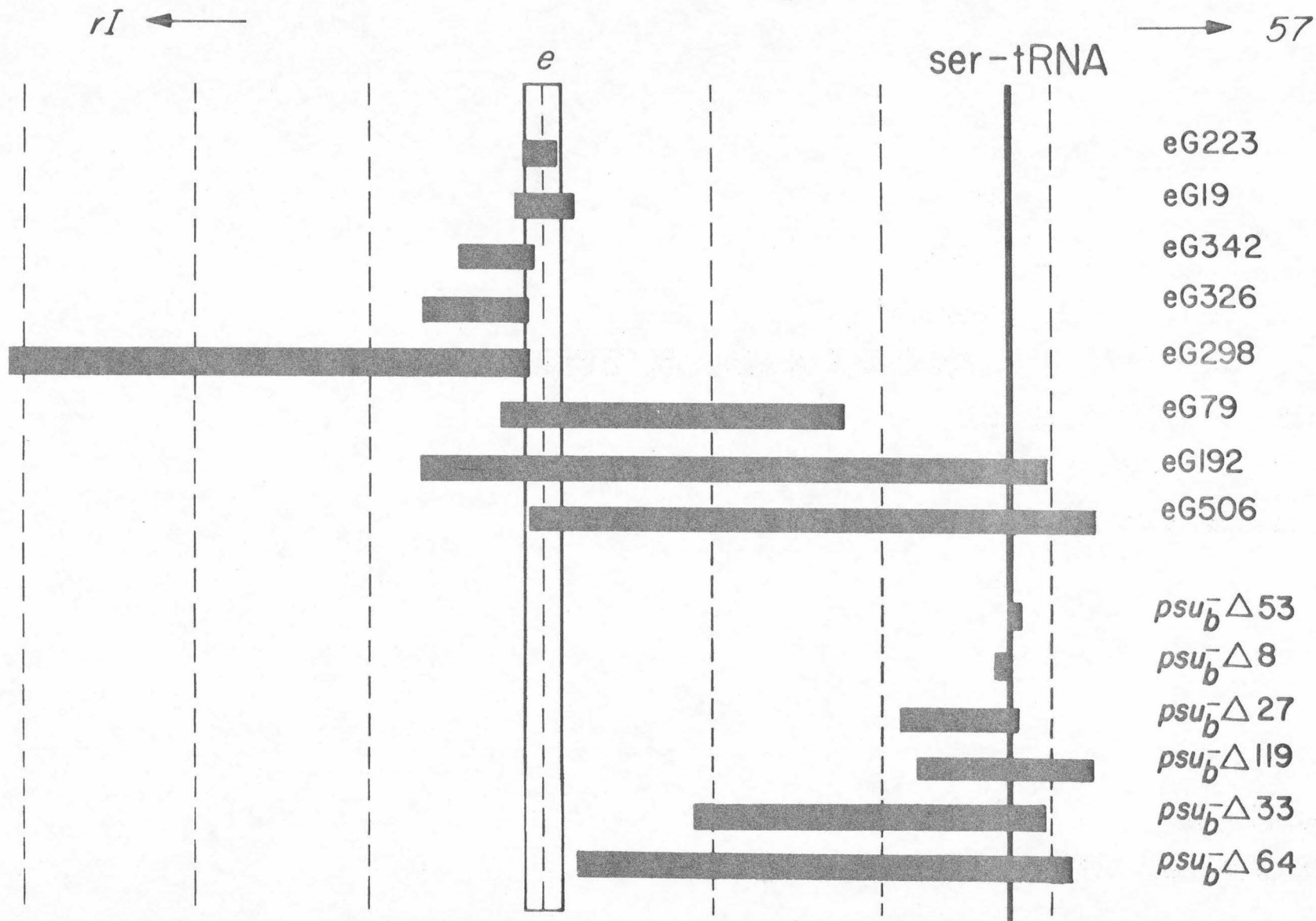
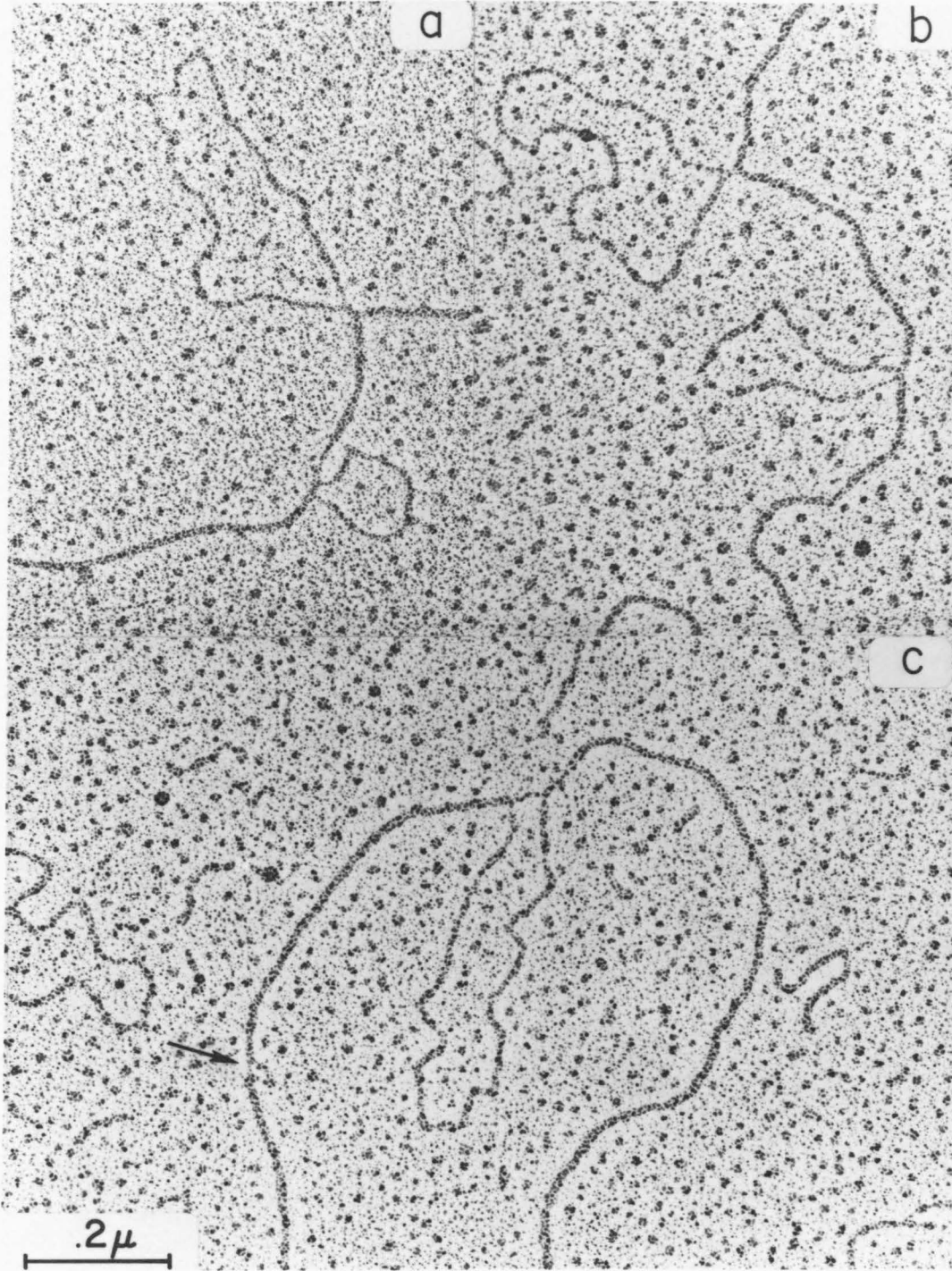


Plate 3. Heteroduplexes of a gene e deletion with ser-tRNA gene deletions. In each case the larger deletion loop corresponds to the gene e deletion eG79.

- (a) eG79/psu_b⁻Δ27 heteroduplex DNA.
- (b) eG79/psu_b⁻Δ119 heteroduplex DNA.
- (c) eG79/psu_b⁻Δ8 heteroduplex DNA.

The micrograph in (c) was selected because it shows the small deletion psu_b⁻Δ8 (indicated by arrow) most clearly. However it was not used in the measurements because the eG79 loop is aberrant.



ser-tRNA deletion loop yields the size of the deletion and the distance between the two deletion loops yields the relative positions of their closest ends. The positions of $\text{psu}_b^- \Delta 8$, $\text{psu}_b^- \Delta 27$ and $\text{psu}_b^- \Delta 119$ were measured relative to both $\underline{e}G19$ and $\underline{e}G79$. The data indicate that these deletions are located to the right of gene \underline{e} as expected from the genetic position of the ser-tRNA gene determined by Wilson and Kells (1972). The physical mapping data for these deletions are shown in Table 1 and the positions of the deletions relative to gene \underline{e} are shown in Fig. 3. The overlap of $\text{psu}_b^- \Delta 8$ and $\text{psu}_b^- \Delta 53$ defines the site of the gene for the ser-tRNA as between genes \underline{e} and 57 about 5400 nucleotides from gene \underline{e} .

By correlating the physical map position of the deletions with the RNA species present in the deletion-infected cells, we can order the genes for the bands containing unique RNA species as shown in Fig. 4. The order shown is of course based on the assumption, unproven for these deletions, that the absence of a band results from the deletion of the gene corresponding to that band. From the position of $\underline{e}G79$, which seems to contain all the RNA species, and $\text{psu}_b^- \Delta 33$ which is missing all the RNA species, we conclude that the maximum size of the cluster is 2500 nucleotides.

Legend for Table 1

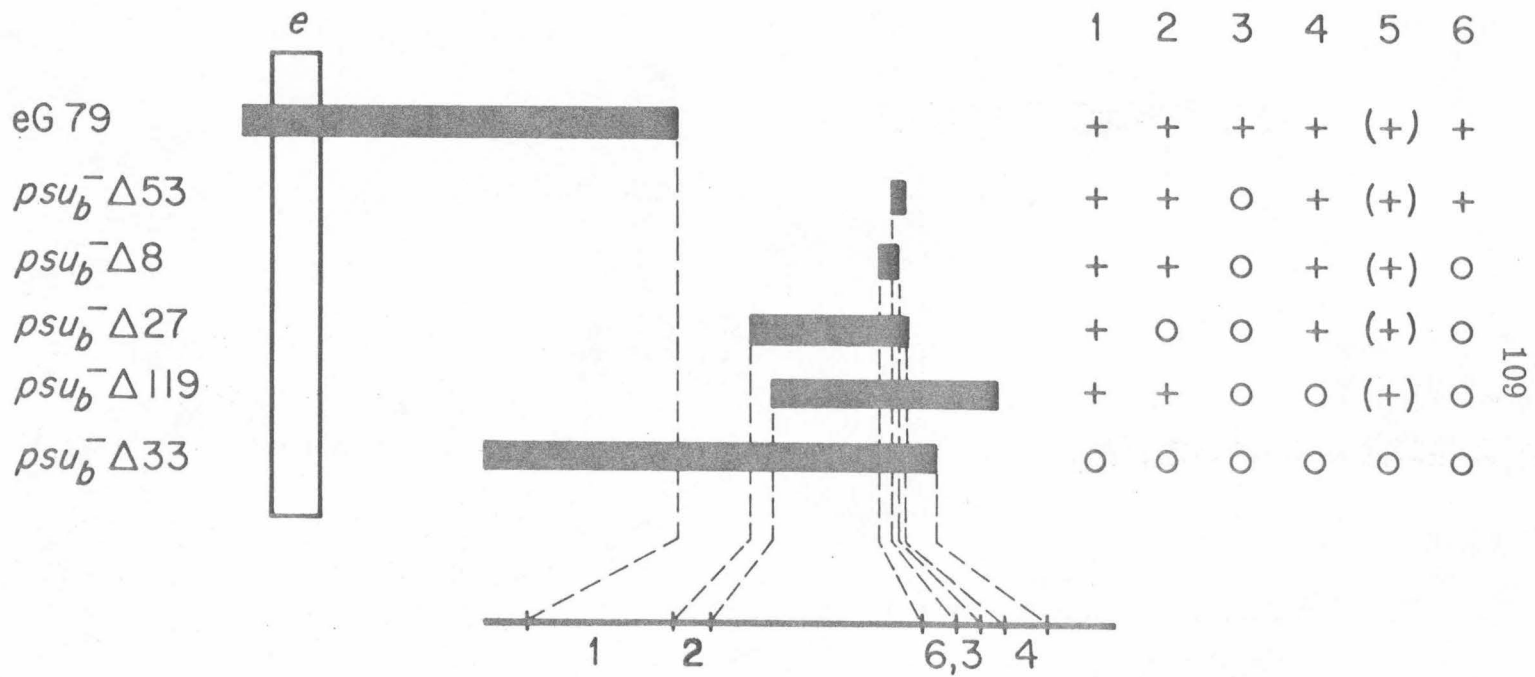
The size of the ser-tRNA deletion was determined by measuring the single strand length of the ser-tRNA deletion loop. The relative positions of the two deletions was determined by measuring the double strand DNA between the deletion loops. The standard deviation is listed with each measurement. Both single and double strand ϕ X174 circles (5200 nucleotides in length) were included in each mixture as an internal standard.

Table 1

Heteroduplex	Number of molecules measured	Size of ser-tRNA deletion (nucleotides)	Distance between deletions (nucleotides)
$\text{psu}_b^- \Delta 53 / \underline{\text{eG19}}$	6	150 ± 30	5330 ± 110
$\text{psu}_b^- \Delta 8 / \underline{\text{eG19}}$	8	200 ± 30	5200 ± 100
$\text{psu}_b^- \Delta 8 / \underline{\text{eG79}}$	12		1950 ± 130
$\text{psu}_b^- \Delta 27 / \underline{\text{eG19}}$	15	1330 ± 100	3940 ± 200
$\text{psu}_b^- \Delta 27 / \underline{\text{eG79}}$	7		800 ± 60
$\text{psu}_b^- \Delta 119 / \underline{\text{eG19}}$	9	2070 ± 190	4180 ± 180
$\text{psu}_b^- \Delta 119 / \underline{\text{eG79}}$	6		1050 ± 120
$\text{psu}_b^- \Delta 33 / \underline{\text{eG19}}$	13	4150 ± 450	1370 ± 100
$\text{psu}_b^- \Delta 64 / \underline{\text{eG19}}$	7	*(5820 ± 350) (700 ± 110)	

* The $\text{psu}_b^- \Delta 64 / \underline{\text{eG19}}$ heteroduplexes showed single substitution loops. The lengths of both strands are given in the Table. The length of $\underline{\text{eG19}}$ has been independently determined to be 700 nucleotides. Thus $\text{psu}_b^- \Delta 64$ must begin near the end of $\underline{\text{eG19}}$.

Fig. 4. Order of the genes for the bands containing unique species of RNA. The RNA band patterns of deletion mutant-infected cells from Plate 1 are summarized at right (data for $\text{psu}_b^- \Delta 119$ are not shown in Plate 1). The numbers correspond to the band numbers of Plate 1. + indicates that the band is present. o indicates that the band is absent. The presence of band 5 is indicated as (+) since we do not know which of the 3 to 5 RNA species are present and which, if any, are absent. The overlap pattern of the deletions uniquely orders the genes for the RNAs in the bands as shown. The comma between 6 and 3 indicates ambiguity in their relative positions; their order depends solely on the physical positions and sizes of the very small and difficult to measure deletions $\text{psu}_b^- \Delta 8$ and $\text{psu}_b^- \Delta 53$ (see Table 1).



Discussion

Certain deletions of T4 gene e and the phage ser-tRNA gene result in the disappearance of the stable, low molecular weight T4 RNA species normally present after T4 infection. These RNA species have been identified as T4 tRNAs and possible T4 tRNA precursors (Pinkerton et al., 1971; W. H. McClain and B. G. Barrell, personal communication; G. Paddock and J. Abelson, unpublished experiments). The lack of hybridization between these RNA species and one of the gene e deletions, eG506, indicates that their disappearance results from the deletion of the corresponding structural genes and not the deletion of some modifying or regulating element. By correlating the physical position of the deletions, as determined by electron microscope examination of heteroduplex DNA, with the presence or absence of RNA species from the deletion mutant-infected cells, we have determined that the genes for the T4 tRNAs are clustered into a region of the genome not more than 2500 nucleotides in length which lies between genes e and 57. These correlations have also allowed us to tentatively order within the cluster some of the genes for those RNA species which are separated on the polyacrylamide gels.

The clustering of the tRNA genes suggests the possibility that they may be transcribed onto a single polycistronic RNA out of which the individual tRNAs are cleaved. W. H. McClain and B. G. Barrell

have demonstrated that at least two different T4 tRNAs are present in a single larger piece of RNA. An RNA species which accumulates under certain conditions of wild type phage growth contains the nucleotide sequences for both a ser-tRNA and a pro-tRNA (W. H. McClain and B. G. Barrell, personal communication). The possibility that the entire cluster is transcribed on one RNA is suggested by another observation. Black and Gold (1971) have calculated that the immediate-early promoter for T4 gene e is located 5,000 to 6,000 nucleotides "upstream" (in the direction of gene 57) from gene e. Given the location of the tRNA gene cluster this observation suggests that the tRNA gene may be transcribed under the control of the same promoter. Two predictions of this arrangement are that the RNAs are immediate-early functions and that they are transcribed from the 1 strand of T4 DNA. Scherberg, Guha, Hsu and Weiss (1970) have demonstrated that the T4 tRNAs are made in the presence of chloramphenicol (a test for immediate-early RNA) and hybridize with the 1 strand of T4 DNA. If the T4 tRNA genes are transcribed under the control of the gene e immediate-early promoter, they must be transcribed onto a single polycistronic RNA.

The viability of T4 strains which lack the phage tRNA genes indicates that these tRNAs are not essential for phage growth under the conditions we have employed. What then is their function? Conceivably they are essential under some conditions encountered in the wild, and therefore have survival value to the phage. Current studies on the growth properties of the deletion mutants described

above in various E. coli host strains appear to support this notion (Wilson and Abelson, in preparation).

We are grateful to Dr. R. L. Russell, Dr. W. B. Wood, Dr. A. Sarabhai, and Dr. W. H. McClain for many helpful discussions. We are especially indebted to Dr. W. H. McClain and Dr. B. G. Barrell for generously communicating to us their unpublished results. This research was supported by grants from the U. S. Public Health Service to Dr. W. B. Wood (GM-06965, AI-09238), to Dr. J. N. Abelson (CA-10984) and to Dr. N. R. Davidson (GM-10991). J. N. A. is a Faculty Research Associate of the American Cancer Society.

References

- Black, L. W. and Gold, L. M. (1971). *J. Mol. Biol.* 60, 365.
- Bolle, A., Epstein, R. H., Salser, W. and Geiduschek, E. P. (1968).
J. Mol. Biol. 31, 325.
- Daniel, V., Sarid, S. and Littauer, U. V. (1968). *FEBS Lett.* 2, 39.
- Daniel, V., Sarid, S. and Littauer, U. V. (1970). *Science* 167, 1682.
- Davis, K. W., Simon, M. and Davidson, N. (1971). *Methods in Enzymology*, Vol. 21 (Grossman, L. and Moldave, K., eds.) Academic Press, New York, p. 413.
- Emrich, J. (1968). *Virology* 35, 158.
- McClain, W. H. (1970). *FEBS Lett.* 6, 99.
- Nygaard, A. P. and Hall, B. D. (1964). *J. Mol. Biol.* 9, 125.
- Pinkerton, T. C., Paddock, G. and Abelson, J. N. (1971). *Fed. Proc.* 30, 1218.
- Scherberg, N. H., Guha, A., Hsu, W.-T. and Weiss, S. B. (1970). *Biochem. Biophys. Res. Commun.* 40, 919.
- Scherberg, N. H. and Weiss, S. B. (1970). *Proc. Natl. Acad. Sci. Wash.* 67, 1164.
- Thomas, C. A. and Abelson, J. N. (1966). *Procedures in Nucleic Acid Research* (Cantoni, G. L. and Davies, D. R., eds.) Harper and Row, p. 553.
- Tillack, T. W. and Smith, D. E. (1968). *Virology* 36, 212.

Weiss, S. B., Hsu, W.-T., Foft, J. W. and Scherberg, N. H. (1968).

Proc. Natl. Acad. Sci. Wash. 61, 114.

Westmoreland, B. C., Szybalski, W. and Ris, H. (1969). Science

163, 1343.

Wilson, J. H. and Kells, S. (1972). J. Mol. Biol., in press.

Wilson, J. H. and Abelson, J. N. (1972). J. Mol. Biol., in press.

PART III

STRUCTURE OF BACTERIOPHAGE T4 GENES 37 and 38

Steven K. Beckendorf, Jung Suh Kim,
and I. Lielausis

Division of Biology

and

Division of Chemistry and Chemical Engineering

California Institute of Technology

Pasadena, California 91109 USA

1. Introduction

Bacteriophages T2 and T₄ are so closely related that a gene product missing from one of the phages due to an amber mutation can usually be replaced by the corresponding gene product from the other phage (Russell, 1967). The only two exceptions are the products of genes 37 and 38 (P37 and P38). These interact during assembly of the distal half of the phage tail fiber (King & Wood, 1969), P37 being incorporated as the major polypeptide of this half fiber (Ward *et al.*, 1970). P38, while necessary for fiber formation, is not incorporated into the assembled structure (King & Laemmli, 1972; Eiserling & Dickson, 1972). During adsorption the distal half fiber interacts with specific receptors on the surface of the bacterium (Wilson, Luftig & Wood, 1970). The specificity of this interaction is at least partially controlled by P37, since host range mutations of T₄ map in gene 37 (Beckendorf, in preparation). P37 and P38 cannot be exchanged by T2 and T₄ because P37 from T₄ (P37^h) cannot interact with P38 from T2 (P38²) and P37² cannot interact with P38^h (Russell, 1967). The T2 and T₄ gene products must also differ functionally, since the two phages attach to very different receptors on the bacterial surface (Jesaitis & Goebel, 1953). Despite these differences there is a low level of am⁺ recombinants in crosses of the type T2 am37 x T₄ am38 or T₄ am37 x T2 am38 (Russell, 1967). These results suggest that, despite the incompatibility of the finished T2 and T₄ gene products, there are at least some regions of the two genes which are mutually compatible.

To determine which regions are compatible and which are incompatible, we have carried out intertype crosses between T2 and T⁴ mutants defective in genes 37 and 38. Analysis of these crosses and of the T2:T⁴ hybrid phage produced has allowed us to locate the host range (h) determinant, the site of P37 interaction with P38, and the regions of these genes which are not homologous between T2 and T⁴.

2. Materials and Methods

(a) Phage and bacterial strains

Phage strains derived from the wild type T⁴D were obtained from the collection of R. S. Edgar and have been described elsewhere (Epstein et al., 1963; Edgar & Lielausis, 1964; Wilson & Kells, 1972; Bernstein, Edgar & Denhardt, 1965). T⁴B rH23 is an rII deletion mutant of T⁴B which is missing both the rIIA and rIIB cistrons (Benzer, 1959). Most of the phage strains derived from wild type T2L were obtained from the collection of R. L. Russell and have also been previously described (Russell, 1967). T2 rH23 is a recombinant between T2L and T⁴B rH23 which was selected to retain T2 host range, and the rII deletion. It is homologous with T2 throughout the tail fiber region (Kim & Davidson, 1972). T2:T⁴ hybrid phage made during this study are described in Table 1.

Escherichia coli strain CR63 was used as permissive host for T⁴ amber mutants, strain CR63r₆⁻r₂₄⁻ as a permissive host for T2 amber mutants (Georgopoulous & Revel, 1971) and strain S/6/5 as restrictive host for both T2 and T⁴ ambers. Strain Bb was used as nonpermissive host for all lysates (Wilson et al., 1970). Strains B/2 and S/4 were used as selective indicators to determine T2 or T⁴ host range (h² or h⁴). Identifica-

Table 1

T2:T4 Hybrid Phage

Hybrid Phage	Composition	Host Range
<u>hyl</u>	<u>aml23</u> ⁺ <u>amB280</u> ⁺ <u>rdf41</u>	<u>h</u> ²
<u>hy2</u>	<u>aml25</u> ⁺ <u>amE2060</u> ⁺ <u>rdf41</u>	<u>h</u> ⁴
<u>hyl1</u>	<u>aml23</u> ⁺ <u>amN52</u> ⁺	<u>h</u> ²
<u>hy⁴4</u>	<u>aml23</u> ⁺ <u>amC290</u> ⁺	<u>h</u> ²
<u>hy⁴5</u>	<u>aml25</u> ⁺ <u>amE2060</u> ⁺	<u>h</u> ⁴
<u>hy215</u>	<u>aml25</u> ⁺ <u>amNG220</u> ⁺	<u>h</u> ⁴
<u>hy217-5</u>	<u>aml29</u> ⁺ <u>amE2082</u> ⁺ <u>rdf41</u>	<u>h</u> ²
<u>hy267</u>	<u>aml23</u> ⁺ <u>amNG182</u> ⁺	<u>h</u> ²

The designation aml23⁺ amB280⁺ for hyl indicates that hyl is an am⁺ recombinant from a cross between T2 aml23 and T4 amB280. This same convention is used for all of the hybrids. The position of the T2 and T4 mutations in genes 37 and 38 are shown in Figure 1 and Figure 2a. hyl, hy2, and hy217-5 also carry the rII deletion rdf41.

tion of both h^2 and h^4 phage on the same plate was done by plating on BIX, a 3:1 mixture of S/6/5 and B/2, each at about 2×10^9 cells/ml. On this indicator h^2 phage made turbid plaques, h^4 phage make clear plaques.

(b) Media

H broth used for phage and bacterial growth and EHA top and bottom agar used for plating assays were prepared as described by Steinberg & Edgar (1962). Dilution buffer was prepared as described by King (1968). Minimal growth medium for preparation of radioactively labeled infected cell lysates contained per liter 7 gm Na_2HPO_4 , 3 gm KH_2PO_4 , 1 gm NaCl, 1 gm NH_4Cl , 0.12 gm $MgSO_4$, and 4 gm glucose.

(c) ^{14}C -labeled lysates

Strain Bb was grown to 5×10^7 cells/ml. in minimal growth medium, collected by centrifugation, and resuspended at $2-4 \times 10^8$ cells/ml. One ml. aliquots of this suspension were warmed to $37^\circ C$, infected with phage at a multiplicity of 4, and aerated by agitation on a rotary shaker. 14 min after infection 2 μC of a uniformly-labeled ^{14}C amino acid mixture (Schwarz-Mann) were added. At 45 min the lysates were added to an equal volume of cold 10% TCA and dialyzed against 0.065 M Tris-HCl, pH 6.8, 1% SDS.

(d) Electron microscopy

Electron microscopic techniques for examining heteroduplex DNA are described in Davis et al. (1971), and Westmoreland, Szybalski & Ris (1969). Details of our procedure are given in Wilson, Kim & Abelson (1972). Briefly, the heteroduplex DNA was prepared by alkaline lysis of a mixture of two phages and renaturation of the DNA in the presence of

formamide, stained with uranyl acetate, and shadowed with platinum-palladium. Under these conditions single-stranded DNA is extended into a measureable form and appears thinner and kinkier than does double-stranded DNA. Both single- and double-stranded ϕ X174 DNA (5200 bases long, Dr. Davidson, personal communication) were added as internal standards.

The crossover points (XOP's) of the hybrid phages were determined by making heteroduplexes of their DNA with that of T4B rH23 and T2L rH23 or, if the hybrids carried the rII deletion rd_f41, with that of T4B and T2L. The rII deletions served as markers to orient the heteroduplexes.

(e) Gel electrophoresis and autoradiography

Procedures for the preparation and running of discontinuous polyacrylamide gels containing SDS were as described by Laemmli (1970). Sample preparation, staining, destaining, and autoradiography of the gels were as described by Wilson & Kells (1972). For molecular weight determinations the gels were standardized as described by Beckendorf & Wilson (1972).

(f) Phage crosses

Standard phage crosses were a modification of the procedure of Steinberg & Edgar (1962). T4D crosses were done at 30°C in CR63. Crosses involving T2L or its mutants as one or more parents were done at 25°C in CR63r₆⁻r₂₄⁻. A stationary culture of the host cells was diluted 1:1000 or 1:500 in H broth and grown for 2.5 hr at 30°C. Cells were collected by centrifugation, resuspended at 4×10^8 cells/ml., and KCN was added to an equal volume of the parental phage strains at a multiplicity of 7.5

each at 30°C or 25°C. After 10 min anti-T₄ serum, anti-T₂ serum, or a mixture of both sera was added to inactivate all unadsorbed phage. 15 min after infection the cells were diluted 1-4 x 10⁴ into H broth at 30°C or 25°C. 90 or 110 min after infection CHCl₃ was added.

(g) Conventions

All maps are represented as they would appear if viewed from the center of the circular T₄ genetic map (see Mosig, 1970, for a recent version of this map). Thus gene 37 is to the left of gene 38. To facilitate comparisons of maps constructed by various means, the positions of markers are often given in fractional parts of T₄ gene 37, measured from its left end. As will be seen in section 3.(d), synthesis of P37 begins at the left end of gene 37.

3. Results

(a) Genetic maps of genes 37 and 38

The genetic map of T₄ genes 37 and 38 presented here (abscissa Fig. 2a) is a composite of two previous maps. The first, a map of gene 37 presented by Bernstein and Fisher (1968), contains three am sites, amA⁴⁸¹, amN⁵², and amB²⁸⁰, and most of the ts sites in gene 37. The data used to construct this map were generously supplied to us by Harris and Bernstein. The second map, which we constructed, contained three gene 37 ts sites, tsL³⁷, tsP⁴³, and tsL⁹³, all of the gene 37 am sites, and the am and ts sites in gene 38. To combine the two maps we crossed am mutants which had been located on our map with ts mutants expected to be nearby.

In this way we determined which ts sites lay in each interval between the am sites on the map we had constructed. The order of the ts sites and their relative spacing within the intervals between am's are essentially as determined by Bernstein & Fisher (1968). The resulting map differs in two important respects from that published by Bernstein & Fisher. We find that tsL19, which is their left-hand terminal marker, is actually in gene 36 not gene 37 (Beckendorf, unpublished). We also find, from the results of two and three-factor crosses, that the ts site defined by tsCB81 is to the left of the tsL37 site rather than to the right of amA481 as published (Beckendorf & Lielausis, unpublished).

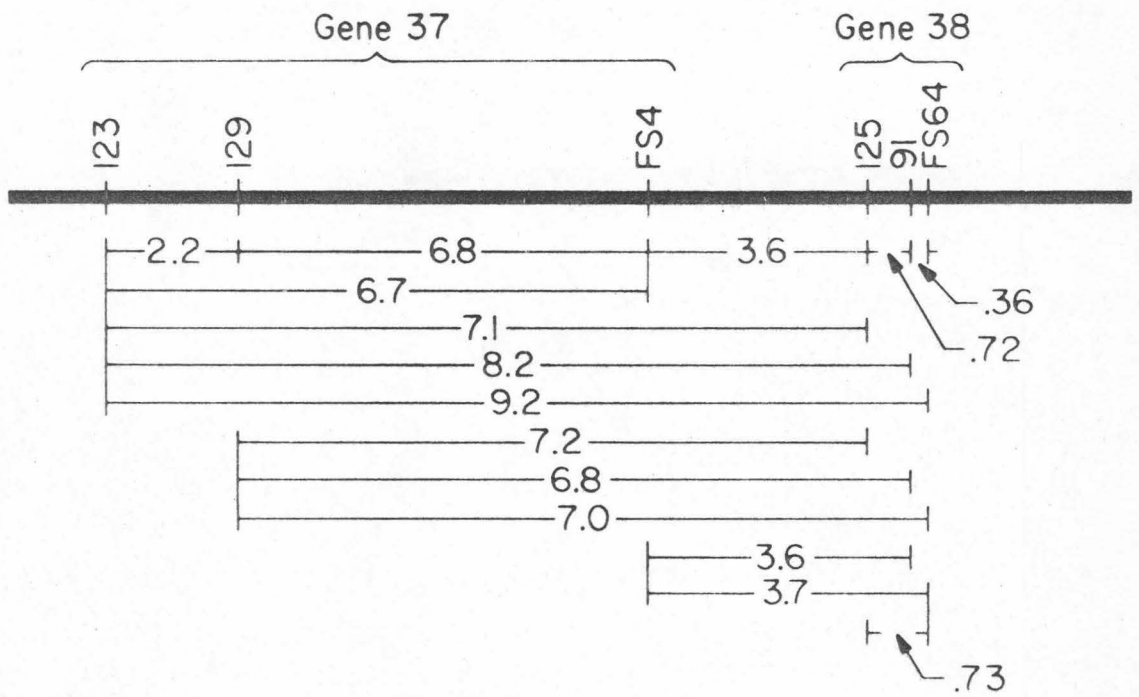
The genetic map of T2 genes 37 and 38 (Fig. 1) was constructed from recombination frequencies determined in two-factor crosses between all of the available am mutants in these genes.

(b) Intertype crosses

We have crossed the ts and am mutants in T⁴ genes 37 and 38 with the three available am's in T2 gene 37 and am125 in T2 gene 38. The results of these crosses show that most of the recombination occurs in one short segment of gene 37. The crosses have also allowed us to locate the region which controls the difference between T2 and T⁴ host range.

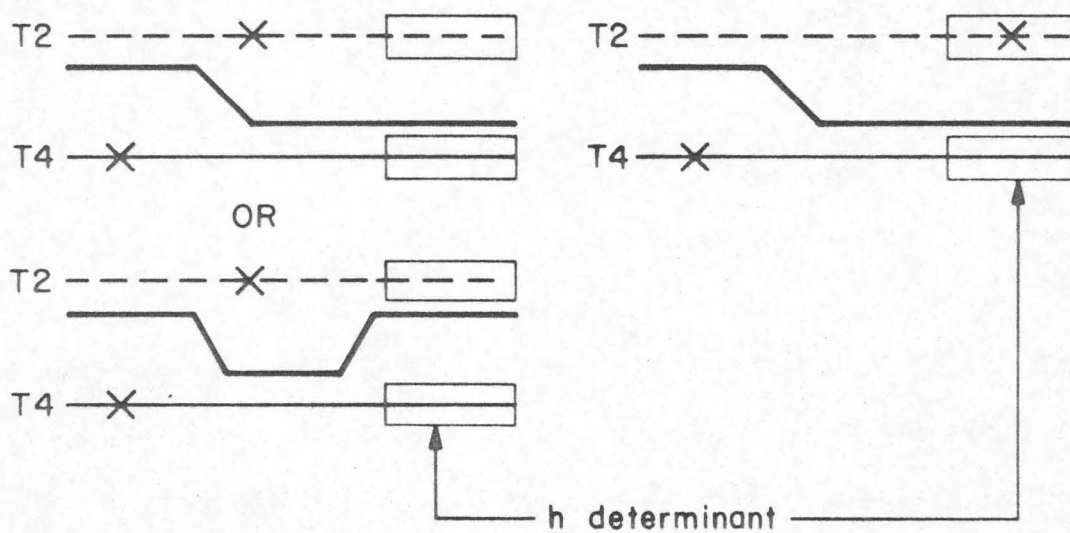
As discussed below, two factors, DNA non-homology and protein incompatibility, might affect the number of recombinants arising in such crosses. Because the DNA molecules would be less likely to pair properly, we would expect a reduction or lack of recombination in nonhomologous regions. The results in section 3.(c) show that most of the T2 and T⁴ DNA in this region is partially or completely non-homologous.

Fig. 1. Genetic map of T2 genes 37 and 38. The % recombination for each interval is listed below the map and was calculated as $(\frac{\text{am}^+ \text{ recombinants}}{\text{total progeny}}) \times 200\%$. All values are the average of recombination frequencies obtained in two independent crosses. All mutants are ambers.



Protein incompatibilities should also affect the apparent frequency of recombination. The interaction of P37 and P38 is an example of such an incompatibility. Any recombinant in which the interacting sites of the two proteins do not come from the same parental phage will be unable to make tail fibers. As another example, a phage carrying part of gene 37 from T2 and part from T4 might make a protein which would be unable to fold correctly. Either of these examples of protein incompatibility would, like DNA nonhomology, lead to apparent low recombination, since recombinant phage would be unable to form a plaque and would not be scored.

To locate the host range (\underline{h}) determinant, we have tested whether the $\underline{am}^+ \underline{ts}^+$ recombinants have T2 or T4 host range (\underline{h}^2 or \underline{h}^4). If, as shown at the left below, the region opposite a mutation is compatible with either host range, both \underline{h}^2 and \underline{h}^4 recombinants will occur. However, as shown at the right, if such a region uniquely determines \underline{h}^4 (is incompatible with \underline{h}^2), all recombinants will be \underline{h}^4 .



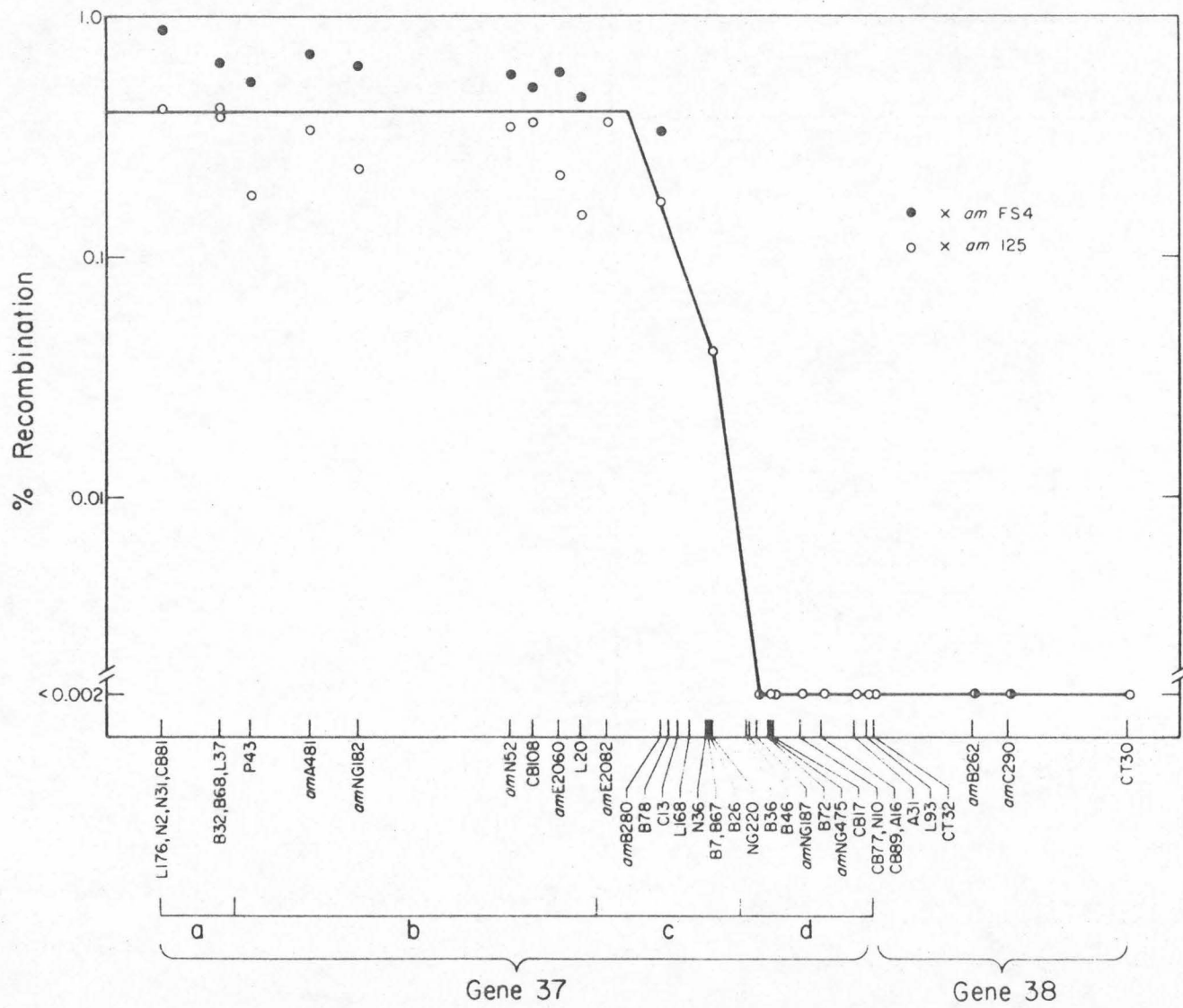
To simplify the discussion of these results, gene 37 has been divided into 4 segments, a, b, c, and d (see Fig. 2a). As will be seen T⁴ phage carrying mutations in the same segment behave similarly in these crosses.

(i) T2 aml25 and T2 amFS4 x T4 mutants. Figure 2a and Table 2 show the results of crosses of T2 aml25 in gene 38 and T2 amFS4 in segment d of gene 37 with T⁴ am and ts mutants defective in genes 37 and 38. These crosses gave two types of results. If the T⁴ mutations were in segment d or gene 38, few if any recombinants were recovered. When the T⁴ mutants were in segment a, b, or c, am⁺ts⁺ recombinants were recovered but all were h⁴. In none of the crosses were any h² recombinants found. Therefore, these crosses are analogous to the second possibility diagrammed above, and the region opposite aml25 and amFS4 (segment d and gene 38, Fig. 2a) must determine h⁴. Since no recombinants were formed when both the T2 and T⁴ mutations were in segment d or gene 38, this region in addition to determining host range must either be non-homologous, specify incompatible polypeptides, or both.

Crosses with T⁴ mutants in the rest of gene 37 yield about 0.5% of recombinants all of which are h⁴. Since these recombinants incorporate at least that part of T2 gene 37 opposite the T⁴ mutation, the left hand part of the T2 gene, segments a, b, c, must not contain a region which specifies h². Since all of the hybrids contain T⁴ gene 38 and it must interact with a T⁴ site in gene 37, this site cannot be in segments a, b, or c, but must be in segment d.

In crosses between two T⁴ mutants or two T2 mutants, the frequency of recombinants increases as the distance between the two mutations

Fig. 2. T2:T4 intertype crosses in genes 37 and 38. Forty am and ts mutants in T4 genes 37 and 38 were crossed to three am mutants in T2 gene 37 and to aml25 in T2 gene 38 (see legend, Table 2). Each graph represents the results of crossing one or two of the T2 mutants to most of the T4 mutants. Both h^2 (Δ) and h^4 (O or \bullet) recombinants are represented when present. a. T2 aml25 (O) and T2 amFS4 (\bullet) by T4 mutants. b. T2 aml23 by T4 mutants. c. T2 aml29 by T4 mutants. The abscissa of the graphs is the genetic map of T4 genes 37 and 38 constructed as described in the text. The prefix ts has been omitted from the designation of all ts mutants. % recombination was calculated as $(\frac{am^+ ts^+}{total\ progeny}) \times 200\%$.



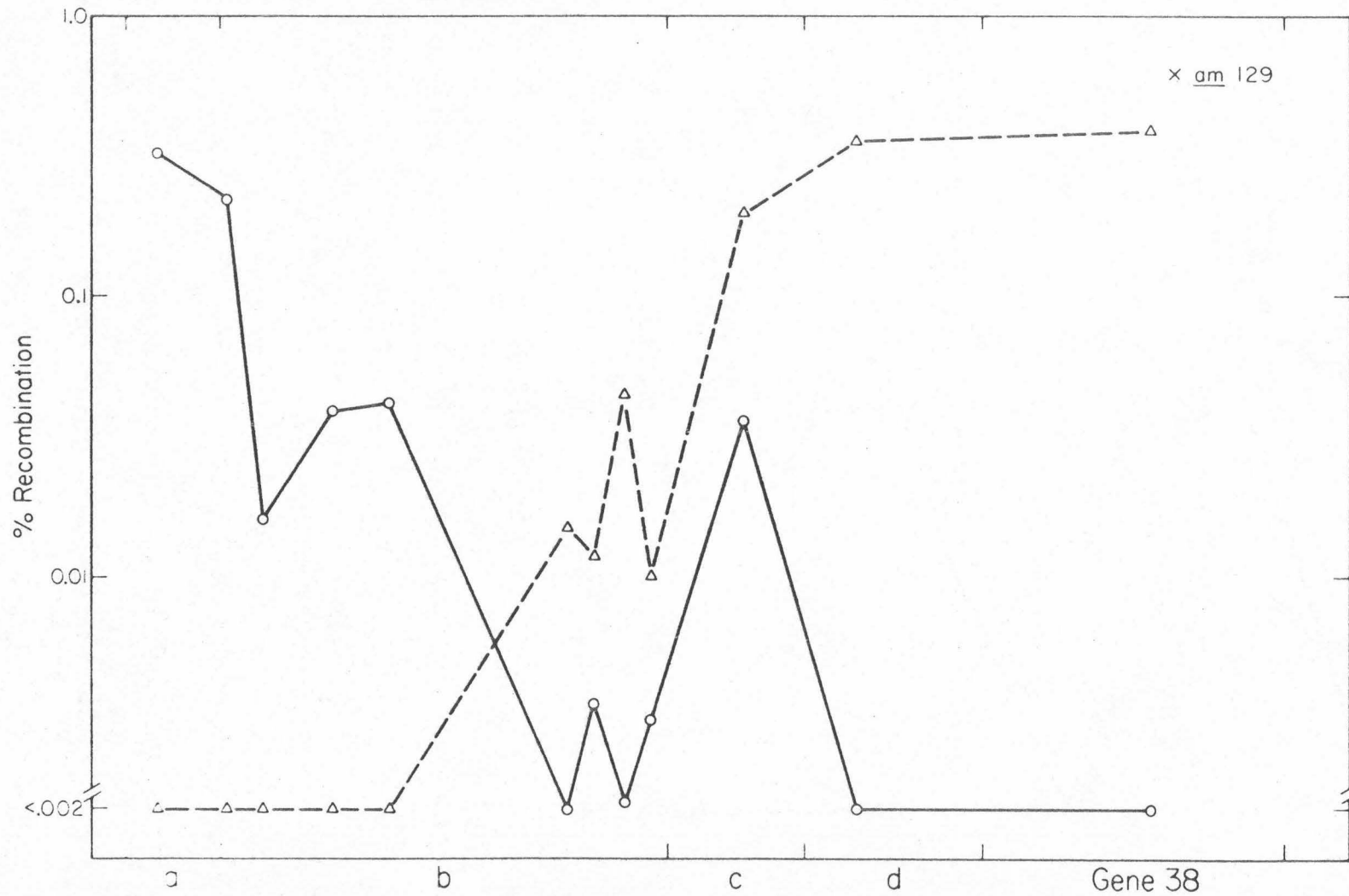


Table 2

Intertype Recombination in Genes 37 and 38

T4 mutants	T2 Mutants					
	<u>aml25</u> <u>h</u> ⁴	<u>amFS4</u> <u>h</u> ⁴	<u>h</u> ⁴	<u>aml23</u> <u>h</u> ²	<u>h</u> ⁴	<u>aml29</u> <u>h</u> ²
<u>tsL176</u>			.45	*		
<u>tsN31</u>			.49	*		
<u>tsN2</u>			.25	*		
<u>tsCB81</u>	.41	.88	.63	*	.32	<.01
<u>tsB32</u>			.26	*		
<u>tsB68</u>	.41		.24	*		
<u>tsL37</u>	.38	.64	.21	*	.22	<.02
<u>tsP43</u>	.18	.53	†	*	.016	†
<u>amA481</u>	.34	.70	†	†	.039	.0017
<u>amNG182</u>	.23	.61	†	.0013	.041	.0019
<u>amN52</u>	.35	.57	.0023	.067	†	.015
<u>tsCB108</u>	.36	.51	.0026	.021	.0035	.012
<u>amE2060</u>	.22	.59	†	.083	.0016	.045
<u>tsL20</u>	.15	.46	.0023	.042	.0031	.010
<u>amE2082</u>	.36		.042	.18		
<u>amB280</u>	.17	.33	.054	.35	.036	.20
<u>tsB78</u>			.057	.19		
<u>tsC13</u>			.026	.31		
<u>tsL168</u>			.023	.18		
<u>tsN36</u>			.020	.13		
<u>tsB7</u>			.015	.12		
<u>tsB67</u>			.018	.16		
<u>tsB26</u>			.016	.14		
<u>amNG220</u>	.040		.0062	.24		
<u>tsB36</u>			†	.29		
<u>tsB46</u>			*	.39		

Table 2 (continued)

T4 mutants	T2 Mutants					
	<u>am</u> 125	<u>am</u> FS4	<u>am</u> 123	<u>am</u> 129		
	<u>h</u> ⁴	<u>h</u> ⁴	<u>h</u> ⁴	<u>h</u> ²	<u>h</u> ⁴	<u>h</u> ²
<u>am</u> NG187	†	†	†	.24	†	.36
<u>ts</u> B72	†		*	.21		
<u>am</u> NG475	†		†	.26		
<u>ts</u> CB17	†		†	.36		
<u>ts</u> CB77	†		†	.32		
<u>ts</u> N10	†		†	.19		
<u>ts</u> A16	†		*	.18		
<u>ts</u> CB89	†		†	.18		
<u>ts</u> A31	†		*	.23		
<u>ts</u> L93	†					
<u>ts</u> CT32	†					
<u>am</u> B262	*	†	*	.47		
<u>am</u> C290	†	†	*	.51	†	.39
<u>ts</u> CT30	†		*	.23		

Phage crosses were as described in Materials and Methods. A mixture of anti-T2 and anti-T4 serum was used to inactivate unadsorbed phage. All values given are per cent recombination calculated as ($\frac{\text{am}^+ \text{ts}^+ \text{ recombinants}}{\text{total progeny}} \times 200\%$). The host range of the am^+ progeny was usually determined by plating the phage on BIX. Occasionally to confirm the host range determined from the BIX plating, plaques were transferred with a sterile pin onto three plates previously seeded with B/2, S/4, and S/6/5 respectively. * <.003% R; † <.001% R.

increases. However in these intertype crosses, the frequency of recombinants remains approximately constant throughout segments a and b. This observation suggests that almost all of the recombination is occurring in segment c and that most of the recombinants carry all of segments a and b from T2.

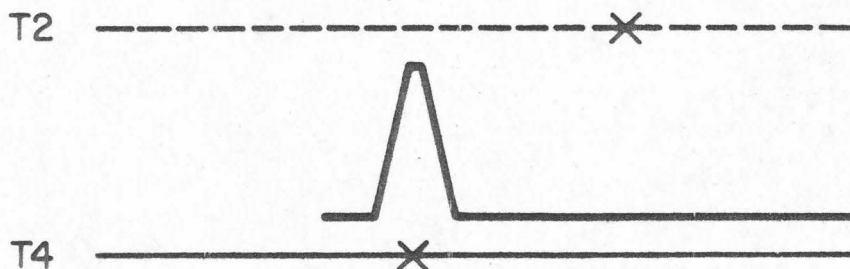
(ii) T2 aml23 and T2 aml29 x T⁴ mutants. The results of crosses with these two mutants are very similar (Table 2 and Figs. 2b and 2c). In the crosses with aml23 the lack of recombinants at the left end of segment b identifies the area on the T⁴ map opposite aml23. No such landmark locates aml29, but its position relative to the T⁴ map can be determined from the molecular weight of the am fragment produced in su⁻ cells infected with aml29 (see section 3f). This fragment of 37,000 daltons locates aml29 opposite the gap on the T⁴ map between amNG182 and amN52 (see Fig. 5).

The finding that crosses of either aml23 or aml29 by T⁴ mutants defective in gene 38 or segment d of gene 37 yield only h² recombinants, confirms that this region controls host range.

In crosses of aml23 and aml29 with T⁴ mutants defective in segment c both h² and h⁴ recombinants occur. Thus the polypeptides coded by this region must be functionally interchangeable.

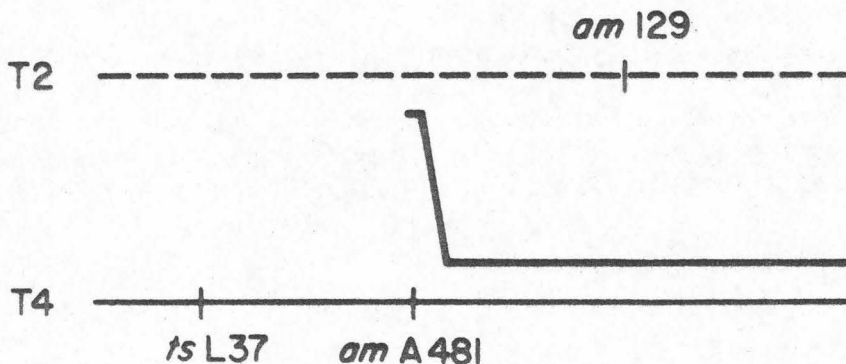
When recombination is forced to occur in segment b because both the T2 and T⁴ mutations are located in b, the number of recombinants found ranges from 5-30% of the number found when recombination can occur in other regions as well. One possible explanation of this low recombination is that the polypeptides made by this region are partially incompatible. This partial protein incompatibility would allow a small piece of

T2 protein to be incorporated from this region, but any large T2 piece combined with the predominantly T4 molecule would, according to this model, render the protein inactive. Thus to produce an active molecule two crossovers would have to occur, one on each side of the T4 marker.



This requirement for a double crossover would account for the decreased recombination in b.

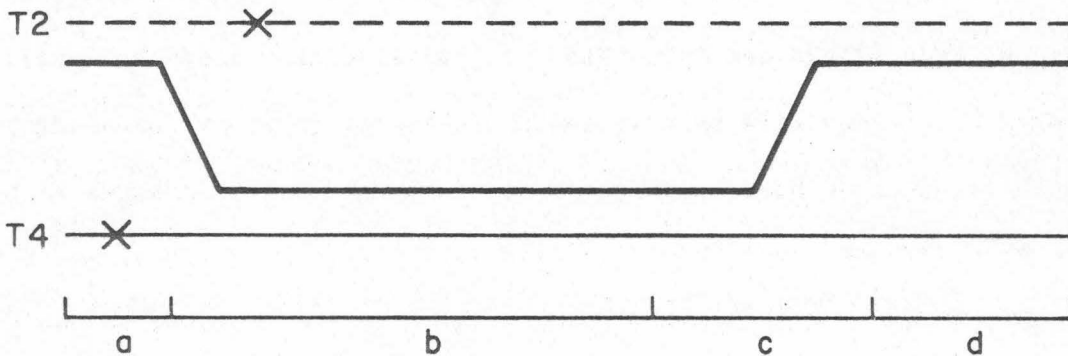
To test this hypothesis, the T4 double mutant tsL37:amA481 was constructed and crossed to T2 am129.



am⁺ recombinants were selected and tested for the presence of the ts marker. If protein incompatibility were causing the low recombination, a large majority of the am⁺ recombinants should carry tsL37. The results showed that only 4.1% of the am⁺ recombinants were also ts. Thus the most likely explanation for the low recombination in segment b is that the DNA molecules are partially nonhomologous. Direct evidence for partial

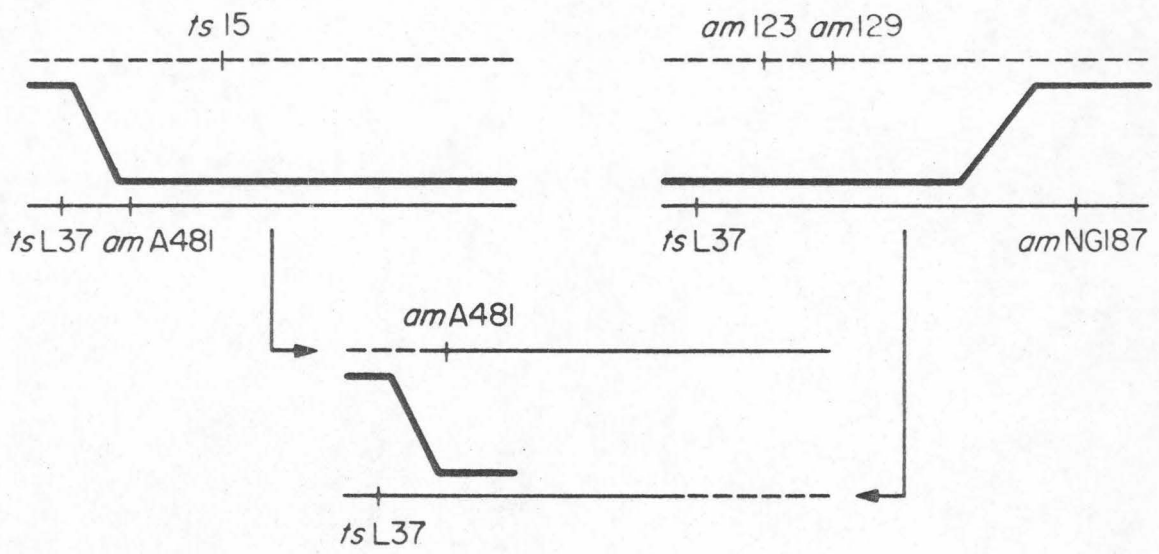
nonhomology in this region is presented in section 3c.

When the T⁴ mutations are in segment a the total number of recombinants is similar to that in c and d, yet no h² recombinants have been found. Since both aml23 and aml29 are in segment b, recombinants in these crosses must incorporate T2 segment a and T⁴ segment b. The lack of h² recombinants would be explained if the combination of the T2 polypeptide coded by segment a with the T⁴ polypeptide coded by segment b caused the phage to have T⁴ host range. Alternatively, since the formation of h²'s in these crosses requires a double crossover, the double



recombinants might be so infrequent that they were not detected. To distinguish these possibilities we constructed two hybrid strains. am⁺ts⁺ recombinants from a cross between these strains will contain T2 segment a and T⁴ segment b, but h² recombinants will be formed by a single crossover, h⁴ recombinants by a double (see Fig. 3). When these strains were crossed 29% of the progeny were am⁺ts⁺h² and 15% were am⁺ts⁺h⁴. These results

Fig. 3. Construction of hybrid phage for test of recombination between segments a and b. The dotted lines represent T2 gene 37 and the thin solid lines represent T4 gene 37. The heavy solid lines represent the selected recombinant. T2 ts15 maps near aml29 and to its right. In the cross T2 ts15 x T4 tsL37:amA481, ts⁺ recombinants were selected and tested for the presence of amA481. In the cross T2 aml23:aml29 x T4 tsL37:amNG187, am⁺ recombinants were selected and tested for the presence of tsL37. In the final cross am⁺ ts⁺ recombinants were selected and scored for host range by plating on BIX.



demonstrate that the combination of T2 segment a and T4 segment b does not specify h⁴ and suggest that the absence of h²'s in the previous crosses was due to nonhomology in segment b which prevented double recombinant formation. In the test cross just described double recombinants (am⁺ts⁺h⁴) were formed at a high frequency, probably because segments b and c of the parental phage were homologous.

(c) DNA heteroduplex mapping of the host range region

Heteroduplex DNA from a mixture of T2 and T4 phage (T2/T4 heteroduplex) shows a characteristic pattern of substitution and deletion loops when examined in the electron microscope. This pattern of loops has been oriented relative to the standard T4 genetic map by using deletions of genes e and rII as markers (Kim and Davidson, 1972). Plate 1 is an electron micrograph of the region near genes 37 and 38. The top line of Figure 4 is a schematic representation of the loop pattern in this region. Loop 4 is present in all T2/T4 heteroduplexes. In contrast loops 2 and 3 are present in only about 50% of the heteroduplexes and are quite variable in size. Occasionally loops 1 and 2 or loops 2 and 3 open up together. Unless it is combined with loop 2, loop 1 is present in all T2/T4 heteroduplexes. These results indicate that from the right end of loop 1 to the right end of loop 3 the T2 and T4 strands are partially non-homologous. In loops 1 and 4 the T2 and T4 strands appear completely nonhomologous by this technique, while in the regions between 0 and 1 and between 3 and 4 they appear completely homologous.

By making heteroduplexes between T2 or T4 and the phages which have a hybrid gene 37, it is possible to map the crossover points (XOP's) of the hybrids onto the heteroduplex loop pattern, as shown by the following examples. hy54 is an am⁺ recombinant from the cross T4 amE2060 x

Plate 1. Electron micrograph of the host range region of a T2/T4 heteroduplex. Heteroduplex molecules were prepared and visualized as described in Materials and Methods.

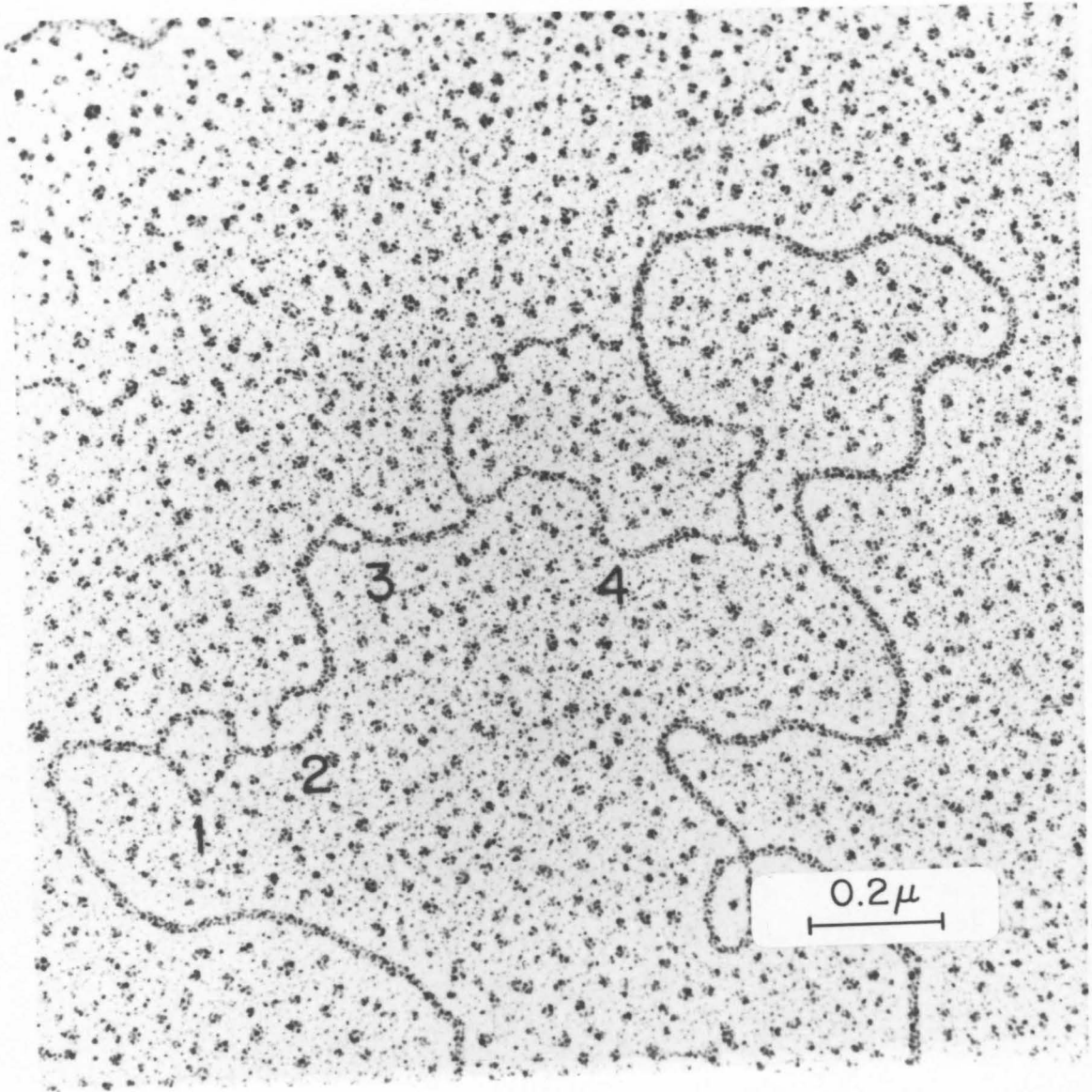
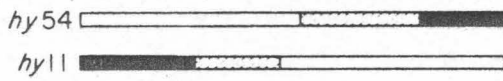
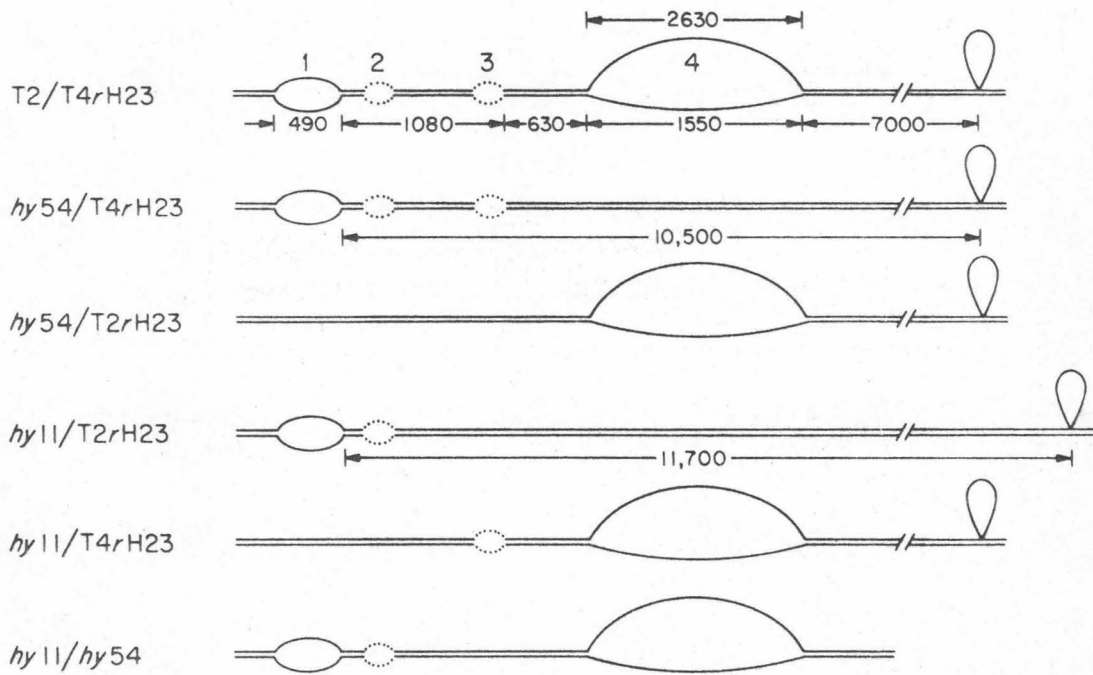


Fig. 4. Heteroduplex loop patterns. Heteroduplex molecules were prepared, visualized and measured as described in Materials and Methods. The loops are numbered 1-4 to correspond to Plate 4. Dimensions are given in nucleotides.



T2 aml25. It has T4 host range and from the results in Figure 2a its XOP must be between amE2060 and the h determinant. A heteroduplex between hy54 and T4 rH23 shows loops 1, 2, and 3 but not 4 (Fig. 4). Thus hy54 must be homologous with T4 in the region of loop 4, but not in the region of loops 1, 2, and 3. The heteroduplex hy54/T2 rH23 demonstrates that hy54 is homologous with T2 in the region of loops 1, 2, 3 and confirms that it is homologous with T4 in the loop 4 region. These two heteroduplex patterns locate the XOP in hy54 between loops 3 and 4.

hy11 is an am⁺h² recombinant from the cross T4 amN52 x T2 aml23. Heteroduplexes between it and T2 or T4 indicate that the region of loops 1 and 2 is homologous to T4 and the region of loops 3 and 4 is homologous to T2 (Fig. 4). Then the XOP in hy11 is between loops 2 and 3, confirming our expectation from the genetic results that the XOP's in hy11 and hy54 are at different points. The heteroduplex hy11/hy54 has loops 1, 2, and 4 but is homologous in the region of loop 3 as predicted from the above results.

From the two heteroduplexes hy54/T4 rH23 and hy11/T2 rH23 it is possible to establish that the longer strand in loop 4 comes from T2 and the shorter from T4. In hy54/T4 rH23 the distance from the rII deletion loop to the right end of loop 1 is 10,500 nucleotides. In this case the region corresponding to loop 4 is duplex T4 DNA. In hy11/T2 rH23 the loop 4 region is duplex T2 DNA and the distance from the rII deletion to the right end of loop 1 is 11,700 nucleotides. Therefore the T2 DNA in loop 4 is longer--1200 nucleotides from this calculation, 1080 nucleotides from directly measuring the strands of the loop.

A number of other hybrid phage have been heteroduplexed with T2 or T4 and the resulting loop patterns determined (Table 3). The results

Table 3

Heteroduplexes of Hybrid Phage

Heteroduplex	XOP	Host Range	Number of molecules with				Total number of Molecules
			Loop 1	Loop 2	Loop 3	Loop 4	
hy11/T2rH23	.21-.48	<u>h</u> ²	9	4	0	0	9
hy11/T4rH23			0	0	6	7	7
hy54/T2rH23	.52-.85	<u>h</u> ⁴	0	0	0	9	9
hy54/T4rH23			23	14	9	0	23
hy11/hy54			9	3	0	9	9
hy1/T4B	.35-.68	<u>h</u> ²	0	0	0	16	16
hy2/T4rH23	.52-.85	<u>h</u> ⁴	6	4	4	0	6
hy44/T2rH23	.21-.85	<u>h</u> ²	7	4	3	0	7
hy44/T4rH23			0	0	0	16	16
hy215/T2rH23	.80-.85	<u>h</u> ⁴	0	0	0	20	20
hy217-5/T4	.35-.58	<u>h</u> ²	13	8	5	0	13

The XOP's and host ranges given refer to the hybrid phage in each heteroduplex. The XOP's are expressed as fractions of gene 37 and were calculated from the position of the appropriate am mutations on the genetic and translational maps (Fig. 2a, Table 4). The heteroduplex molecules were prepared and visualized as described in Materials and Methods.

demonstrate that the origin of the DNA in the region corresponding to loop 4 determines the host range of the phage.

The location of XOP's in two different regions of the heteroduplex loop pattern and the correspondence of the h determinant with loop 4 partially align T⁴ genes 37 and 38 with the heteroduplex map. To directly compare the results of the intertype crosses with the regions of non-homology, we need a physical map of mutations in gene 37 and a precise way of positioning it relative to the heteroduplex loop pattern. These requirements are met in the next section.

(d) Translational mapping of T⁴ gene 37

Since polypeptide chain termination occurs at the amber codon under nonpermissive conditions, the site of an amber mutation can be physically positioned within a gene by determining the relative sizes of the wild type product and the amber fragment, using the technique of polyacrylamide gel electrophoresis in the presence of sodium dodecyl sulfate (SDS). ¹⁴C-labeled lysates of T⁴ and seven different T⁴ gene 37 am's grown under nonpermissive conditions were analyzed on discontinuous SDS gels (Laemmli, 1970). From autoradiographs of the gels we were able to identify five P37 amber fragments (Plate 2) and, by comparison with a standard curve, to determine their molecular weights (Table 4). Two other fragments, that from amB280 and that from amN52, were not visible apparently because they coelectrophoresed with other bands. To visualize these fragments we constructed multiple mutants carrying either amB280 or amN52 and am mutations in genes whose product was thought to be obscuring the P37 fragment. Gels of these multiple mutants revealed that the amB280 fragment runs at the same position as P20 and the amN52

Plate 2. Identification of P37⁴ am fragments. ¹⁴C-labeled lysates were prepared as described in Materials and Methods and electrophoresed on 7.5% discontinuous polyacrylamide gels containing SDS. After staining and destaining the cylindrical gels were sliced longitudinally. The slices were dried and autoradiographed on Kodak No Screen X-ray film. The differences in absolute migration of corresponding bands in the three groups reflects normal daily fluctuations.

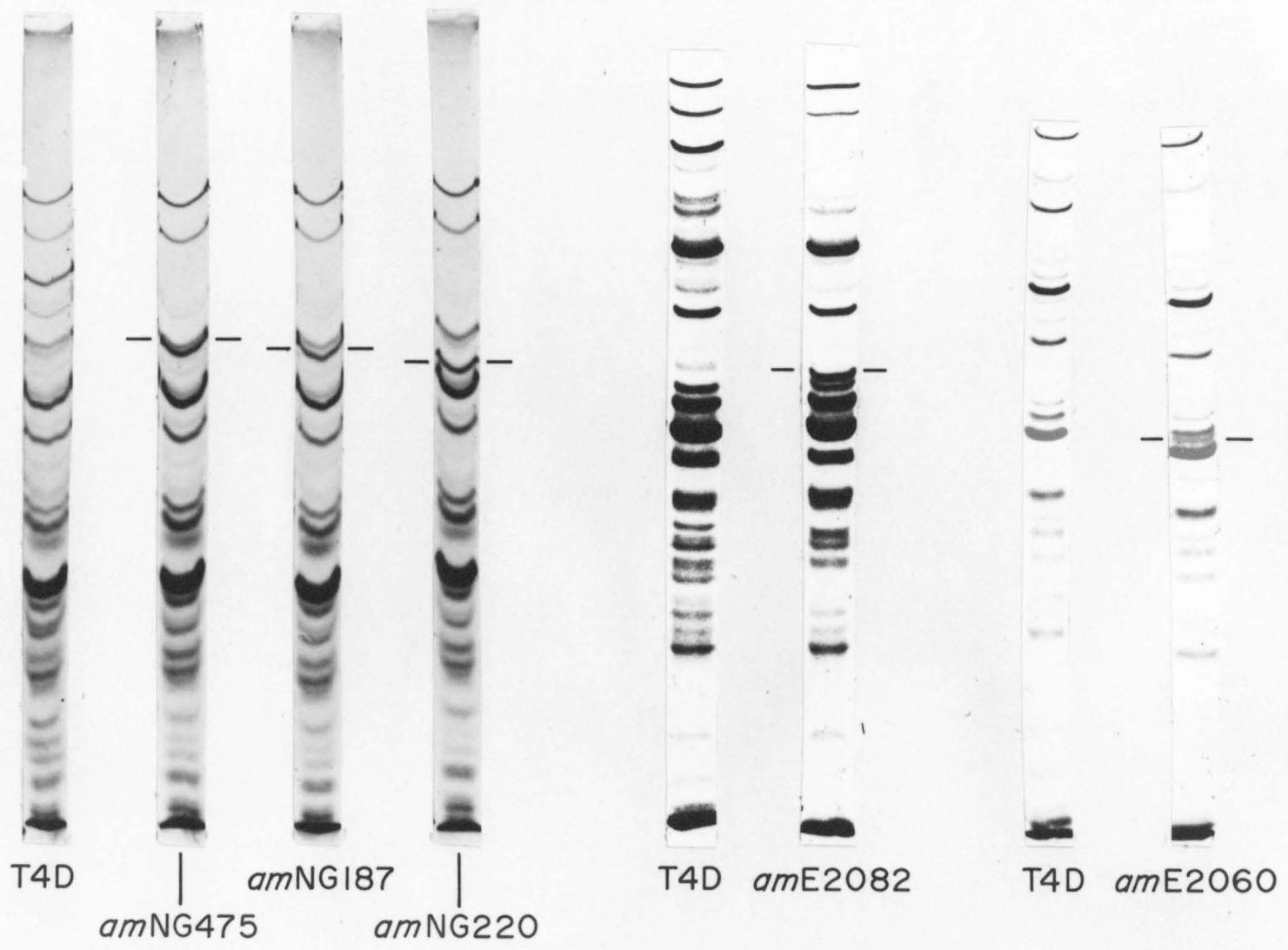


Plate 3. Identification of amb280 and amN52 fragments in multiple mutants. For procedure see Plate 2. Mutants used: 20⁻ - amN50; 23⁻24⁻ - amb272 amb26.

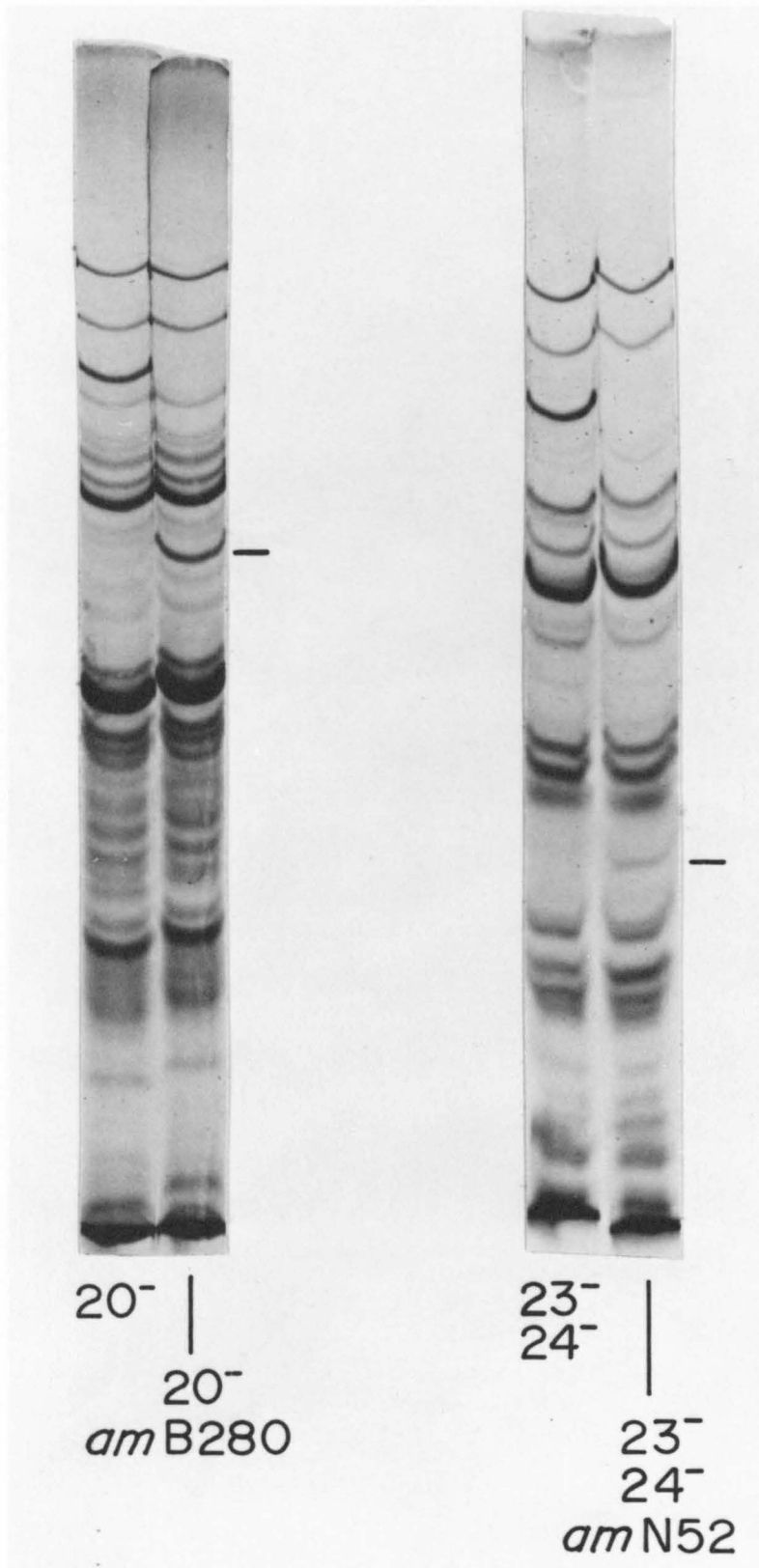


Table 4

Molecular Weights of P37⁴, P37², and Amber Fragments of Each

	MW($\times 10^{-3}$)
P37 ⁴ <u>am</u> Fragments	
<u>am</u> N52	50
<u>am</u> E2060	55
<u>am</u> E2082	61
<u>am</u> B280	72
<u>am</u> NG220	84
<u>am</u> NG187	89
<u>am</u> NG475	90
P37 ⁴	105
P37 ² <u>am</u> Fragments	
<u>am</u> 129	37
<u>am</u> FS4	124
P37 ²	120

Molecular weights of the gene products and am fragments was determined by comparing their migration on SDS polyacrylamide gels with the migration of standard proteins as described in Materials and Methods and Beckendorf & Wilson (1972).

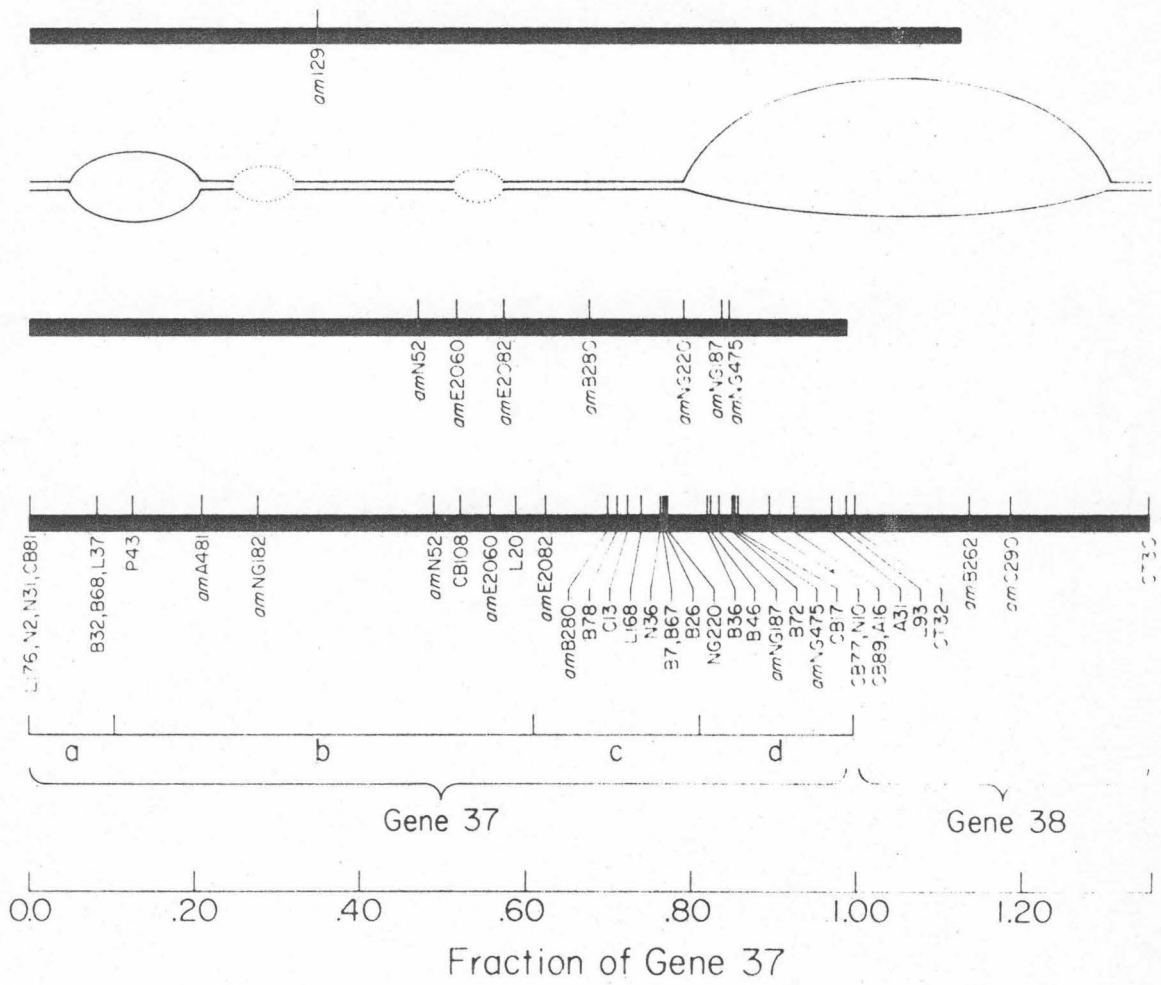
fragment runs very close to the position of P23 (Plate 3). From the molecular weights of these two fragments (Table 4) and the previously determined five fragments, we have constructed the translational map of T4 gene 37 shown in Figure 5.

The nearer the am mutation is to the right end of gene 37, the larger is the size of the am fragment. Thus the direction of translation is from left to right. Studies of the polarity of a gene 36 am mutation (amE1) on the production of P37 and the polarity of a gene 37 am mutation (amN52) on the production of P38 have shown that the direction of transcription of gene 37 is also from left to right (King and Laemmli, 1972).

This translational map can be aligned with the DNA heteroduplex map in the following way. hy215 is an am⁺ recombinant from the cross of T4 amNG220 by T2 am125. Therefore amNG220 must be located to the left of the XOP in this hybrid. hy217-5 is an am⁺ recombinant from the cross of T2 am129 by T4 amE2082 rdf41; amE2082 must be to the right of the XOP in this hybrid. Heteroduplexes of these hybrids with T2 rH23 show that the XOP's in both hybrids lie between loop 3 and loop 4 (Table 3). Thus both am mutations must also lie between loops 3 and 4. The distance from loop 3 to loop 4 is about 630 nucleotides (Fig. 4). The same figure, 630 nucleotides, is obtained when the interval between the two am mutations is calculated from their separation on the translational map (assuming 3 nucleotides per amino acid and an average residue molecular weight of 110 per amino acid). Therefore we have aligned the translational and heteroduplex maps so that amE2082 coincides with the left end of loop 4.

This alignment permits the left end of gene 37 to be located on

Fig. 5. Comparison of heteroduplex, translational, and genetic maps of genes 37 and 38. From top to bottom the maps are T2 gene 37 translational map, T2/T⁴ heteroduplex map of genes 37 and 38, T⁴ gene 37 translational map, T⁴ genetic map of genes 37 and 38. The scale at the bottom is calibrated in fractional parts of T⁴ gene 37. The maps were oriented so that the ends of T⁴ gene 37 were aligned. The prefix ts has been omitted from the designation of all ts mutants.



the heteroduplex map. The amber fragment of amNG220 is 84,000 daltons, which corresponds to 2310 nucleotides. The left end must then be 2310 nucleotides to the left of the left end of loop 4 or 110 nucleotides to the left of loop 1. By similar calculations the right end of gene 37 is within loop 4, 560 nucleotides from the left end.

The alignment of the translational and heteroduplex maps also determines the positions of the seven translationally mapped am mutants on the heteroduplex map (Fig. 5). To understand the results of the intertype crosses, it would be useful to know the positions of the ts mutants and the other am mutants as well. The genetic map can be used to locate these positions, since the frequency of recombination per unit length is nearly constant throughout the gene. Figure 6 compares the am fragments map with the recombination map by plotting the per cent recombination per 1000 mol. wt. of protein (R_{1000}) for each interval on the translational map. Since the value of R_{1000} varies only slightly throughout the gene (.12-.36), the genetic map can be aligned with the two physical maps as shown in Figure 5.

(e) Translational mapping of T2 gene 37

In SDS polyacrylamide gel patterns of ^{14}C -labeled lysates of T4-infected cells, the three most slowly migrating bands have been identified as P34, P7, and P37 (King and Laemmli, 1972; Ward and Dickson, 1972; King and Laemmli, in preparation). When a gel pattern from T2-infected cells is compared with the T4 pattern, it is clear that bands corresponding to P34 and P7 are present but that no band corresponding to P37⁴ is present. Instead another band, which migrates more slowly than P7, is present in the T2 pattern (Plate 4). This new band is P37²,

Fig. 6. Comparison of genetic and translational maps of T₄ gene 37. The heavy bar near the bottom of the graph is the translational map of the gene with am mutants located along it. R_{1000} , the per cent recombination per 1000 mol. wt. of protein, is plotted for each interval on the translational map.

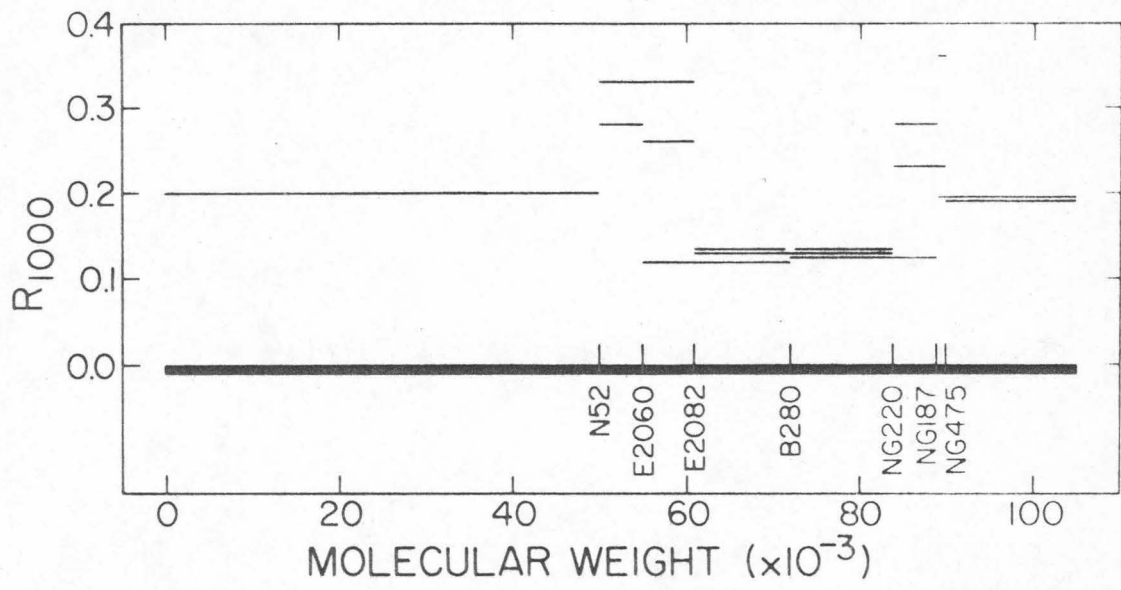
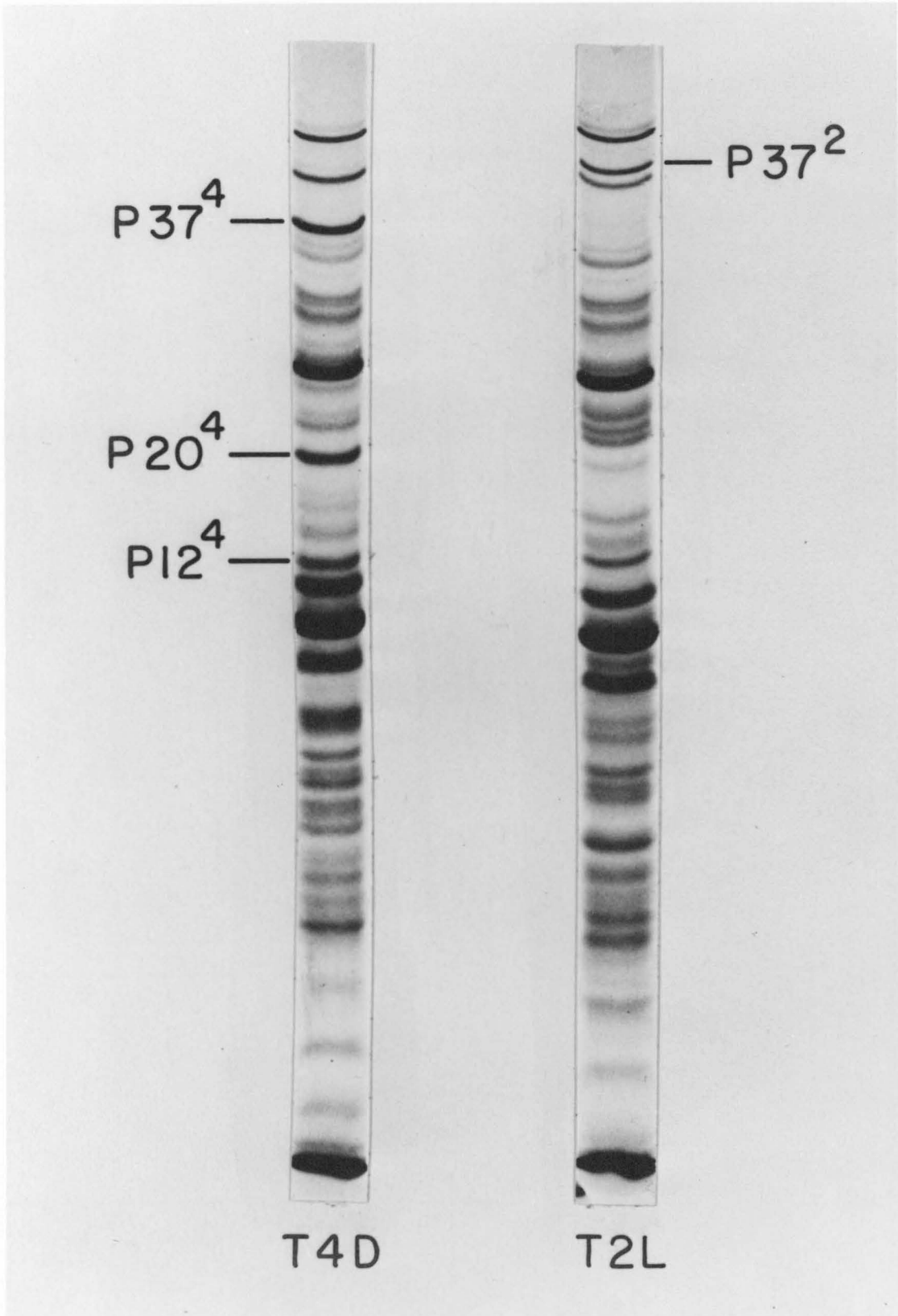


Plate 4. Comparison of T⁴D and T²L proteins. For procedure see Plate 2. Besides the difference in mobility of P₃₇, a number of other bands do not correspond on the two gels, notably P₂₀ and P₁₂.



as shown by its basence in T2 aml23- and aml29-infected cells (Plate 5). The difference in the rates of migration of the two polypeptides suggests that P37² is 13,000 mol. wt. larger than P37⁴ (Table 4).

The molecular weights of T2 gene 37 am fragments were determined in the same way as the T4 fragments. Two of the three T2 gene 37 mutants produced recognizable am fragments (Plate 5). The molecular weight of the aml29 fragment is 37,000 which places aml29 opposite the large gap in the T4 genetic map (Fig. 5), as expected from the reversal of h² and h⁴ frequencies in this region in the crosses of aml29 by the T4 mutants (Fig. 2c). The amFS4 gel shows no band at the position of P37², but there is a band with lower mobility between the positions of P37² and P34. A gene 22 am fragment with a lower mobility than the wild type product has previously been reported (Laemmli, 1970), but no explanation for this effect has been found.

(f) Location of the molecular weight difference between P37² and P37⁴

To determine whether the molecular weight difference between P37² and P37⁴ is localized in one part of the gene or dispersed throughout it, we analyzed ¹⁴C-labeled lysates made with hybrid phages which have part of their gene 37 from T2 and part from T4. As shown in Plate 6 the P37 from these hybrid phages has either the mobility of P37² or P37⁴. Since there are no bands with intermediate rates of migration, the difference in molecular weight must be localized in one region of the gene. As shown in Table 5, the molecular weight difference is controlled by the right end of gene 37. If segment d comes from T2, the P37 band corresponds to P37²; if d comes from T4, the P37 band corresponds to P37⁴.

Plate 5. Identification of P37² and its am fragments. For procedure see Plate 2. The banding pattern on the first gel is identical to that of T2L. No am fragment can be seen on the aml23 gel.

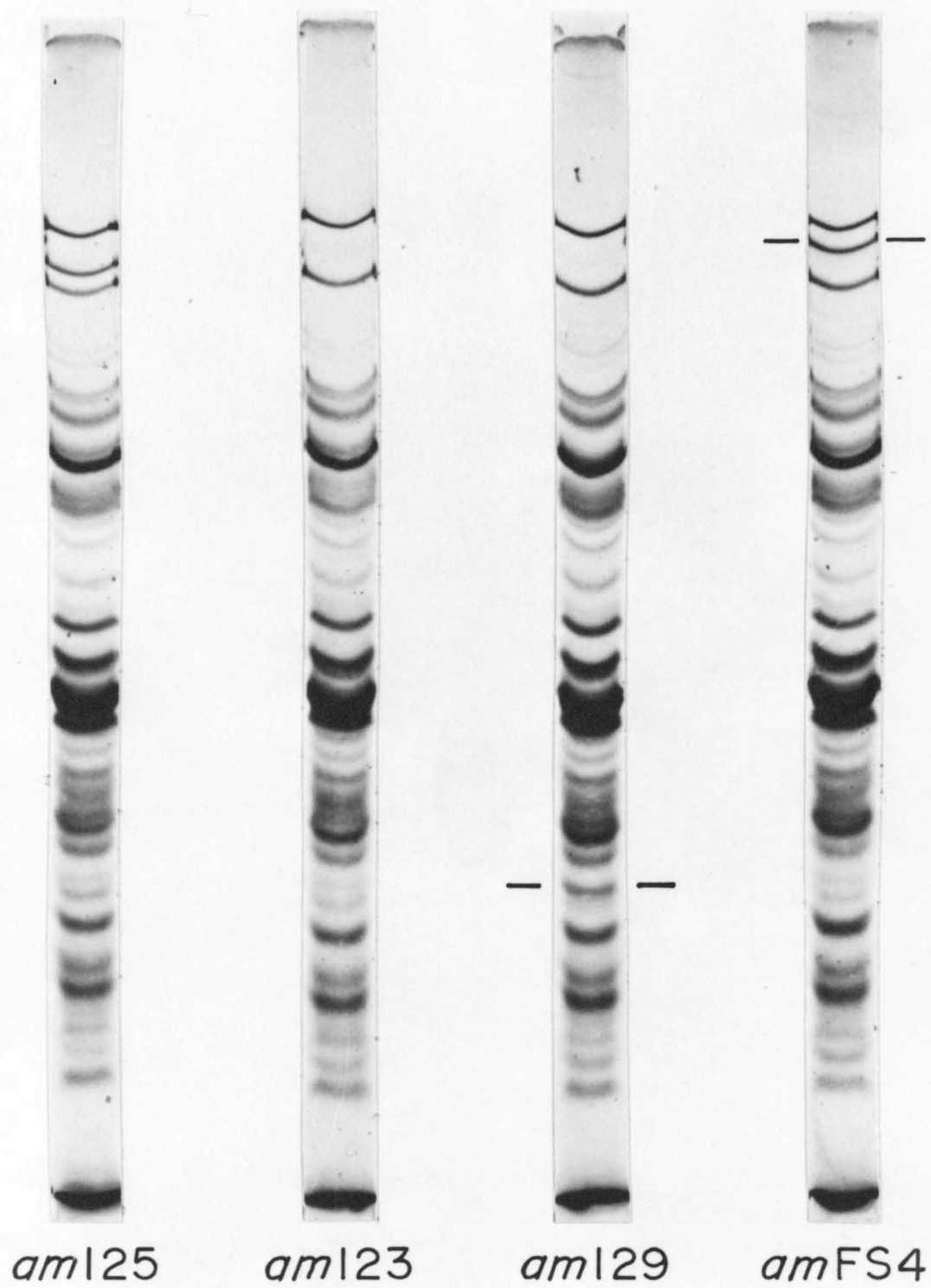


Plate 6. Migration of P37 in T2:T4 hybrid phage. For procedure see Plate 2. ^{14}C -labeled lysates of four independent am⁺ recombinants from the cross T2 am123 x T4 amC290 were run on the first four gels. ^{14}C -labeled lysates of three independent am⁺ recombinants from the cross T2 am125 x T4 amE2060 were run on the last three gels. That the recombinants are in fact hybrids can be seen from the pattern of the lower molecular weight bands (compare with Plate 4). The bars at the bottom represent the composition of gene 37. The filled-in region represents T4 DNA; the open region T2 DNA. The XOP lies within the hatched region.

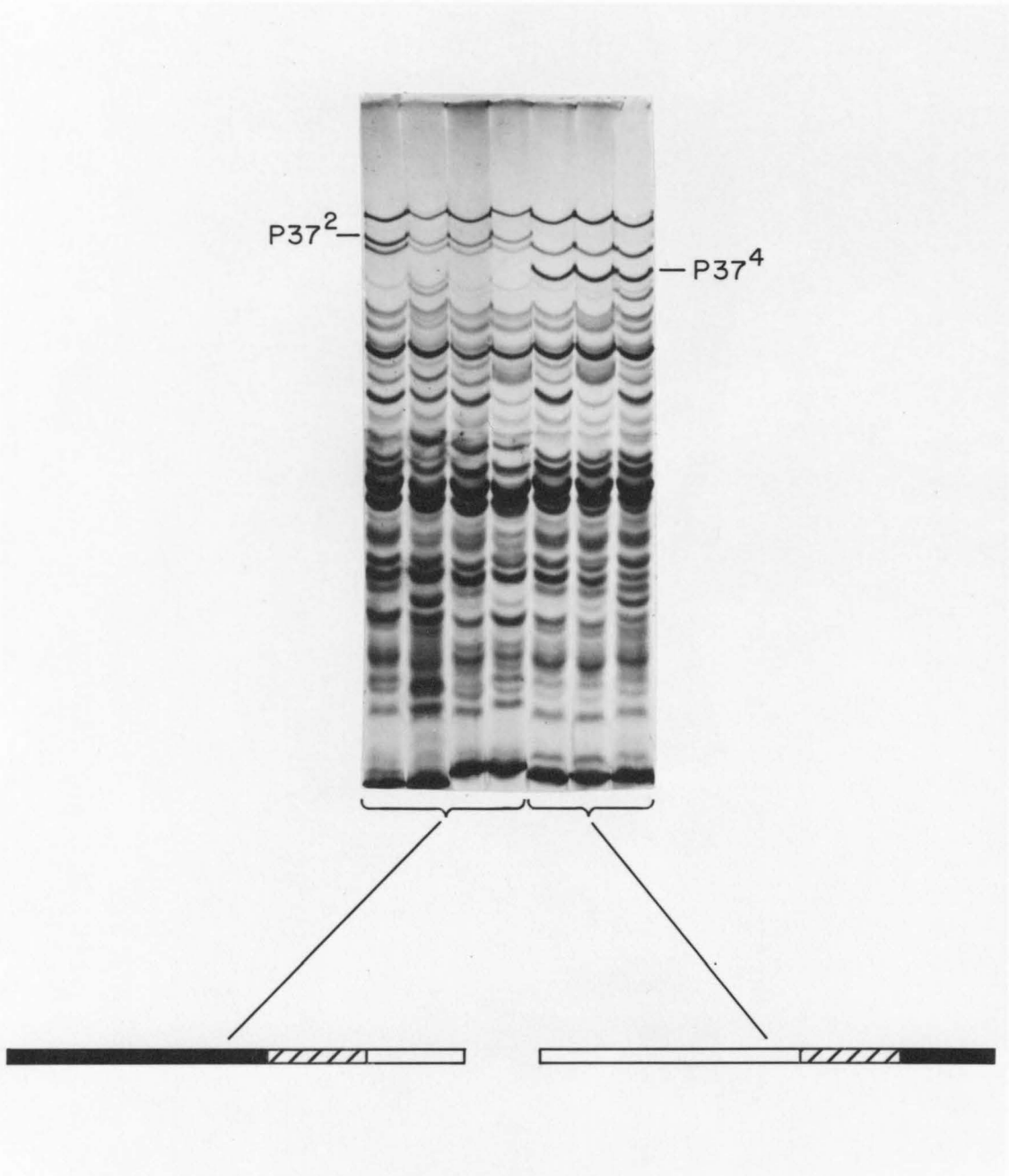


Table 5

Migration of P37 from Hybrid Phage

Hybrid	Host Range	XOP	P37 ²	P37 ⁴
<u>hy11</u>	<u>h</u> ²	.21-.48	+	
<u>hy44</u>	<u>h</u> ²	.21-.85	+	
<u>hy54</u>	<u>h</u> ⁴	.52-.85		+
<u>hy215</u>	<u>h</u> ⁴	.80-.85		+

The XOP's are expressed as fractions of gene 37 and were calculated from the position of the appropriate am mutations on the genetic and am fragment maps (Fig. 2a, Table 4).

4. Discussion

(a) Recombination frequencies between T2 and T4 markers in genes 37 and 38

It was previously noted that in T2 by T4 crosses recombination between genes 37 and 38 was much lower than expected from the T2 by T2 or T4 by T4 crosses (Russell, 1967). The results in this paper provide some explanations for this low frequency. There are two regions of genes 37 and 38 which in T2 and T4 are nonhomologous. We have not detected recombination in either of them. T2 aml23 does not recombine with two T4 mutants which are 1.7 map units apart on the T4 chromosome (tsP43 and amA481, Table 2). Although these mutants have not been physically mapped, they are opposite the nonhomologous loop 1 when the genetic map is aligned with the heteroduplex map (Fig. 5). Similarly, no recombination has been detected between mutants in gene 38 and segment d of gene 37, which correspond to nonhomologous loop 4. Also contributing to decreased recombination in gene 37 is segment b to the right of amA481, in which there is only 5-30% of the number of recombinants as in segments a and c. This low recombination is correlated with partial nonhomology of the DNA in this region.

Thus most of the recombination in genes 37 and 38 in T2:T4 crosses occurs in two relatively short regions, a and c. But even in c the frequency of recombination is strikingly low. It is possible to calculate R_{1000} for two intervals in c using the am fragment molecular weights for amNG220, amB280, and amE2082 and the recombination frequencies from crosses of T2 aml25 by these T4 mutants. These calculations give values of 0.011 and 0.017 for R_{1000} , or about tenfold less than for

T₄ x T₄ crosses in gene 37. This low value might be explained if crosses of T₂ x T₄ give drastically fewer recombinants in all regions of the map than do the T₂ x T₂ or T₄ x T₄ crosses. However, Russell (1967) found that in gene 3₄ T₂ x T₄ crosses gave 40 to 50% as many recombinants as did the corresponding T₂ x T₂ or T₄ x T₄ crosses. [These results are calculated only for the N-terminal end of gene 3₄--from amB25 to amN58 in T₄ and from aml2 to aml35 in T₂. This part of gene 3₄ does not show abnormally high values of R₁₀₀₀ (Beckendorf & Wilson, 1972).] Since DNA with a small amount of mismatching will appear annealed in the electron microscope, the low recombination in region c might be due to partial nonhomology. Alternatively a normal number of recombinants might be formed but only a few would produce active protein and thus be scored by our techniques. A third alternative is that the nonhomologous and partially nonhomologous regions flanking c might sterically inhibit pairing and genetic exchange in c. This last alternative differs from the first two by not requiring region c to be different in T₂ and T₄.

(b) Structural and functional observations

Although T₂ and T₄ are similar enough to be called members of the same species (Russell, 1967), their genes 37 and 38 have diverged sharply. At least 75% of the length of gene 37 and all of gene 38 are partially or completely nonhomologous between the two phages. This nonhomology can be separated into two classes. The functional specificities of gene 38 and segment d of gene 37 have changed during divergence while those of segments a, b and c have apparently been unaltered.

Segment d codes for two functions, the interaction of the tail fiber with its specific receptor on the bacterial surface and the interaction

of P37 and P38 during assembly of the tail fiber. Both of these functions are type specific. Whether or not the host range determinant is the same as the site of interaction between P37 and P38 has not been established. Since we have not been able to detect any recombination in d in inter-type crosses, it has not been possible to determine whether the two specificities are genetically separable. Host range mutations of T⁴ which allow it to infect T⁴ resistant strains of E. coli K12 map at two very tightly linked sites within segment d rather than throughout the segment (Beckendorf, in preparation).

Along with the functional changes, the physical sizes of segment d and possibly gene 38 have changed during the divergence of T2 and T⁴. Segment d of T2 is 60% larger than T⁴ segment d. If we assume that there is no space between genes 37 and 38 and that gene 38 extends from the end of gene 37 to the right end of loop 4, we can calculate a molecular weight for P38⁴ of 35,000. The molecular weight has been estimated from SDS gels as 26,000 (King & Laemmli, 1971). If T2 gene 38 also occupies the right hand portion of loop 4, its predicted molecular weight would be 60,000.

The functional specificity of segments a, b and c has apparently not changed during the divergence of T2 and T⁴. In the formation of hybrid phage the T2 and T⁴ protein coded by these regions has been spliced in a number of places, indicating that the proteins are functionally interchangeable. Since the DNA of segment b is largely non-homologous, it is surprising that splices in b produce active proteins. This suggests that the structure of the protein coded by b is quite simple without much interaction between amino acids which are separated

in the primary sequence.

Despite the sequence divergence of the rest of the gene, segments a and c have been conserved with the same or very similar sequences. It may be that their function is more strictly prescribed than that of segment b. As discussed in the accompanying paper the portion of P37 coded by segment a is located in the assembled tail fiber adjacent to P36 and probably interacts with it (Beckendorf, 1972). Since P36 does not seem to be type specific (Russell, 1967 and Beckendorf, unpublished), the requirement that the portion of P37 coded by segment a interact with P36 might cause its sequence to be conserved. The function of the portion of P37 coded by segment c has not been determined. Two possibilities are discussed at the conclusion of the accompanying paper (Beckendorf, 1972).

REFERENCES

- Beckendorf, S. K. (1972). Manuscript in preparation.
- Beckendorf, S. K. and Wilson, J. H. (1972). Manuscript in preparation.
- Benzer, S. (1959). Proc. Natl. Acad. Sci., Wash. 45, 1607.
- Bernstein, H., Edgar, R. S. and Denhardt, G. H. (1965). Genetics, 51, 987.
- Bernstein, H. and Fisher, K. M. (1968). Genetics 58, 307.
- Davis, R. W., Simon, M. N., and Davidson, N. (1971). Chapter in Methods in Enzymology, XXID, p. 413.
- Edgar, R. S. and Lielausis, I. (1965). Genetics 52, 1187.
- Epstein, R. H., Bolle, A., Steinberg, C. M., Kellenberger, E., Boy de la Tour, E., Chevalley, R., Edgar, R. S., Susman, M., Denhardt, G. H. and Lielausis, A. (1963). Cold Spring Harbor Symp. Quant. Biol. 28, 375.
- Georgopoulous, C. P. and Revel, H. R. (1971). Virology 44, 271.
- Jesaitis, M. A. and Goebel, W. F. (1953). Cold Spring Harbor Symp. Quant. Biol. 18, 205.
- King, J. (1968). J. Mol. Biol. 32, 231.
- King, J. (1972). J. Mol. Biol., in press.
- King, J. and Laemmli, U. K. (1972). J. Mol. Biol., in press.
- King, J. and Wood, W. B. (1969). J. Mol. Biol. 39, 583.
- Laemmli, U. K. (1970). Nature 227, 680.
- Mosig, G. (1970). Adv. Genetics 15, 1.

- Russell, R. L. (1967). Ph.D. Thesis, California Institute of Technology.
- Steinberg, C. M. and Edgar, R. S. (1962). *Genetics* 47, 187.
- Ward, S. and Dickson, R. C. (1972). *J. Mol. Biol.*, in press.
- Ward, S., Luftig, R. B., Wilson, J. H., Eddleman, H., Lyle, H. and
Wood, W. B. (1970). *J. Mol. Biol.* 54, 15.
- Westmoreland, B. C., Szybalski, W. and Ris, H. (1969). *Science* 163,
1343.
- Wilson, J. H., Luftig, R. B. and Wood, W. B. (1970). *J. Mol. Biol.* 51,
423.

Part IV

Electron Microscope Heteroduplex Studies of the DNA of a Deletion
Mutant of ϕ X-174 Bacteriophage

Jung-Suh Kim, Phillip A. Sharp, * and Norman Davidson

* Present address: Cold Spring Harbor Laboratory,
Cold Spring Harbor, New York 11724.

ELECTRON MICROSCOPE HETERODUPLEX STUDIES OF THE DNA
OF A DELETION MUTANT OF ϕ X-174 BACTERIOPHAGE

JUNG-SUH KIM, PHILLIP A. SHARP, AND NORMAN DAVIDSON

A population of double-stranded ϕ X-RF DNA molecules carrying a deletion of about 9% of the wild-type DNA has been discovered in a sample cultivated under conditions where the phage lysozyme gene is nonessential. The structures of deleted monomers, dimers, and trimers have been studied by the electron microscope heteroduplex method. The dimers and trimers are shown to be head-to-tail repeats of the deleted monomers. Some interesting examples of the dynamical phenomenon of branch migration in vitro have been observed in heteroduplexes of deleted dimer and trimer strands with undeleted wild-type monomer viral strands.

* * * * *

In our laboratory both single-stranded ϕ X-174 DNA and the nicked double-stranded intracellular form, RFII, are used as internal standards for length measurements of other DNA molecules in the basic protein film method of preparing samples for electron microscopy. The ϕ X-174 DNA samples are always gifts from members of the Sinsheimer group. We have observed that one of the RF-II ϕ X DNA samples actually consists of a mixture of two kinds of molecules: in one kind, about 9% of the DNA is deleted; the other kind is of the normal size. We report here our electron microscope studies of the structure of this

deleted DNA. Some interesting examples of the dynamical phenomenon of branch migration [Lee, Davis, and Davidson (1); Broker and Lehman (2)] have been observed in heteroduplexes of a deleted dimer strand with undeleted, wild-type ϕ X-174 DNA.

Our serendipitous discovery of a deletion mutant illustrates the effectiveness of electron microscopy as a tool for the study of DNA molecules. At the same time, Zuccarelli, Benbow, and Sinsheimer were independently conducting a systematic search for deletion mutants of ϕ X. Their biological and physical studies are reported in an accompanying publication.

MATERIALS AND METHODS

DNA. A sample (sample 1) of ϕ X-174 RF (double-stranded) DNA was given to us by Dr. John Sedat. Its history appears to be as follows: Drs. C. Hutchison and M. Edgell grew a 300-liter batch of amber 3 (lysis defective) low-reverting phage at a multiplicity of 1 using artificial lysis [according to the procedure of Hutchison and Sinsheimer (3); see also Eisenberg, Benbow, and Sinsheimer (4)]. Approximately 40% of the progeny were viable on a permissive host (Hfr 4714) indicating that the sample did not consist entirely of deletion mutants at this time. The sample was stored in a refrigerator for one year in borate buffer. J. Sedat then infected a 3-liter culture of the nonpermissive Hfr 4704 (UVR⁻) host in the presence of 30 γ /ml of chloroamphenicol (which inhibits synthesis of the viral single strands but permits multiplication of the RF form) [Komano and Sinsheimer (5)]. After 90 minutes, the sample was lysed with Brij and divided

into a pellet and a supernatant fraction. The pellet contained 10% of all the RF and was enriched in multiple length DNA. We were given a sample of the supernatant fraction which was relatively enriched in monomer forms. Sample 2 was a gift from R. Benbow. It was also derived from the original Hutchison and Edgell culture by a similar method, but had been enriched in multiple length forms by sedimentation. It is probable that the deletion mutant was present and propagated in the original 300 liter growth.

Electron Microscopy. Our electron microscope techniques have been described [Davis, Simon and Davidson (6)]. The essential point of the heteroduplex method is that if a duplex is formed by re-naturation between a complete viral (plus) strand of wild-type ϕ X DNA and a minus strand from a deletion mutant, the region present in the wild-type DNA, but deleted in the mutant, will form a single-strand loop in an otherwise duplex structure. By using suitable concentrations of formamide in the spreading solution and in the hypophase for the basic protein film technique, the single strand is displayed in an extended, measurable form (6, 7). Single-strand DNA looks a little thinner and wigglier than does double-strand DNA.

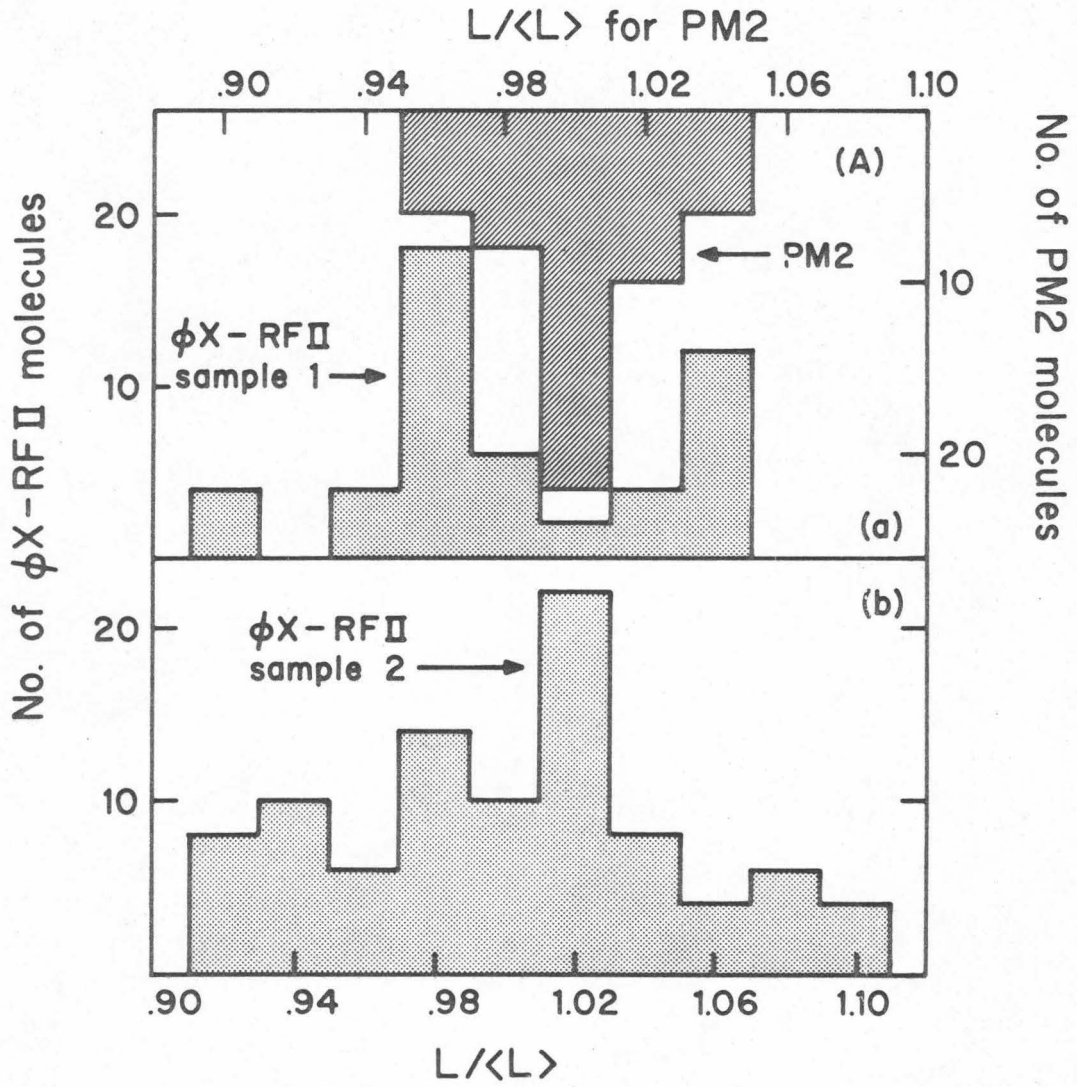
Hybridization was conducted as follows: A quantity of about 0.05 microgram of ϕ X-RF DNA and an excess of single-stranded, wild-type viral strands was denatured by treatment with 50 μ l of 0.10 M NaOH, 20 mM EDTA at room temperature for ten minutes. The sample was neutralized and renatured by adding 5 μ l of 1.8 M Tris-HCl, 0.2 M Tris-OH and 50 μ l of formamide. The renaturation time was varied from about 10 minutes to 2 hours. Self-renatured sample of the

ϕ X-RF DNA were made similarly but without adding any viral DNA. For preparing a basic protein film, 2.5 μ l of 1 mg/ml cytochrome C was added to 50 μ l of the hybridization mixture. This was spread onto 0.01 M Tris, pH 8.5, 0.001 M EDTA, 10% formamide. Grids were stained with uranyl acetate and shadowed with platinum-palladium. For heteroduplex experiments, at least a tenfold excess of single-stranded viral ϕ X DNA was present to serve as a length standard for single-strand measurements.

RESULTS

Existence of a Deletion. In a course of studies on T2/T4 heteroduplexes, we frequently mounted both ϕ X-RF (from sample 1) and λ c₂₆ DNA on the same grid as standards for double-strand length measurements. The observed length ratio was 0.105 (\pm .002). (Measurements were made only on the RF-II of the ϕ X-RF sample.) Results of many other workers in this laboratory on other ϕ X-RF samples had invariably given a ratio of 0.112 (\pm .002). Histograms of the length distribution of a homogeneous DNA (PM2) and of these two ϕ X-RF samples are shown in Fig. 1. The histogram and the length ratio to λ DNA suggest that sample 1 contains about 60% of a deleted form. To test this hypothesis, a mixture of the ϕ X-RF DNA sample and a tenfold excess of viral ϕ X single strands (mostly intact) was denatured and renatured. In the resulting preparation there were a number of heteroduplexes showing a single clear deletion loop (Fig. 2a).

Figure 1. Length distribution of PM2 DNA and of the ϕ X-RFII DNA in each of the two samples. PM2 DNA and ϕ X-RF DNA of sample 1 were on the same grid. The samples were spread from 40% formamide on to 10%.



Length measurements of the single-strand deletion loop give a size of $0.09 (\pm 0.01)$ relative to ϕX . We take the molecular weight of double λ DNA as $30.8 (\pm 1) \times 10^6$, corresponding to 46,500 nucleotide pairs (8); therefore ϕX contains 5200 nucleotides. Therefore, the deletion consists of 470 (± 100) nucleotides. (The two main peaks in the histogram of Fig. 1a suggest a deletion of $0.075 (\pm .02) \phi X$ units, in satisfactory agreement with the direct measurements.)

Sample 1 was denatured and renatured by itself. A deletion loop of the same size as seen in the heteroduplex preparation was observed. This is presumably a heteroduplex between deleted and nondeleted DNA in the sample. For sample 2, deletion loops of size 490 (± 140) and 420 (± 110) were seen in the heteroduplex and self-renatured preparations, respectively. In sample 1 homoduplexes, no structure with substitution loops, two deletion loops, or a small deletion loop were seen. Thus, within a resolution of about 50 nucleotides, only one deletion was present. When sample 2 was self-renatured, there was a low frequency of structures with two small deletion loops, suggesting that there is a low frequency of molecules with a different nonoverlapping deletion. A denatured-renatured mixture of 1 and 2 showed mainly perfect duplexes or the single deletion loop; samples 1 and 2 must have the same deletion.

Statistical considerations predict a fractional standard deviation of 0.16 in the length distribution of a homogeneous single-strand segment of length $0.09 \phi X$ units and a fractional standard deviation of 0.035 in the length distribution of a homogeneous duplex preparation

of ϕ X-RF size (6). The standard deviations of the distributions observed here are in agreement with these predictions and are thus consistent with the hypothesis of a single deletion.

Another laboratory stock of ϕ X-RF received at an earlier time as a gift from the Sinsheimer group and used frequently as a length standard contained about 1% of deleted molecules, as indicated by a heteroduplex experiment.

Structure of the Dimer. Samples 1 and 2 contained approximately 2% and 16% of the dimer forms, respectively, and slightly more than 0.2% and 3% of trimers and other multimers, respectively. The length ratios for dimer to monomer in the two samples were 2.04 (\pm .08) and 1.99 (\pm .11), respectively.

In order to ascertain whether the deleted dimer is a head-to-tail (tandem) duplication of the deleted monomer, we have observed the dimer structures after heteroduplexing a sample with an eightfold excess of circular ϕ X viral strands. Photographs of the two structures observed are displayed in Fig. 2A and 2B; schematic explanations of the structures are given in Fig. 3 as A and B. (Sample 1 consisted mostly of RF-II nicked open circular forms. In sample 2, about 60% of the molecules were nicked open circles and 40% were RF-I supercoils. The latter do not participate in heteroduplex formation. Over 90% of the ϕ X viral DNA was circular. Due to topological restrictions, only a linear strand can renature with a circular viral strand. Accordingly, in Fig. 3 we depict the heteroduplexes as having a nick in the deleted strand.) Structure B can only occur for a head-to-tail dimer. In any one heteroduplex of type A the two distances from

Figure 2.a) Electron micrograph of a monomer heteroduplex between a complete viral strand and a deleted complementary (minus) strand; the deletion loop is indicated by an arrow.

A) Heteroduplex of type "structure A" between a deleted linear dimer strand and two circular viral strands. The two deletion loops are indicated by arrows; they are equidistant from the fusion point. A schematic representation is shown in Fig. 3A.

B) Heteroduplex of "structure B"; in this structure the two deletion loops (arrows) have migrated to the fusion point; see Fig. 3B.

A' and B') Heteroduplexes of a deleted linear dimer strand with only one circular viral strand, to give structures A' and B' respectively; the deletion loop in A' and deletion strand in B' are indicated by arrows. Schematic representations are shown in Figs. 3A' and 3B'. A tracing of structure B' is shown at the lower right of Fig. 2; duplex regions are thick; single-strand regions are thinner.

E and F) Heteroduplexes of deleted trimer strands with 3 viral monomer circles. The deletion loops are indicated by arrows, schematics are in Fig. 3. A tracing of F is shown in the lower right. In this particular molecule, one of the duplex circles is incomplete because of single strand breaks, as indicated in the tracing.

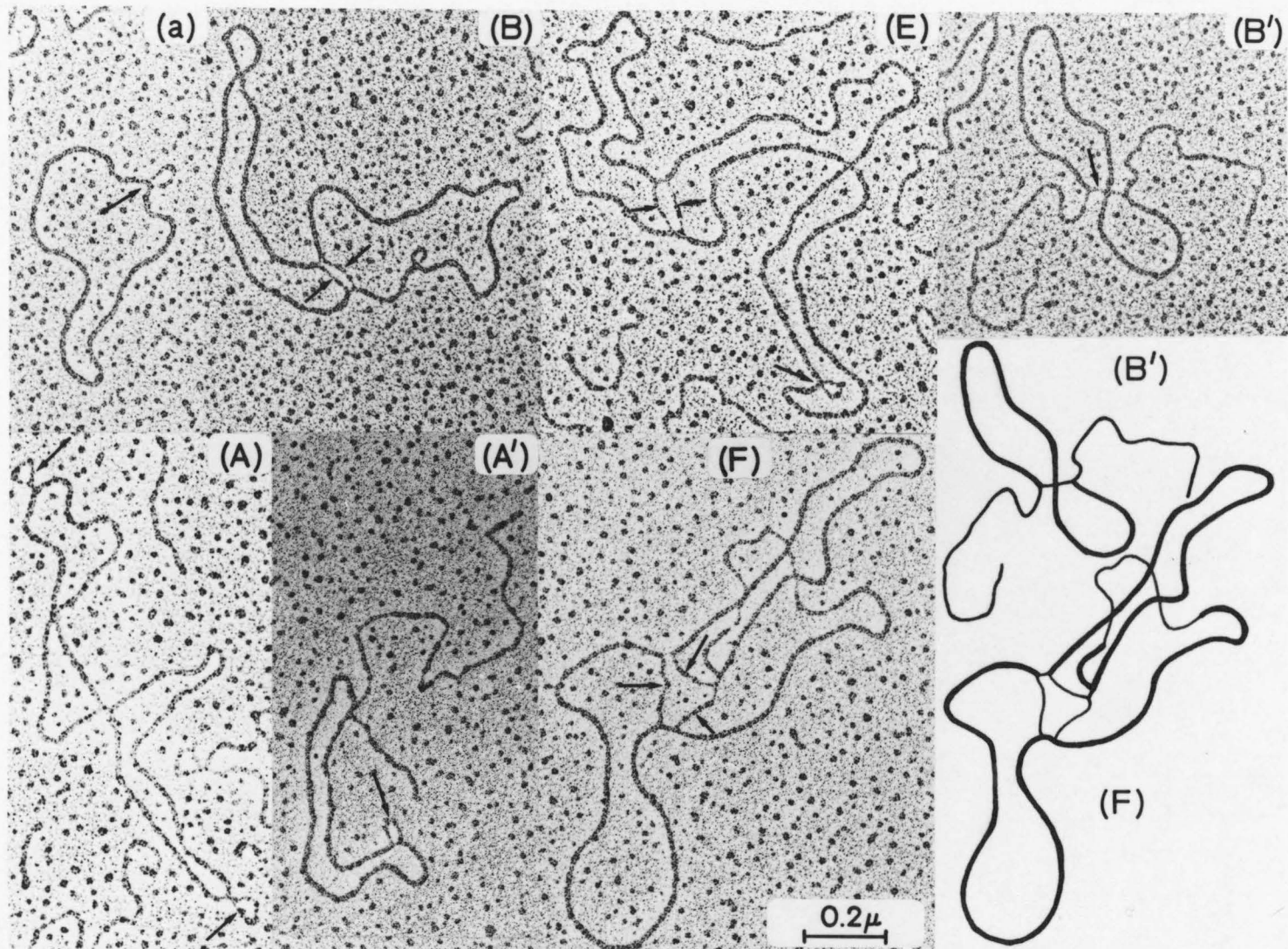
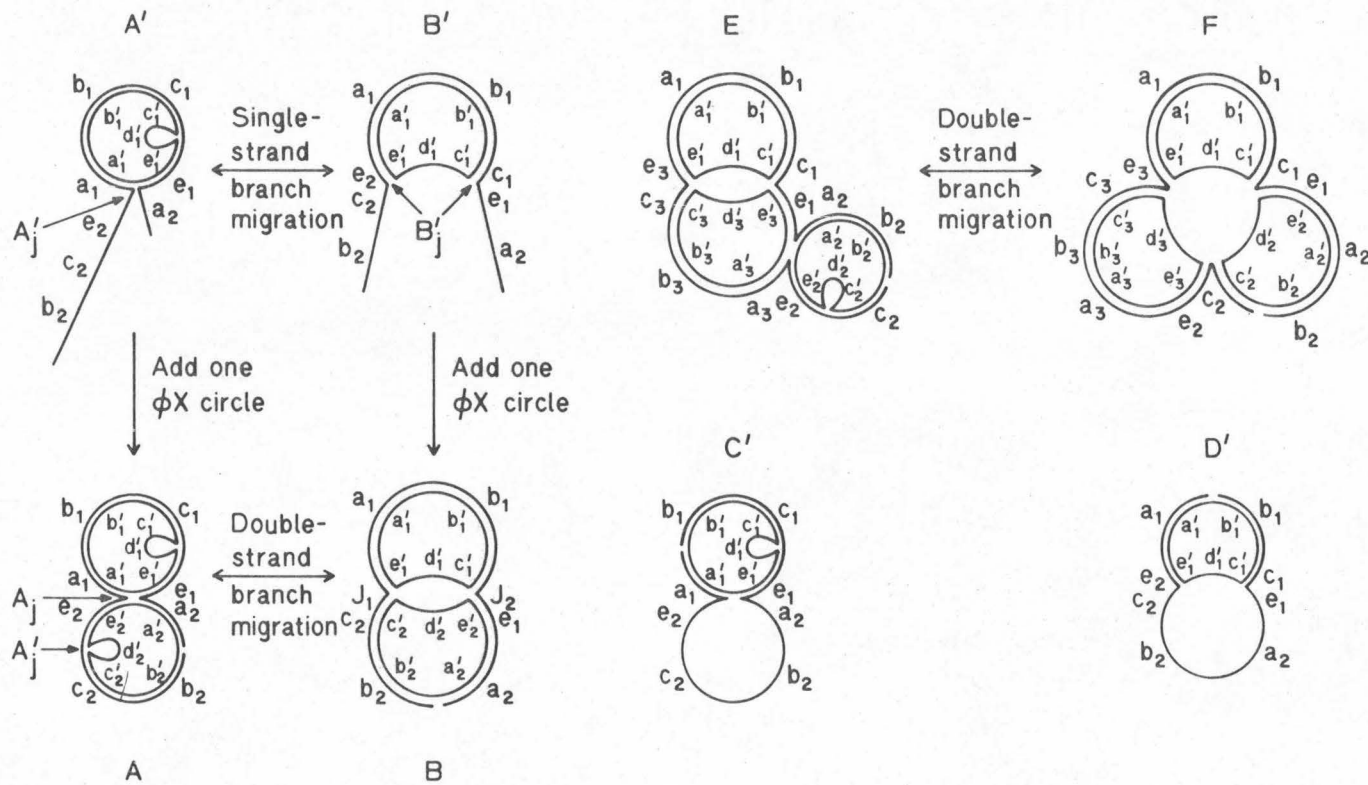


Figure 3. Schematic representations of the several heteroduplex structures for which electron micrographs are shown in Fig. 2. The symbols are explained in the text. Micrographs of structures C' and D' are not included in Fig. 2.



the fusion point of the two circles to the two deletion loops were equal. This distance was different in different heteroduplexes. (These distances are shown as the sequences e_1 and e_2 in Fig. 3A.) The only simple and reasonable interpretations of all these observations is that the dimer is a head-to-tail duplication of the monomer.

Branch Migration. One hundred-fifty examples of structure B and three examples of structure A were observed in the sample scored. Renatured structures in which a linear dimer strand had associated with only one circular viral strand were also observed. The two structures mainly seen are displayed in Fig 2A' and 2B' and are schematically depicted in Fig. 3 as A' and B'. Observations on the relative numbers of the several structures after different renaturation times are recorded in Table 1. There appear to be more B' type structures than A' by a ratio of about 2:1. This ratio seems to be independent of renaturation time.

The phenomenon of single-strand branch migration in vitro has been described (1). Its occurrence as a part of the mechanism of in vivo recombination has been proposed (9). In a structure such as A' in Fig. 3, there are two identical sequences, e_1 and e_2 , complementary to the sequence e_1' . If the sequence e_1 shown mated to e_1' dissociates, nucleotide by nucleotide, and is replaced by the identical sequence e_2 , there is no change in the number of base pairs, but the deletion loop migrates with respect to the point where the two single-strand branches emerge from the duplex circle. This is branch migration. If migration occurs to the point where the sequence d' of the wild type strand missing

Table I

Numbers of Dimer Structures as a Function of Renaturation Time*

<u>Time of Renaturation (min)†</u>	<u>A'</u>	<u>B'</u>	<u>Uncertain A'‡</u>	<u>B</u>
11	4	5		0
19	11	27	(26)	2
25	6	14	(24)	14
73	9	17		23

* The results in this table, crude as they are, have been confirmed in repeat experiments with other samples.

† Sample 2 renatured with a fourfold excess of viral strands; except that 25 minute point is with an eightfold ratio of viral strands to RF II.

‡ These are ambiguous structures. Some are due to catenanes in the preparation, some are linear strands accidentally crossing duplex circles, and some are probably true A'.

in the deleted DNA is between the two single-strand branches, structure B' results.

Similarly, in the duplex structure A, e_1 is mated to e_1' and e_2 to e_2' . By breaking and remaking base pairs, one by one, e_1 can mate to e_2' and e_2 to e_1' , resulting finally in structure B. This is the phenomenon of double-strand branch migration. Double-strand branch migration was clearly and explicitly described by Broker and Lehman (2) who postulated that it occurred in vivo as a part of the mechanism of recombination between the DNA molecules of T-even phages after infection.

If single-strand branch migration is slow compared to the rate of association of a linear deleted dimer strand with a circular ϕ X viral strand, then the observed ratio of structure B' to A' of 2:1 is an indication of their relative rates of formation from the dissociated strands. If, however, branch migration is fast, structures A' and B' rapidly interconvert, and the observed ratio is primarily determined by the equilibrium constant of the reaction $B' \rightleftharpoons A'$. It does not appear to us to be feasible, in the present system, to do decisive experiments to distinguish between the two hypotheses. We believe, however, that branch migration is sufficiently rapid so that the B' to A' ratio is approximately the equilibrium one. This surmise is supported by two considerations: (a) the B' to A' ratio is constant with time; (b) there is evidence that in the similar systems of renatured circularly permuted DNA's from the coliphage of E. coli 15 (1) and T4 (10) branch migration is rapid. The topological requirement discussed

below that one or both strands wind around through the circle as branch migration occurs may decrease the rate for the smaller circle involved in the present case, but we believe it is unlikely that this effect is large.

Structure B' can react with a circular viral strand to give structure B. Similarly, A' gives A. We expect the rate-constants of the two reactions to be about the same. Since $B'/A' \approx 2$, the ratio B/A should be 2, unless there is interconversion between A and B by double-strand branch migration. Since the observed ratio is $B/A \approx 50$, we conclude that double-strand branch migration does occur under the renaturing conditions used and that the equilibrium ratio of B to A under these conditions is about 50. We believe that this is the first direct experimental evidence for the occurrence of double-strand migration.

Several heteroduplexes of deleted trimers with three undeleted monomer circles were observed. Micrographs of the two kinds of structures seen are shown in Figs. 2E and 2F and schematically explained as structures E and F in Fig. 3. About equal numbers of structures E and F are seen. For a tandem trimer, it is a necessary condition in structures of type E that the distances e_1 and e_2 should be equal. This was observed to be the case. The three-leaf clover structure, F, is of course, consistent with the head-to-tail tandem structure of the trimer.

If the equilibrium ratio of B to A is 50, we expect an equilibrium ratio of F to E of 50, which is not in agreement with observation. The indications thus are that the system is not at equilibrium but that E may be formed by stepwise renaturation of ϕ X circles to a trimer strand and that the interconversion between structures F and E by double-strand branch migration is slow.

At present, there is insufficient information as to the factors influencing the kinetics of branch migration, especially in circular molecules. We shall, therefore, refrain from an effort to discuss the rates of all of the possible reaction paths leading to the several dimer and trimer structures observed. Several points, however, are sufficiently clear to merit discussion.

It seems probable that branch migration processes involve successive opening and closing of base pairs. Accordingly, the rate should be faster under renaturing conditions than under conditions where base pairs are very stable. Indeed, it is possible that the rate increases as the solvent conditions approach T_m .

There are topological constraints on the rate of branch migration in circular structures. In a branch migration reaction such as $A' \rightarrow B'$, one or the other of the dangling single strands (presumably the shorter) must wind around through the circle once for every ten base pairs exchanged by branch migration. This would slow down the rate for the present case as compared to that observed in linear structures or in very large circular ones (1). On the other hand, in a double-strand branch migration such as $A \rightarrow B$, the two intersecting

duplexes can rotate about their respective helix axes and it is not necessary for one circle to rotate through the other. This is easy to see by construction of a model, but hard to depict in a drawing. However, in the branch migration of the trimer structure E to F, it is necessary for the circle with subscripts numbered 2 to rotate through circle 3 once for every ten base pairs migrated. The duplex structures involved are more rigid and more extended in space than the single strands that wind through the circle for the A' → B' reaction. We therefore propose that branch migration from E to F is slow because of this topological constraint.

Equilibrium Considerations. Several structural and statistical parameters influence the relative stabilities of structures A' and B' and of A and B. These parameters are not all known with sufficient accuracy to permit a theoretical prediction of the equilibrium ratios. However, by assuming that equilibrium obtains, we can compute a numerical value for the product of several unknown parameters that occur in the theory, for use in interpreting future experiments on other systems.

There is a statistical factor, $\underline{g}_1(A')/\underline{g}_1(B')$, for structure A' relative to B' of 5000, because of the 5000 nucleotide sites at which the deletion loop can be situated around the circle in A'. A second statistical factor, $\underline{g}_2(A')/\underline{g}_2(B')$, favoring structure B', arises because of factors associated with the probability of ring closure. Structure A' consists of two closed circles; a closed duplex loop of length $\underline{L}_D = 5000$ nucleotide pairs and a closed single-strand loop of length $\underline{L}_S = 500$ nucleotides, whereas structure B' contains only a single

composite circle of duplex length, \underline{L}_D , plus single-strand length, \underline{L}_S . There are protruding single strands in both A' and B'; these have the same partition functions.

The two structures have the same number of base pairs. However, there is a difference in free energy between A' and B' because the two structures have different kinds of junctions between duplex regions and single-strand regions. Denote this factor by $\underline{g}_3(A')/\underline{g}_3(B')$.

The quantity $\underline{g}_2(A')/\underline{g}_2(B')$ may be calculated according to the well known Jacobsen-Stockmayer (11) treatment for ring closure in random coils as follows: The statistical weight of a circular duplex, relative to a linear duplex, is $(3/2\pi \underline{L}_D \underline{b}_D)^{3/2} d\underline{V}_D$, where \underline{b}_D is the Kuhn statistical segment length of duplex DNA, and $d\underline{V}_D$ is a volume element for double-strand ring closure (12). Similarly, the statistical weight of a single-strand deletion loop of length \underline{L}_S (relative to the linear strand of the same length) is $(3/2\pi \underline{L}_S \underline{b}_S)^{3/2} d\underline{V}_S$, where \underline{b}_S is the Kuhn statistical segment length of single-strand DNA under renaturing conditions. Structure B' contains a composite circle consisting of a duplex of length \underline{L}_D and a single strand of length \underline{L}_S . It is fairly easy to show that the statistical weight of this structure is $[3/2\pi(\underline{L}_S \underline{b}_S + \underline{L}_D \underline{b}_D)^{3/2} d\underline{V}_{DS}]$, where $d\underline{V}_{DS}$ is the volume element for ring closure at a junction between double- and single-strand DNA. In the present instance $\underline{L}_D \underline{b}_D \gg \underline{L}_S \underline{b}_S$; therefore

$$\frac{\underline{g}_2(B')}{\underline{g}_2(A')} = \frac{[3/2\pi(\underline{L}_S \underline{b}_S + \underline{L}_D \underline{b}_D)]^{3/2} d\underline{V}_{DS}}{(3/2\pi \underline{L}_S \underline{b}_S)^{3/2} (3/2\pi \underline{L}_D \underline{b}_D)^{3/2} d\underline{V}_D d\underline{V}_S} \approx \frac{1}{(3/2\pi \underline{L}_S \underline{b}_S)^{3/2} d\underline{V}} \quad (1)$$

where $d\underline{V}$ represents $d\underline{V}_D d\underline{V}_S / d\underline{V}_{DS}$.

To apply eq. (1), we take a contour length of 3.2_2 \AA per nucleotide for both single- and double-strand DNA. Thus, for the ϕX deletion loop, $L_S = 0.16_1 \mu$. The principal uncertainties are the values of $d\underline{V}$ and of \underline{b}_S . We must estimate \underline{b}_S for denatured DNA under renaturing conditions, where no hydrodynamic measurements are available. To do this, we follow Wetmur and Davidson (13) and estimate the sedimentation coefficient of single-stranded T7 DNA under renaturing conditions as $50S$. We then apply eq. (11) of Gray *et al.* (14), using $\epsilon = 0.110$, $\underline{M}_L = 100 \text{ daltons/\AA}$, $\underline{v} = 0.555 \text{ cm}^3/\text{gram}$, $M = 1.26 \times 10^7 \text{ daltons}$ for T7 DNA, and the diameter of a DNA strand as 10 \AA , and calculate $\underline{b}_S = 45 \text{ \AA}$. A similar value can be deduced from calculations presented by Bloomfield (15).

We expect $d\underline{V}$ to be of the order of 10^{-21} cm^3 , and write $d\underline{V} = \underline{f} 10^{-21} \text{ cm}^3$, where \underline{f} is hopefully of the order of unity. We then find that

$$[g_1(B)/g_1(A')] [g_2(B)/g_2(A')] = 12/\underline{f} \quad (2)$$

The factors affecting $\underline{g}_3(B')/\underline{g}_3(A')$ are the following: The structure A' contains two junctions of the type identified as A_j' in Fig. 3 and drawn in magnified scale in Fig. 4. The structure B' contains two junctions depicted as B_j' in Figs. 3 and 4. There may be some steric crowding in A_j' , relative to B_j' , but there is a favorable stacking interaction in A_j' that is lost in B_j' . We write

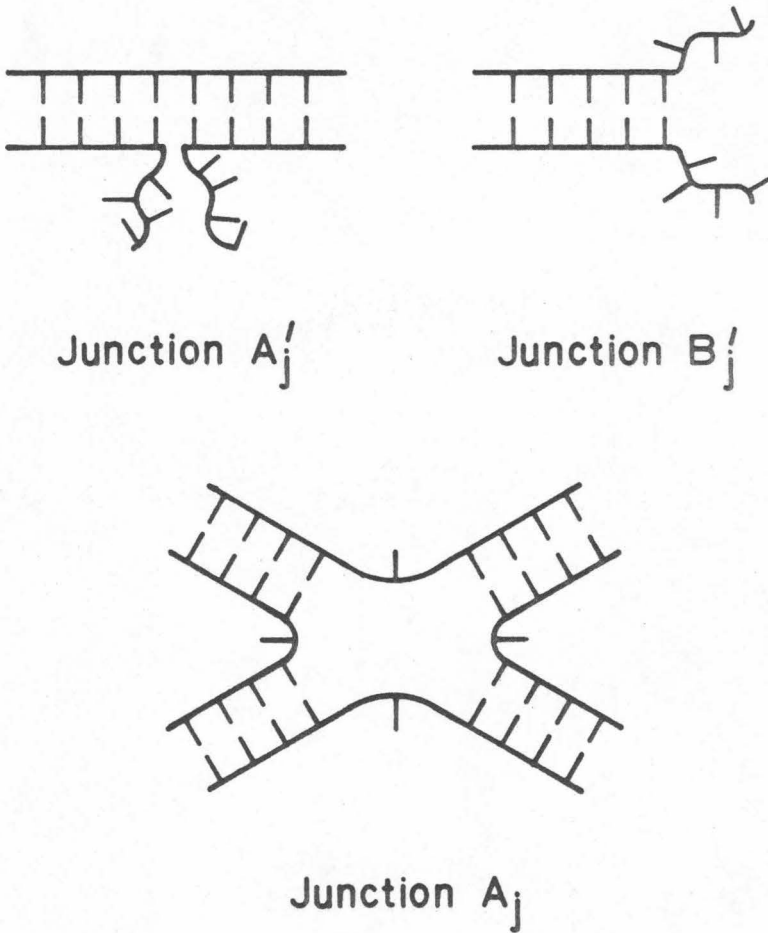


Fig. 4. Schematic representation of the junctions A'_j , B'_j and A_j .

$$\underline{g}_3(B')/\underline{g}_3(A') = [\underline{g}(B_j')/\underline{g}(A_j')]^2 \quad (3)$$

and we expect that $\underline{g}(B_j')/\underline{g}(A_j') > 1$. If the equilibrium ratio $\underline{g}_1(B')$ $\underline{g}_2(B')\underline{g}_3(B')/\underline{g}_1(A')\underline{g}_2(A')\underline{g}_3(A')$ is 2, as suggested by the experiments, then from (2) and (3)

$$(1/f)[\underline{g}(B_j')/\underline{g}(A_j')]^2 = 2/12 = 1/6 \quad (4)$$

This numerical parameter, deduced from our experimental data, is available for prediction of equilibria in other systems.

It is probable that structures C' and D' (Fig. 3) are much less stable than structures A' and B', respectively, because they involve an additional ring closure as well as a nick in a duplex. Nevertheless, structures with this topology are seen at a frequency of about 1/10 A' and B', respectively. This suggests that the rate of branch migration is sufficiently slow compared to the rate of renaturation so that the observed system is not quite at equilibrium.

The stabilities of the duplex structures A and B can be similarly discussed. Structure A involves two closed duplexes and two closed single-strand deletion loops. Structure B is more complicated. It can be approximately discussed as follows: The two duplex strands, $e'_1a'_1b'_1c'_1$ and $c'_2b'_2a'_2e'_1$, start at J_1 and meet at J_2 . The two single strands, d_1' , and d_2' , also start at J_1 and meet at J_2 . The root mean square end-to-end distance of a duplex strand, $(\underline{L}_D b_D)^{3/2}$, is much greater than that, $(\underline{L}_S b_S)^{3/2}$, for a single strand. Therefore, the two duplex paths between J_1 and J_2 have approximately zero end-to-end distance and

the constraint in the two duplexes is the same in B as for the two duplex circles in A. The constraint on the single strands in B is effectively ring closure for a strand of contour length, $\underline{d}_1' + \underline{d}_2'$, that is, $2\underline{L}_S$. Then.

$$\frac{g_2(B)}{g_2(A)} = \frac{[3/2\pi(2\underline{L}_S b_S)]^{3/2} dV}{\{[3/2\pi\underline{L}_S b_S]^{3/2} dV\}} = \frac{1}{2^{3/2}(3/2\pi\underline{L}_S b_S)^{3/2}} = \frac{1/3 \times 10^4}{f} \quad (5)$$

There is a statistical factor $\underline{g}_1(B)/\underline{g}_1(A) = 1/5000$. Structures A and B both contain two junctions of type A_j' . Structure A contains the additional junction labeled A_j in Figs.3 and 4 where four duplex strands meet. There are presumably several base pairs broken in this junction to accommodate the steric strains; thus $\underline{g}_3(B)/\underline{g}_3(A) = 1/\underline{g}(A_j) > 1$. If the equilibrium ratio of B to A is 50:1, we find that

$$\frac{\underline{g}_1(B)}{\underline{g}_1(A)} \cdot \frac{\underline{g}_2(B)}{\underline{g}_2(A)} \cdot \frac{\underline{g}_3(B)}{\underline{g}_3(A)} = \frac{1.3 \times 10^4}{(5 \times 10^3)\underline{f}g(A_j)} = 50 \quad (6)$$

or

$$\underline{f}g(A_j) \approx 0.05$$

This product too is available for application to other problems.

ACKNOWLEDGEMENT

This research was supported by NIH grant GM-10091. Phillip A. Sharp was supported by a U.S.P.H.S. fellowship. Our indebtedness to John Sedat is evident from the text. We wish also to acknowledge our cordial interaction with A. Zuccarelli, R. L. Benbow, and R. L. Sinsheimer.

REFERENCES

1. Lee, C. S., R. W. Davis, and N. Davidson, J. Mol. Biol., 23, 163 (1970).
2. Broker, T. R., and I. R. Lehman, J. Mol. Biol., 60, 131 (1971).
3. Hutchison, C. A., and R. L. Sinsheimer, J. Mol. Biol., 18, 429 (1966).
4. Eisenberg, M. G., R. M. Benbow, and R. L. Sinsheimer, J. Mol. Biol., in press.
5. Komano, T., and R. L. Sinsheimer, Biochim. Biophys. Acta, 155, 295 (1968).
6. Davis, R. W., M. Simon, and N. Davidson, Chapter in Methods in Enzymology, XXID, 413 (1971).
7. Westmoreland, B. C., W. Szybalski, and H. Ris, Science, 163, 1343 (1969).
8. Davidson, N., and W. Szybalski, Chapter 3 in The Bacteriophage Lambda, 45 (1971).
9. Cassuto, E., and C. M. Radding, Nature New Biology, 229, 13 (1971); 230, 128 (1971).
10. Kim, J. P., and N. Davidson, private communication.
11. Jacobsen, H., and W. H. Stockmayer, J. Chem. Phys., 18, 1600 (1950).
12. Wang, J. C., and N. Davidson, J. Mol. Biol., 19, 469 (1966).

13. Wetmur, J. G., and N. Davidson, J. Mol. Biol., 31, 349 (1968).
14. Gray, H. B., V. Bloomfield, and J. E. Hearst, J. Chem. Phys., 46, 1493 (1967).
15. Bloomfield, V., Biochem. and Biophys. Res. Commun., 34, 765 (1969).

Proposition I

Physical Studies on Bacteriophage T5 DNA

Experiments are proposed to: (a) map the sites of the single-strand breaks and to map the deletion in T5 st(0) DNA; (b) study the relation, if any, between the single strand-breaks and the piece of DNA (FST DNA) first transferred during phage infection; and (c) study the biological significance of the breaks.

Bacteriophage T5 DNA is unusual in that it contains three major single-strand breaks at specific sites so that it will produce one intact strand and four fragments upon denaturation (Abelson and Thomas, 1966; Bujard, 1969; Jacquemin-Sablon and Richardson, 1970; Haywood and Smith, 1972a and 1972b). The breaks can be repaired in vitro with DNA ligase (Jacquemin-Sablon and Richardson, 1970). There is an evidence that such repair occurs in vivo as well (Thomas, 1966). A heat stable mutant of T5⁺, called T5st(0), appears to have a deletion covering the position of one of the single strand breaks in T5⁺ DNA (Fig. 1).

The injection of the T5 chromosome into E. coli proceeds in two stages (Lanni, 1968). After adsorption of the virus to the host cell, a segment called FST DNA (first-step transfer DNA) is injected first into the cell. There is a pause which allows protein synthesis to occur in order to transfer the rest of the molecule. Therefore

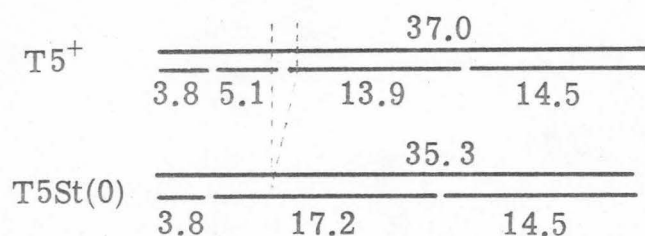


Fig. 1. A model for the T5⁺ and T5St(0) molecules, showing the locations of single-strand breaks. This model is redrawn from Haywood and Smith (1972b). The relative position of the first two fragments is based on the Bujard's observation (1969).

in the absence of protein synthesis the FST DNA can be separated from the rest of the molecule by blending the host cell-phage complexes. Blending would simply shear off the untransferred portion of each DNA molecule, leaving a double-stranded DNA fragment associated within the cell. Genetic and biochemical evidence indicated that the FST DNA consists of homogeneous phage DNA of uniform size of about 8.3% of the mature T5 DNA (McCorquodale and Lanni, 1968; Lanni, McCorquodale and Wilson, 1964; Lanni, Lanni and Tevethia, 1966). The FST DNA region controls two functions associated with phage infection: breakdown of bacterial DNA and injection of the rest of the phage DNA molecule. It has been suggested that discontinuous transfer of T5 DNA is associated with single-strand breaks and that the smallest fragment in Fig. 1 could be one strand of FST DNA.

Haywood and Smith (1972a) have developed a high resolution method for separating single-stranded DNA fragments by agarose gel electrophoresis. They found that the molecular weight of the single-strands of FST DNA is 3.0×10^6 daltons (3.0 MD; MD = Mega Daltons) which is smaller than that of any known major fragment (Haywood and Smith, 1972b). In the gel, the band corresponding to 3.0 MD DNA was clearly separated from that corresponding to 3.8 MD DNA. Furthermore, there was only one distinct band in the gel at the position of 3.0 MD when the single-stranded FST DNA itself was electrophoresed. From these results they suggested that two-step transfer was not related to single-strand breaks. It is not known, however that the first-step transfer stops when the DNA is injected at the point of break into the host cell, or beyond the break point, or when a single-strand break reaches a certain point of the tail. Therefore it is possible that the single-strand break is somehow used as a stop signal for transfer of DNA while the break remains inside the tail. In such a case the FST DNA will be smaller than the 3.8 MD or the 14.5 MD fragments. Thus the size difference between the FST DNA and the smallest fragment is by no means conclusive evidence that two step transfer is not associated with the single-strand breaks.

T5 DNA appears to be terminally repetitious (personal communication with Dr. Snustad through Dr. Broker). Then the nucleotide sequence of part or all of the FST DNA is also repetitious, so that either end could be transferred first.

The present proposition will describe methods to answer the following question:

1. Where does the deletion in T5st(0) map on the T5 chromosome? The experiments will also independently determine the sites of the single-strand breaks depicted in Fig. 1.
2. Is there a real size difference between the FST DNA and 3.8 MD fragments as obtained by Haywood and Smith (1972b)?
3. Is the FST DNA a unique segment of the left- or the right-end of T5 DNA or a repetitious?
4. Are the single-strand breaks repaired soon after infection? If they are not repaired at all, is T5 DNA without any single-strand breaks transfective?

Intact strands and fragments are prepared by preparative gel electrophoresis or by sedimentation. To map the deletion in T5st(0) on the T5 chromosome by electron microscopy, the intact strand of T5st(0) is hybridized with a mixture of two fragments as shown in Fig. 2.

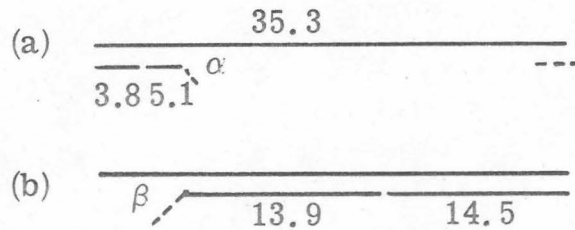


Fig. 2. Schematic representation of the hybridized molecules (a) between T5st(0) intact strand and (3.8 + 5.1) MD fragments from T5⁺; (b) between T5st(0) intact strand and (13.9 + 14.5) MD fragments from T5⁺.

A single-stranded region is well resolved when DNA is mounted under proper conditions (Davis, Simon and Davidson, 1971).

α represents the amount of deletion in the 5.1 MD fragment and β in the 13.9 MD fragment. Therefore the combined length of α and β will correspond to 1.8 MD (refer to Fig. 3 for reciprocal hybridization). Furthermore, if the 3.8 MD fragments hybridize to the sequence both end of the molecule, T5 DNA is in fact terminally repetitious. The length of the duplex region on the right end gives a measure of the length of the terminal repetition.

To determine the size of the FST DNA, the FST DNA is isolated from infected cells with ³²P-labelled T5 phage by the procedures described by Haywood and Smith (1972b). The denatured FST DNA is mounted for the electron microscopy and their lengths are determined. As a comparison, the single-stranded 3.8 MD fragments from mature phage are measured. These length

measurements will determine size of the FST DNA and the difference in size, if any, between the FST DNA and the 3.8 MD fragments. The results obtained by Haywood and Smith (1972b) indicated that the FST DNA is smaller. This experiment is an independent determination of the lengths.

The FST DNA can be mapped in the following way. The intact strand from T5⁺ DNA is hybridized with the denatured FST DNA. If T5 DNA is terminally repetitious, the FST DNA will hybridize to the sequence at both ends. Therefore it will be impossible to distinguish the left end from the right end regardless of the size of terminal repetitious region. Thus the additional 17.2 MD fragments from T5st(0) are hybridized to the heteroduplexes between the 37.0 MD strands and the denatured FST DNA. The possible structures for such heteroduplex molecules are shown in Fig. 3. The deletion loop

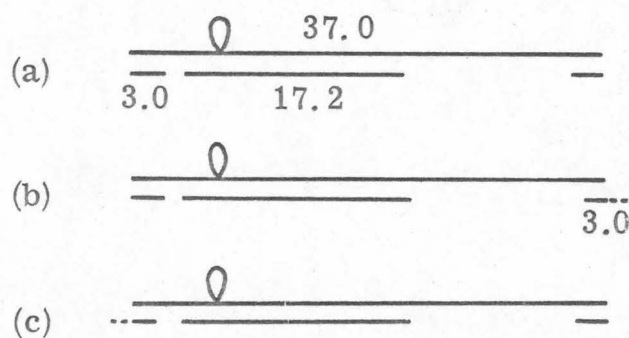


Fig. 3. Hypothetical heteroduplex molecule (37.0 MD/17.2 MD + FST), when the size of the FST is equal (a) to or larger (b, c) than the terminal repetition.

will be used as a position marker. When the structure shown in Fig. 3(a) is observed, the size of the terminal repetition is the same as that of the FST DNA. In this case it can't be determined whether one end or either end is transferred first. The observation of the structure shown in Fig. 3(b) suggests that the left end is preferentially transferred first, that is, the FST DNA maps on the left end. If the structure shown in Fig. 3(c) is observed, the right end is most likely injected first. If the two structures in Fig. 3(b) and 3(c) are observed with equal frequency, one would conclude that phage can inject the FST DNA from either end. As a result, reannealed FST DNA may not be all double-stranded throughout the molecule.

According to Thomas (1966), preliminary experiments indicated that the nicks in T5 were repaired four min after injection. No later experiments confirmed his observation. E. coli F (a fast-adsorbing host for T5 but a nonpermissive host for amber phage mutants) can be infected with labelled T5 phage carrying an amber mutation in DNA polymerase to prevent replication (Hendrickson and McCorquodale, 1971). At various times of infection, intracellular DNA is gently extracted. Denatured DNA is examined in the agarose gel electrophoresis to see if all the single-strand breaks are repaired.

If the above study indicate that the single-strand breaks are repaired during T5 replication, possible function, if any, of the breaks immediately after infection can be studied by transfection. However, if the single-strand breaks are never repaired, their essentiality can also be studied by a similar way. Usually the efficiency of transfection

is very low compared with normal infection: one infection center per 1×10^5 T5 phage DNA (Lawhorne and Benzinger, 1970). By using a strain lacking endonuclease I (E. coli 238/4), the transfectivity of T4 was shown to be increased (Baltz, 1971).

Spheroplasts of E. coli 238/4 are transfected with ligase-treated T5⁺ DNA to see if viable progeny are produced. The two-step transfer process would not be observed in transfection. If the ligase-treated T5 DNA is transfective, its progeny DNA can be examined to determine whether all the single-strand breaks are re-introduced. If not, a study to define which single-strand breaks are essential could be performed as follows: one can partially repair T5 DNA with ligase. First the intact strand can be hybridized with the mixture of 3.8 and 5.1 MD fragments. The hybridized molecules are then treated with ligase to seal the break between the 3.8 and the 5.1 fragments and finally these partial duplexes are hybridized with the 13.9 and the 14.5 fragments mixture. This partially repaired DNA is used to transfect E. coli to determine if viable progeny are produced. If not, the break between the 3.8 and the 5.1 fragments must be essential for T5 DNA replication. Similarly the break between the 5.1 and the 13.9 fragments is ligase-treated, and E. coli is transfected with this DNA. It is likely that viable progeny are produced, because T5st(0), having a deletion covering this break is perfectly viable. For further studies on the indispensability of the break, the same steps can be used.

It will be also interesting to infect a mutant of E. coli which overproduces DNA ligase (Gellert and Bullock, 1970) with T5 phage, and to determine whether all three normally occurring nicks appear. They might be expected to if the single-strand breaks are under the genetic control of the phage.

References

- Abelson, J. and Thomas, C. A., Jr. (1966). *J. Mol. Biol.* 18, 262.
- Baltz, R. H. (1971). *J. Mol. Biol.* 62, 425.
- Bujard, H. (1969). *Proc. Natl. Acad. Sci., Wash.* 62, 1167.
- Davis, R. W., Simon, M. N. and Davidson, N. (1971). In "Methods in Enzymology", XXIX, 413.
- Gellert, M. and Bullock, M. L. (1970). *Proc. Natl. Acad. Sci.* 67, 1580.
- Haywood, G. S. and Smith, M. G. (1972a). *J. Mol. Biol.* 63, 383.
- Haywood, G. S. and Smith, M. G. (1972b). *J. Mol. Biol.* 63, 397.
- Henderickson, H. E. and McCorquodale, D. J. (1971). *J. Virology* 7, 612.
- Jacquemin-Sablon, A. and Richardson, C. C. (1970). *J. Mol. Biol.* 47, 477.
- Lanni, Y. T. (1968). *Bact. Rev.* 32, 227.
- Lanni, Y. T., Lanni, F. and Tevethia, M. J. (1966). *Science* 152, 208.
- Lanni, Y. T., McCorquodale, D. J. and Wilson, C. M. (1964). *J. Mol. Biol.* 10, 19.
- Lawhorne, L. and Benzinger, R. (1970). *Abstracts of Phage Meeting at Cold Spring Harbor*, p. 41.
- McCorquodale, D. J. and Lanni, Y. T. (1964). *J. Mol. Biol.* 10, 10.
- Thomas, C. A., Jr. (1966). *J. Gen. Physiol.* 49 (No. 6, Part 2), 43.

Proposition II
On Condensed T4 DNA

DNA in bacteriophages appears to be packaged into the head in a highly ordered and condensed configuration. In order to model this process, methods for producing condensed T4 DNA are proposed. The properties of the condensed DNA will be investigated by electron microscopy, sedimentation velocity and circular dichroism.

DNA in bacteriophage appears to be packaged into the head in a highly ordered and condensed configuration, since the available volume is only slightly greater than that of the DNA molecule alone.

Recent studies by Lerman (1971) showed that DNA undergoes a cooperative structural change in the presence of high concentration of polyethylene oxide (PEO) and salt. Sedimentation studies under these conditions indicate that in dilute DNA solutions, each molecule collapses into compact particle approaching the dimensions of a phage head. Lerman has suggested that this system is a model for the condensation of DNA in the bacterial cell before packaging. He reasons that, in both cases, there is a high concentration of macromolecules in the environment--either polyethylene oxide or the various proteins and other macromolecules associated with DNA inside cell.

Under the same conditions that caused sedimentation changes the circular dichroism (CD) spectrum was drastically altered (Jordan, Lerman and Venable, 1972). CD spectra of DNA brought into a more or less compact state are also available from studies on complexes with f-1 histone, DNA in ethylene glycol and complexes with polylysine (Fasman, Schaffhausen, Goldsmith and Adler, 1970; Nelson and Johnson, 1970; Shapiro, Leng and Felsenfeld, 1969). The CD spectrum of DNA alone consists of roughly equal positive and negative bands (near 275 and 245 $m\mu$, respectively) with a zero near 260 $m\mu$. In PEO at high salt concentrations, however, the positive band at 275 $m\mu$ diminishes or disappears. Apparently the CD spectra of T5 and T7 viruses show a collapse of the 275 $m\mu$ maximum (Dorman and Maestre, unpublished data). Therefore the condensed DNA formed under the several conditions previously described might imitate the in vivo structure of DNA inside a phage head.

In addition to DNA, bacteriophage T4 contains polyamines, acid-soluble peptides (Eddleman and Champe, 1966) and basic internal proteins. Internal proteins bind to DNA at low salt concentration (Mingawa, 1961). These materials are released when the phage is osmotically shocked. The amount of the internal proteins packaged corresponds to 7% of the total head protein. Polyamines in the T4 head can neutralize 30% of the negative charge on the viral DNA (Ames, Dubin and Rosenthal, 1958). The polypeptides comprise 1% of the total carbon of the phage.

Purified internal proteins do reduce RNA transcription on phage DNA (Bachrach and Friedman, 1967). The viscosity of phage or thymus DNA is reduced by association with internal proteins (Chaproniere-Rickenberg, Mahler and Fraser, 1964). Also the internal proteins cause a change in melting profiles of DNA. Thus these proteins apparently do interact with DNA.

I propose that a study of the effects of internal proteins, polyamines and phage heads on DNA might provide a more realistic model for condensation than does the PEO system. I propose the following experiments.

¹⁴C-Labelled T4 DNA is gently extracted. Internal proteins, polyamines and polypeptides are isolated from the phage (Black and Ahmad-Zadeh, 1971; Ames et al., 1958; Eddleman and Champe, 1966). Defective heads can be accumulated by infection with a mutant in gene 49 and can be purified (Lutfig, Wood and Okinawa, 1971).

At a salt concentration lower than 0.1 M, a dilute solution (1 μ g/ml) of ¹⁴C-labelled T4 DNA is mixed with each of internal proteins, polyamines, polypeptides and phage heads. Structures of the complexes or DNA molecules are examined as a function of the concentrations of the several components by electron microscopy, sedimentation velocity and circular dichroism studies. Effects on structural change using a combination of two, three and four components can also be studied. The complexes can be mounted without further dilution for electron microscopy by the procedures described by Griffith (1970).

If the binding of DNA to the internal proteins is tight, the complexes (whether in the presence or absence of polyamines, polypeptides or phage heads) can be sedimented through sucrose gradients. Since T4 DNA is labelled with ^{14}C , the complexes can be detected without being confused with 300 S defective heads. CD spectra of DNA in several different concentrations of internal proteins, polyamines and phage heads would be compared with those previously obtained for condensed DNA.

References

- Ames, B. N., Dubin, D. T., and Rosenthal, S. M. (1958). *Science* 127, 814.
- Bachrach, V. and Friedmann, A. (1967). *Biochem. Biophys. Res. Commun.* 26, 596.
- Black, L. W. and Ahmad-Zadeh, C. (1971). *J. Mol. Biol.* 57, 71.
- Chaproniere-Rickenberg, D. M., Mahler, H. R. and Fraser, D. (1964). *Virology* 23, 96.
- Eddleman, H. L. and Champe, S. P. (1966). *Virology* 30 471.
- Fasman, C. D., Schaffhausen, B., Goldsmith, L., and Adler, A. (1970). *Biochemistry* 9, 2814.
- Griffith, J. (1970). Ph. D. Thesis, California Institute of Technology.
- Jordan, C. F., Lerman, L. S. and Venable, J. H., Jr. (1972). *Nature New Biol.* 236, 67.
- Lerman, L. S. (1971). *Proc. Natl. Acad. Sci.* 68, 1886.
- Luftig, R. B., Wood, W. B. and Okinawa, R. (1971). *J. Mol. Biol.* 57, 555.
- Mingawa, T. (1961). *Virology*, 13, 515.
- Nelson, R. G. and Johnson, W. C. (1970). *Biochem. Biophys. Res. Commun.* 41, 211.
- Shapiro, J. T., Leng, M., and Felsenfeld, G. (1969). *Biochemistry* 8, 3219.

Proposition III
Specificities of a Single-strand Break on Replicating
Molecules of Bacteriophage λ

During the early stage of replication of bacteriophage λ , the structure involved is a branched monomeric open circle. In this proposition methods will be described to study specificities of the single-strand break by electron microscopy.

Linear DNA molecules of phage λ are converted into covalently closed circles shortly after infection (Bode and Kaiser, 1965). There are two stages in λ replication: 1) the production of closed circular molecules is completed by about 15 min (Young and Sinsheimer, 1968; Carter and Smith, 1970); 2) this is followed by the formation of "fast-sedimenting DNA" or concatemers, which in turn acts as precursor of linear phage size molecules (Smith and Skalka, 1966; Weissbach, Bartl and Salzman, 1968; Carter and Smith, 1970). Open circles (circles with one strand open and the other strand closed, (Ogawa and Tomizawa, 1967)) appear to be intermediates in the replication of closed circles, and also of concatenated DNA. The transition between the first and the second stages occurred between 9 and 15 min after infection (Carter and Smith, 1970).

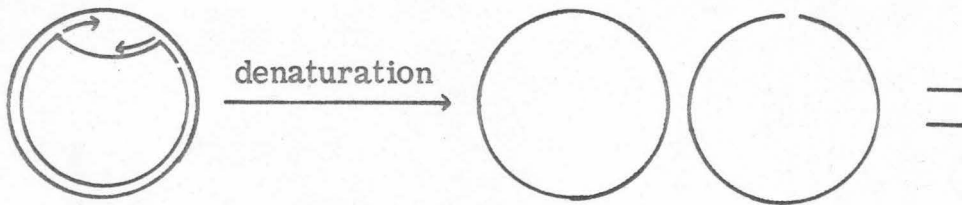
During the early round of replication, the structure involved in λ replication is a branched monomeric open circle (Ogawa, Tomizawa

and Fuke, 1968; Schnös and Inman, 1970). In general replication proceeds bidirectionally. A specific nick may be introduced into closed circles to relieve constraint—such a nick would probably occur near the origin of replication. Alternatively, a nonspecific nick may be formed and move around as λ replication proceeds. Either nick makes it possible for the replicated region to turn once for the replication of every 10 base pairs.

Schnös and Inman (1970) located the origin of the first stage replication at 0.82 ± 0.03 fractional map position from the left end. Stevens, Adhya and Szybalski (1971) located the origin of the replication between positions 0.79 and 0.815, that is between the right end of imm^{434} and gene O.

It is proposed to study the specificity of the single-strand nick of replicating open circles and to map its location on the λ map by electron microscopy.

Sensitive bacteria grown in heavy medium (^{15}N , D_2O) are infected with ^3H -labelled light λ phage. Seven min after infection, DNA replication is stopped. λ replicating open circular molecules can be purified on the basis of density difference (between light and hybrid density) by the procedures described by Schnös and Inman (1970). Denaturation of replicating open circles would produce the molecules as shown below.



The linear single-stranded DNAs are separated from the circles and fragments by sedimentation. If replication proceeded very far, the separation of the whole linear strand from some replicated fragments would not be possible. Therefore it is desirable to pool the fraction in lighter side in CsCl density gradient (used to separate replicating circles, to get in early stages of replication) and to sediment replicating circles in sucrose gradient to have relatively homogeneous sample.

A specific single-strand break will produce non-permuted sequences of the linear strand, on the other hand, a random break will give permuted sequences of the linear strand.

To find strand-specificity of the single-strand break, the linear strands are hybridized with each of the H and L strands of $\lambda_{b_2b_5c}$ separated in a CsCl density gradient in the presence of poly U, G (Szybalski, 1967). If it hybridizes to the L strand, the single-strand break appears on the H strand or vice versa. If it hybridizes with both strands, the break could be considered as random one. Since it is probable that the single-strand break does not occur between two cohesive ends as in mature λ DNA, resulting hybrid duplexes will be circular molecules. Therefore when examined in

the electron microscope, the heteroduplex molecules would not reveal the single-strand break. If the single-strand break happen to be at AT-rich region upon partial denaturation of the heteroduplex one of the denatured loops will contain a broken single-strand while the other strand is intact. However partially denatured replicating molecules (Schnös and Inman, 1970) did not show this break, suggesting that the break might be specific. The origin of replication mapped is the region of GC-richest sequences in the right half. If the break maps in either the b_2 or the b_5 region, it can be identified in the heteroduplex $\lambda/\lambda b_2 b_5 c$ (Fig. 1).

Suppose the single-strand break is somewhere between gene A and att. One way to map in this region is to use λdg strains. All the λdg strains mapped have the same right end point in att^L. The size of the λdg substitution varies from 54.6% ($\lambda dg P71$) to 34.6%

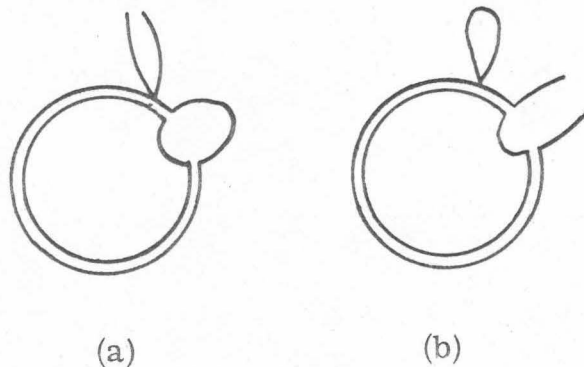


Fig. 1. $\lambda/\lambda b_2 b_5 c$ heteroduplex molecule when the break is in the b_2 region (a) or in the b_5 region (b).

(λ dgP72) of λ (Davis and Parkinson, 1971). The linear strands separated from λb_5 intracellular replicating open circles are hybridized with λ dgP71. A schematic representation of the $\lambda b_5/\lambda$ dgP71 heteroduplex is shown in Fig. 2a. Since the distance between att and b_5 loop is known (Davis and Parkinson, 1971) it is possible to map the single-strand break, which would appear in one of the strands of the substitution loop. λ bio 10 (13.5% substitution) is used to examine between genes att^R (0.574) and cIII (0.709) (Fig. 2b).

Similarly nin 5 deletion, qin A₃, Q₃ substitution and a₃ deletion mutants are used to study region of the λ map between 0.838 and 0.892, between 0.838 and 0.950 and between 0.979 and 0.995, respectively (Fiandt, Hradecna, Lozeron and Szybalski, 1971).

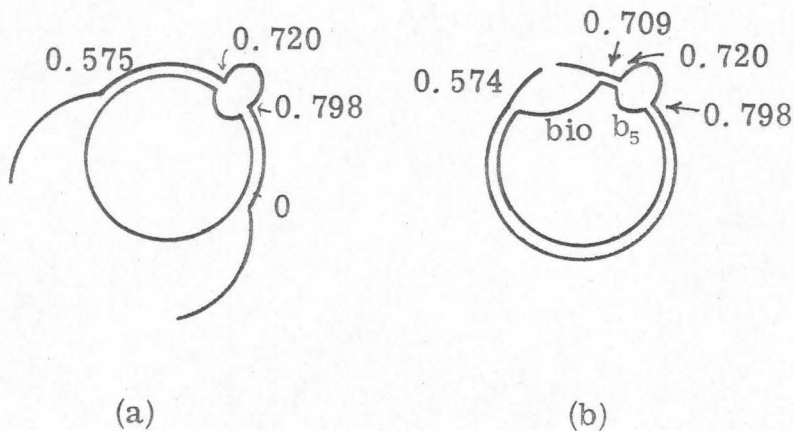


Fig. 2. $\lambda b_5/\lambda$ dgP71 (a) and $\lambda b_5/\lambda$ bio 10 (b) heteroduplex molecule when the break in dgP71 and bio 10 regions, respectively.

If the single-strand break is not detected in the above experiments or does not seem to be random, it must be in the rest of the regions which have not been studied. For these regions (between 0.709 and 0.720 and between 0.798 and 0.829), there is no immediate way to map the single-strand break. Let us assume the single-strand break is in the region between genes *cII* and *O* of the H strand (Fig. 3a). The cohesive ends of linear λ DNA from mature phage can be digested with an exonuclease specific for single-stranded DNA attacking 5'-ends. L strands are separated from H strand in poly U, G-CsCl density gradients and are hybridized with the linear H strand from the wild type intracellular replicating open circles. Circular molecules will be formed but there is a gap (about 15 bases) on the L strand (Fig. 3b). A break is introduced on H strand opposite to cohesive end of the L strand by lamb brain endonuclease (Heally, Stollar, Simm and Levine, 1963) (Fig. 3c). This enzyme is highly specific

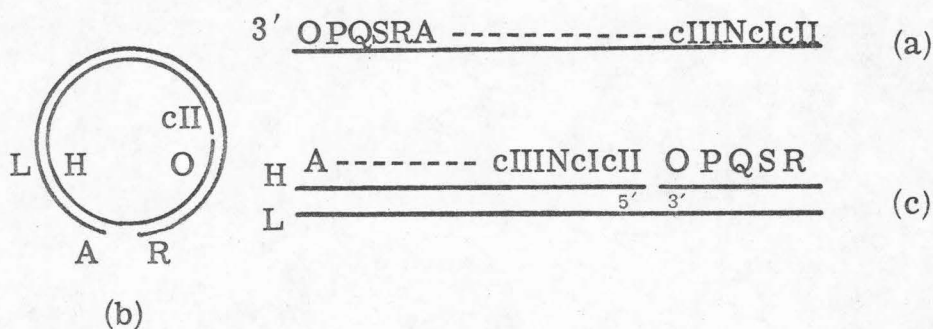


Fig. 3. Several steps of introducing a break in the region of cohesive end into the linear strand of replicating open circles.

for single-stranded DNA. Three single-stranded molecules are separated by alkaline sedimentation velocity. Larger H strand is hybridized with L strand of various λ dg and λ bio DNA to map 5'-ends. 3'-ends of the smaller H strand is mapped by hybridizing with nin 5 deletion, qin A₃, Q₃ substitution and a₃ deletion.

References

- Bode, R. and Kaiser, A. D. (1965). *J. Mol. Biol.* 54, 417.
- Carter, B. J. and Smith, M. G. (1970). *J. Mol. Biol.* 50, 713.
- Davis, R. W. and Parkinson, J. S. (1971). *J. Mol. Biol.* 56, 403.
- Fianndt, N., Hradecna, A., Lozeron, H. and Szybalski, W. (1971).
In "The Bacteriophage λ " (A. D. Hershey, editor), Cold Spring Harbor, New York, p. 329.
- Heally, J. W., Stollar, D., Simm, M. I. and Levine, L. (1963).
Arch. Biochem. Biophys. 103, 461.
- Ogawa, T. and Tomizawa, J. (1967). *J. Mol. Biol.* 23, 265.
- Ogawa, T., Tomizawa, J. and Fuke, M. (1968). *Proc. Natl. Acad. Sci.* 60, 861.
- Schnös, M. and Inman, R. B. (1970). *J. Mol. Biol.* 51, 61.
- Smith, M. G. and Skalka, A. (1966). *J. Gen. Physiol.* 49, No. 6, Part 2:127.
- Stevens, W. F., Adhya, S. and Szybalski, W. (1971). In "The Bacteriophage λ " (A. D. Hershey, editor), Cold Spring Harbor, New York.
- Szybalski, W. (1967). *J. Mol. Biol.* 29, 217.
- Weissbach, A., Bartl, P. and Salzman, L. A. (1968). *Cold Spring Harbor Sym. Quant. Biol.* 33, 525.
- Young, E. T. II and Sinsheimer, R. L. (1968). *J. Mol. Biol.* 33, 49.

PROPOSITION IV

On a Mechanism for the Antidotal Effect of Several Drugs on
the Poison α -Amanitin

The toxicity of α -amanitin can be partly protected by drugs, penicillin, phenylbutazone and 'bactrim'.

A mechanism of the antidotal effect of these drugs will be tested by equilibrium dialysis and renal extraction studies of α -amanitin.

α -Amanitin, a bicyclic octapeptide of the toadstool *Amanita Phalloides* (Wieland, 1968) causes necrosis of liver and kidney cells.

The action of α -amanitin begins shortly after the toxin reaches the organ although toxication symptoms do not appear for several hours. Death usually follows ingestion in two to five days. The nuclei of liver are primarily affected. The toxin binds to RNA polymerase in eukaryotic cells and inhibits the enzyme (Novello, Fiume and Stripe, 1970; Jacobs, Sadjel and Munro, 1970; Kedinger, Gniazdowski, Mandel, Gissinger and Chambon, 1970).

Floersheim (1972) found that penicillin, phenylbutazone, and 'Bactrim' provide curative potentialities against lethal doses of α -amanitin. The activity of the drugs depends on the time of their application. For example, if penicillin is injected into the mice 30 minutes or 8 hours after the α -amanitin, 50% and 30% of the mice, respectively, survive.

No cures were observed with chloramphenicol, sulfadimethoxine or refampicin. Combinations of two drugs (also given 30 minutes or 2 hours after α -amanitin) were more effective than either of the two drugs alone. Even drugs which were not antidotes could increase the effectiveness of a mild antidote. With a third drug added, more profound therapeutic effects were observed.

Penicillin, chloramphenicol and sulfonamides bind to serum proteins (Goldstein, Aronow and Kalman, 1969). Interference of drugs with the binding of other agents are known. For example, sulfonamides inhibit the binding of penicillin (Kunin, 1966), and phenylbutazone reduces the binding of sulfonamides and penicillin (Anton, 1960; Brodie, 1965).

The toxicity of amanitin increases several times when it is conjugated to albumin, probably because of a slow rate of elimination of the toxin through the glomeruli (Fiume, Campadelli-Fiume and Wieland, 1971).

A mechanism for the antidotal effect of drugs against α -amanitin was proposed (Floersheim, 1972) It involves inhibition of α -amanitin-protein binding. The hypothesis assumes that amanitin does in fact bind to serum proteins. The drugs compete for the limited number of binding sites on albumin. When the drugs are present in excess they remove α -amanitin from its albumin binding sites and enhance excretion of α -amanitin.

I therefore propose that the validity of this hypothesis may be tested by equilibrium dialysis and renal excretion studies of α -amanitin in the following way.

α -Amanitin can be labelled by injecting ^{14}C -glycine into the poisonous mushroom. α -Amanitin is purified from the rest of the toxins by paper chromatography. Uptake of C^{14} -labelled α -amanitin by liver cells is measured as a function of time. A drug is applied after injection of C^{14} α -amanitin, and renal excretion and uptake of α -amanitin are also measured as a function of time. The same experiment is repeated with a combination of two drugs and three drugs. The above hypothesis predicts that there will be more excretion of α -amanitin in the presence of drugs and that the degree of excretion will be increased in the order: single drug, double drugs and triple drugs.

To see whether α -amanitin binds to serum albumin, albumin can be dialyzed against C^{14} -labelled α -amanitin for several hours. After the dialysis has gone to completion, radioactivities of the outside and the inside of the dialysis bag are measured. If there is no difference, no binding has occurred.

A binding isotherm can be constructed by measuring the difference between the inside concentration (bound plus free) and the outside concentration (free) of α -amanitin as a function of free concentration.

Incidentally, the mechanism of functioning of the toxin could be studied by measuring its binding to RNA polymerase in the same apparatus.

A competition experiment may be performed as follows:

Albumin is dialyzed against a mixture of radioactive α -amanitin and unlabelled penicillin (single drug), penicillin and phenylbutazone (double drugs), and finally penicillin, phenylbutazone and chloramphenicol (triple drugs). If the hypothesis is correct, one will find less binding of C^{14} α -amanitin to albumin in the presence of single drug, and much less binding in the presence of double and triple drugs.

References

- Anton, A. H. (1960). *J. Pharmacol. Exp. Ther.* 129, 282.
- Brodie, B. B. (1965). *Proc. Roy. Soc. Med.* 58, 946.
- Fiume, L., Campadell-Fiume, G. and Wieland, Th. (1971).
Nature New Biology, 230, 219.
- Floersheim, G. L. (1972). *Nature New Biology* 236, 115.
- Kunin, C. M. (1966). *Clin. Pharmacol. Ther.* 7, 180.
- Goldstein, A., Aronow, L. and Kalman, S. M. (1969). *Principles of Drug Action*, 137 (Hoeber, New York).
- Jacob, S. T., Sajdel, E. M. and Munro, H. N. (1970). *Nature* 225, 60.
- Kedinger, C., Gniazdowski, M., Mandel, Jun., J. L., Gissinger, F., Chambon, P. (1970). *Biochem. Biophys. Res. Commun.* 38, 165.
- Novello, F., Fiume, L. and Stirpe, F. (1970). *Biochem. J.* 116, 177.
- Wieland, Th. (1968). *Science* 159, 946.

Proposition V

Synthesis of Ribulose-1, 5-diphosphate Carboxylase on
the Cytoplasmic and the Chloroplast Ribosomes

Messenger RNA for ribulose-1, 5-diphosphate carboxylase is transcribed in the nucleus in higher green plants and algae. However, its translation requires the functioning of the cytoplasm and the chloroplast ribosomes. The enzyme consists of two types of subunits. Specificity for translation of the subunits will be studied by using specific antibodies.

Chloroplasts contain ribosomes which are different from those found in the cell cytoplasm. Chloroplasts, however, are clearly not genetically autonomous; for genetic studies of both higher plants and algae indicate that some chloroplast components are encoded in the nuclear DNA (Kirk, 1971).

One example of such a component is ribulose-1, 5-diphosphate carboxylase (RuDPCase) which catalyzes the primary carbon dioxide fixation of the photosynthetic Calvin cycle of most green plants and algae. In the unicellular green algae, it was shown that chloroplast DNA transcription is not required for the synthesis of RuDPCase, and that its translation entails the function of both 70S chloroplast ribosomes and 80S cytoplasmic ribosomes (Armstrong, Surzycki, Moll and Levine, 1971).

RuDPCase is a large protein with a molecular weight of about 500,000 (Paulsen and Lane, 1966; Matsumoto, Sugiyama, and

Akazawa, 1969). In higher green plants and algae it contains two non-identical subunits, one having a molecular weight of 55,000 and the other having a molecular weight of around 12,000 (Ruther, 1970; Sugiyama, Ito and Akazawa, 1971). The native enzyme appears to consist of eight of the heavy subunits and 8 of the light subunits (Rutner, 1970). There seems to be 8 binding sites of this enzyme for ribulose-1,5-diphosphate (RuDP) at low ionic strength (Wishnick and Lane, 1970).

It has been suggested that polypeptide chains of one subunit are formed on cytoplasmic ribosomes and that those of the other subunit are formed on chloroplast ribosomes. In barley leaves, chloramphenicol, an inhibitor of chloroplast ribosomes, specifically inhibited the synthesis of the large subunit of RuDPCase (Criddle, Dau, Kleinkopf and Huffaker, 1970). Cycloheximide, an inhibitor of cytoplasmic ribosomes exerted a primary effect upon synthesis of the smaller subunit. However it also influenced production of the large subunit because it has a general effect in inhibiting total protein synthesis.

Both chloramphenicol and cycloheximide affect cellular metabolism other than protein synthesis (Ellis, 1969; Ellis and MacDonald, 1970). Recently Ellis and Hartly showed that lincomycin is more useful than chloramphenicol for selectively inhibiting the activity of chloroplast ribosomes in vivo in detached pea apices.

I therefore propose to show that chloroplast ribosomal activity is necessary for the synthesis of one subunit of RuDPCase by using

antibiotic lincomycin in detached pea apex system to extend the observation by Criddle et al. (1970).

The enzyme can be purified by the procedure described by Kleinkopf, Huffaker and Matheson (1970). Native RuDPCase can be reversibly dissociable into enzymatically active (large) and inactive (small) subunits by treatment with 4.0 M urea provided that the enzyme is preincubated with either RuDP or NaHCO₃ and MgCl₂. These subunits are separable in sucrose gradients; the large subunits then retain the enzymatic activity (Matsumoto et al., 1969).

Antibodies are prepared against native enzyme, the large subunits and the small subunits (Kleinkopf et al., 1970).

Detached etiolated pea apices are illuminated for several hours in the presence of lincomycin (2 μ g/ml) and ¹⁴C-leucine. Apices are ground and the homogenate are centrifuged at 20,000 g for 10 min. The supernatant in an equal volume is incubated with each of antibodies prepared against the native enzyme, the large subunit and the small subunit. The observation by Criddle et al. (1970) predicts that there will be precipitation of the ¹⁴C-labelled smaller subunit with antibodies specific for the native enzyme and the smaller subunit. C¹⁴ counts in the two precipitates may be same. However, no precipitation will be observed with antibodies specific for the larger subunit.

It seems to be reasonable that the smaller subunit is synthesized in the cytoplasm with subsequent transport into the chloroplast, where it is united with the larger subunit. In the absence of synthesis

of the larger subunit, is the smaller subunit transported into the chloroplast? To investigate this problem, chloroplasts are isolated from detached etiolated pea apices illuminated in the presence of lincomycin and ^{14}C -leucine. Each antibody is added to the chloroplast extracts. If the smaller subunit is transported, C^{14} counts will be found in precipitate upon addition of antibody specific for the native enzyme and the smaller subunit.

References

- Armstrong, J. J., Surzycki, S. J., Mall, B. and Levine, R. P.
(1971). *Biochem.* 10, 692.
- Criddle, R. S., Dau, B., Kleinkopf, G. E. and Huffaker, R. C.
(1970). *Biochem. Biophys. Res. Commun.* 41, 621.
- Ellis, R. J. and MacDonald, I. R. (1970). *Plant Physiol.* 46, 227.
- Ellis, R. J. and Hartley, M. R. (1971). *Nature New Biol.* 233, 193.
- Kirk, J. T. O. (1971). *Ann. Rev. Biochem.* 40, 161.
- Kleinkopf, G. E., Huffaker, R. C. and Matheson, A. (1970).
Plant Physiol. 46, 204.
- Matsumoto, C., Sugiyama, T. and Akazawa, T. (1969). *Arch.*
Biochem. Biophys. 135, 282.
- Paulsen, J. M. and Lane, M. D. (1966). *Biochemistry* 5, 2350.
- Rutner, A. C. (1970). *Biochem. Biophys. Res. Commun.* 39, 923.
- Sugiyama, T., Ito, T. and Akazawa, T. (1971). *Biochemistry* 10,
3406.
- Wishnick, M. and Lane, M. D. (1970). *J. Biol. Chem.* 245, 4939.